ANALYSIS OF ENTROPY GENERATION DUE TO MAGNETOHYDRODYNAMIC COUPLE STRESS FLUID

BY

OPANUGA, ABIODUN ADEGBOYEGA

Matriculation Number: 13PCD00575

JUNE, 2017

ANALYSIS OF ENTROPY GENERATION DUE TO MAGNETOHYDRODYNAMIC COUPLE STRESS FLUID

BY

OPANUGA, ABIODUN ADEGBOYEGA

Matriculation Number: 13PCD00575

JUNE, 2017

ANALYSIS OF ENTROPY GENERATION DUE TO MAGNETOHYDRODYNAMIC COUPLE STRESS FLUID

BY

OPANUGA, ABIODUN ADEGBOYEGA

B.Sc (Ed) Mathematics, University of Ado-Ekiti, Ekiti.

M.Sc Mathematics, Olabisi Onabanjo University, Ago-Iwoye.

Matriculation Number: 13PCD00575

A THESIS SUBMITTED TO THE DEPARTMENT OF MATHEMATICS, COLLEGE OF SCIENCE AND TECHNOLOGY, COVENANT UNIVERSITY, OTA, OGUN STATE, NIGERIA IN PARTIAL FULFILLMENT OF THE REQUIREMENTS FOR THE AWARD OF Ph.D DEGREE IN INDUSTRIAL MATHEMATICS.

JUNE, 2017

ACCEPTANCE

This is to attest that this thesis is accepted in partial fulfilment of the requirements for the award of the degree of Doctor of Philosophy in Industrial Mathematics, College of Science and Technology, Covenant University, Ota.

Mr. Philip John. Ainwokha .....
(Secretary, School of Postgraduate Studies) Signature & Date

Prof. Samuel T. Wara .....
(Dean, School of Postgraduate Studies) Signature & Date

DECLARATION

I, **OPANUGA Abiodun Adegboyega** (13PCD00575) declare that this research was carried out by me under the supervision of Prof. Jacob A. Gbadeyan of the Department of Mathematics, University of Ilorin, Ilorin, Nigeria and Prof. Samuel A. Iyase of the Department of Mathematics, Covenant University, Ota, Nigeria. I attest that the thesis has not been presented either wholly or partly for the award of any degree elsewhere. All the sources of materials and scholarly publications used in the thesis are duly acknowledged accordingly.

OPANUGA Abiodun Adegboyega .....
(Student) Signature & Date

CERTIFICATION

We certify that this thesis titled "Analysis of Entropy Generation Due to Magneto-hydrodynamic Couple Stress Fluid" is an original work carried out by **OPANUGA Abiodun Adegboyega** (13PCD00575), in the Department of Mathematics, College of Science and Technology, Covenant University, Ota, Ogun State, Nigeria, under the supervision of Prof. Jacob A. Gbadeyan and Prof. Samuel A. Iyase. We have examined and found the work acceptable for the degree of Doctor of Philosophy in Industrial Mathematics.

Prof. Jacob A. Gbadeyan .....
(Supervisor) Signature & Date

Prof. Samuel A. Iyase .....
(Co-supervisor) Signature & Date

Dr. Timothy A. Anake .....
(Head of Department) Signature & Date

Prof. Alagbe W. Gbolagade .....
(External Examiner) Signature & Date

Prof. Samuel T. Wara .....
(Dean, School of Postgraduate Studies) Signature & Date

DEDICATION

To the Almighty God, my father and my mother whose vehicle conveyed my existence. And to my love, Comfort for being there for me.

ACKNOWLEDGEMENTS

I want to give Glory and Praise to the Almighty God for helping me through the course of this programme.

I appreciate the Chancellor, Dr D.O. Oyedepo, the Vice Chancellor, Professor AAA. Atayero and the entire management of Covenant University for funding my doctorate studies and providing an enabling environment for research.

I acknowledge the intellectual tutelage and fatherly understanding of my supervisor, Professor J. A. Gbadeyan for his inspiration, immense contribution(s) and guidance towards the commencement and completion of this research. I remain indebted to his invaluable advice. A pillar of inspiration he has been to me. I am grateful also to my Co-Supervisor, Professor S. A. Iyase for his concern, encouragements, criticisms and directions for the successful completion of this research work.

My deep appreciation goes to the current *Ag.* Head of the Department of Mathematics, Covenant University, Dr. T.A. Anake for recommending me suitable for this programme. I cannot forget the former *Ag.* Head of the Department of Mathematics, Covenant University, Dr. E.A. Owoloko, for his love and concern. Getting through this research work required more than academic support. I therefore appreciate my colleagues and all the staff of the Department of Mathematics, Covenant University who made my life enjoyable in Covenant University.

I am grateful to Pastor Folarin whose spiritual support for my family knows no limit. May God keep him, his family and God's sheep under his care. I sincerely appreciate the guidance provided to me by Mr. V. O. Akinyemi of Isara Secondary School, Isara Remo.

I am particularly grateful to my wife, Comfort Opanuga and my children- Stephen and Philip. Their patience and support enabled me to complete this research in a record time.

TABLE OF CONTENTS

COVER PAGE i

TITLE PAGE ii

ACCEPTANCE iii

DECLARATION iv

CERTIFICATION v

DEDICATION vi

ACKNOWLEDGEMENTS vii

TABLE OF CONTENTS viii

LIST OF TABLES xii

LIST OF FIGURES xiii

LIST OF SYMBOLS xvi

ABSTRACT xviii

CHAPTER ONE: INTRODUCTION 1

1.1 Background to the Study 1
1.1.1 Couple Stress Fluid 2
1.1.2 Magnetohydrodynamic 3
1.2 Basic Equations of Flow 9
1.2.1 Continuity Equation 10
1.2.2 Momentum Equation 14
1.2.3 Energy Equation 19
1.3 Statement of the Problem 22
1.4 Aim and Objectives 22
1.5 Motivation 23
1.6 Justification for Research 24
1.7 Significance of the Study 24
1.8 Scope of Research 24
1.9 Limitation 25

1.10 Delimitation 25
1.11 Definition of Terms 25
1.12 Organisation of the Study 32

CHAPTER TWO: LITERATURE REVIEW 33
2.1 Introduction 33
2.2 Review of Related Literature 34
2.3 Magnetohydrodynamic 34
2.4 Flow through Porous Medium 36
2.5 Flow through Vertical Channel 37
2.6 Boundary Layers Flows 38
2.7 Reactive Flows 38
2.8 Entropy Generation 39

CHAPTER THREE: METHODOLOGY 43
3.1 Introduction 43
3.2 Description of Methods 43
3.2.1 Adomian Decomposition Method 44
3.2.2 Differential Transform Method 46
3.3 Mathematical Models 48
3.3.1 Model 1: Influence of Magnetic Field on Couple Stress Flow Through Porous Channel with Entropy Generation 48
3.3.2 Formulation of Model 1 48
3.3.3 Solution by Adomian Decomposition Method (ADM) 51
3.3.4 Solution by Differential Transform Method (DTM) 53
3.3.5 Entropy Generation Analysis 56
3.3.6 Model 2: Second Law Analysis of Hydromagnetic Couples Stress Fluid Embedded in a Non-Darcian Porous Medium 58
3.3.7 Formulation of Model 2 58
3.3.8 Solution by Adomian Decomposition Method (ADM) 61
3.3.9 Solution by Differential Transform Method (DTM) 63
3.3.10 Entropy Generation 66
3.3.11 Model 3: Inherent Irreversibility Analysis in Buoyancy Induced Magnetohydrodynamic Couple Stress Fluid 67
3.3.12 Formulation of Model 3 67
3.3.13 Solution by Adomian Decomposition Method 70
3.3.14 Entropy Generation 72

3.3.15 Model 4: Combined Effects of Velocity Slip, Temperature Jump and Thermal Radiation on Entropy Generation of a Reactive Hydromagnetic Couple Stress Fluid Through Vertical Porous Medium . . . 73
3.3.16 Formulation of Model 4 . . . 73
3.3.17 Solution by Adomian Decomposition . . . 77
3.3.18 Entropy Generation . . . 79

CHAPTER FOUR: RESULTS AND DISCUSSION 80
4.1 Introduction . . . 80
4.2 Model 1 . . . 80
4.2.1 Effects of Parameter Variation on Velocity and Temperature Profiles . . . 80
4.2.2 Effects of Parameter Variation on Entropy Generation Rate . . . 88
4.2.3 Effects of Parameter Variation on Bejan Number . . . 92
4.2.4 Effects of Parameter Variation on Skin Friction . . . 96
4.2.5 Effects of Parameter Variation on Nusselt Number . . . 98
4.3 Model 2 . . . 100
4.3.1 Effects of Parameters Variation on Velocity and Temperature Profiles . . . 100
4.3.2 Effects of Parameter Variation on Entropy Generation . . . 109
4.3.3 Effects of Parameter Variation on Bejan Number . . . 114
4.4 Model 3 . . . 119
4.4.1 Effects of Parameters Variation on Velocity Profile . . . 119
4.4.2 Effect of Parameters Variation on Temperature Profile . . . 124
4.4.3 Effect of Parameters Variation on Entropy Generation Rate . . . 130
4.4.4 Effect of Parameters Variation on Bejan Number . . . 136
4.5 Model 4 . . . 142
4.5.1 Effect of Parameter Variation on Velocity Profile . . . 142
4.5.2 Effect of Parameters Variation on Temperature Profile . . . 147
4.5.3 Effect of Parameters Variation on Entropy Generation . . . 152
4.5.4 Effects of Parameters Variation on Bejan number . . . 157

CHAPTER FIVE: CONCLUSION AND RECOMMENDATIONS 162
5.1 Introduction . . . 162
5.2 Summary of the Research Aim and Objectives . . . 162
5.3 Conclusion . . . 163
5.4 Contributions to Knowledge . . . 164

5.5 Further Study 164

REFERENCES **165**

APPENDIX **175**

Appendix A: Mathematica Codes for ADM **175**

Appendix B: Maple Codes for ADM **178**

Appendix C: Maple Codes for DTM **182**

LIST OF TABLES

Table 1.1 Typical values of Prandtl number 32

Table 3.1 Comparison between ADM and DTM solutions for velocity profile 55
Table 3.2 Comparison between Adesanya and Makinde (2015b), ADM and DTM solutions of velocity profile 57
Table 3.3 Comparison between ADM and DTM solutions 65

Table 4.1 Effect of Magnetic field variation on Skin friction 97
Table 4.2 Effect of suction/injection on variation on Skin friction 97
Table 4.3 Effect of Pressure gradient variation on Skin friction 97
Table 4.4 Effect of Magnetic field variation on Nusselt number 99
Table 4.5 Effect of suction/injection variation on Nusselt number 99
Table 4.6 Effect of couple stress variation on Nusselt number 99

LIST OF FIGURES

Figure 1.1 Magnetohydrodynamic Ship Propulsion 7
Figure 1.2 Magnetohydrodynamic Generator 8
Figure 1.3 Fluid element in three-dimensional flow 9
Figure 1.4 Infinitesimally small, moving fluid element 13
Figure 1.5 Energy fluxes associated with an infinitesimally small, moving fluid element 18
Figure 1.6 Application of Porous Medium 28

Figure 3.1 Schematic diagram for Model 1 49
Figure 3.2 Schematic diagram for Model 2 59
Figure 3.3 Schematic diagram for Model 3 68
Figure 3.4 Schematic diagram for Model 4 74

Figure 4.1 Effect of magnetic field parameter (H^2) on velocity profile . . 82
Figure 4.2 Effect of suction/injection (s) on velocity profile 83
Figure 4.3 Effect of couple stress inverse parameter (a) on velocity profile 84
Figure 4.4 Effect of magnetic field parameter (H^2) on temperature profile 85
Figure 4.5 Effect of suction/injection (s) on temperature profile 86
Figure 4.6 Effect of couple stress inverse parameter (a) on temperature profile 87
Figure 4.7 Effect of magnetic field parameter (H^2) on entropy generation rate 89
Figure 4.8 Effect of suction/injection (s) on entropy generation rate . . . 90
Figure 4.9 Effect of couple stress inverse parameter (a) on entropy generation 91
Figure 4.10 Effect of magnetic field parameter (H^2) on Bejan number . . 93
Figure 4.11 Effect of suction/injection (s) on Bejan number 94
Figure 4.12 Effect of couple stress inverse (a) on Bejan number 95
Figure 4.13 Effect of magnetic field parameter (H^2) on velocity profile . . 102
Figure 4.14 Effect of porous media shape factor parameter (β) on velocity profile 103
Figure 4.15 Effect of second order porous media resistance parameter (α) on velocity profile 104
Figure 4.16 Effect of couple stress inverse parameter (a) on velocity profile 105
Figure 4.17 Effect of magnetic field parameter (H^2) on temperature profile 106
Figure 4.18 Effect of porous media shape factor parameter (β) on temperature profile 107
Figure 4.19 Effect of couple stresses (a)on temperature profile 108

Figure 4.20 Effect of magnetic field parameter (H^2) on entropy generation rate 110
Figure 4.21 Effect of porous media shape factor parameter (β) on entropy generation rate 111
Figure 4.22 Effect of second order porous media resistance parameter (α) on entropy generation rate 112
Figure 4.23 Effect of couple stresses (a) on entropy generation rate 113
Figure 4.24 Effect of magnetic field parameter (H^2) on Bejan number . . 115
Figure 4.25 Effect of porous media shape factor parameter (β) on Bejan number 116
Figure 4.26 Effect of Brinkman number (Br) on Bejan number 117
Figure 4.27 Effect of Prandtl number (Pr) on Bejan number 118
Figure 4.28 Effect of Grashof number (Gr) on velocity profile 120
Figure 4.29 Effect of suction/injection (s) on velocity profile 121
Figure 4.30 Effect of Prandtl number (Pr) on velocity profile 122
Figure 4.31 Effect of couple stress inverse (a) on velocity profile 123
Figure 4.32 Effect of Grashof number (Gr) on temperature profile 125
Figure 4.33 Effect of magnetic field parameter (H^2) on temperature profile 126
Figure 4.34 Effect of suction/injection (s) on temperature profile 127
Figure 4.35 Effect of lower Biot number (Bi_1) on temperature profile . . . 128
Figure 4.36 Effect of upper Biot number (Bi_2) on temperature profile . . . 129
Figure 4.37 Effect of Grashof number (Gr) on entropy generation rate . . . 131
Figure 4.38 Effect of magnetic field parameter (H^2) on entropy generation rate 132
Figure 4.39 Effect of suction/injection (s) on entropy generation rate . . . 133
Figure 4.40 Effect of lower Biot number (Bi_1) on entropy generation rate . 134
Figure 4.41 Effect of upper Biot number (Bi_2) on entropy generation rate 135
Figure 4.42 Effect of Grashof number (Gr) on Bejan number 137
Figure 4.43 Effect of magnetic field parameter (H^2) on Bejan number . . 138
Figure 4.44 Effect of suction/injection (s) on Bejan number 139
Figure 4.45 Effect of lower Biot number (Bi_1) on Bejan number 140
Figure 4.46 Effect of upper Biot number (Bi_2) on Bejan number 141
Figure 4.47 Effect of velocity slip parameter (γ) on velocity profile 143
Figure 4.48 Effect of temperature jump parameter (k_n) on velocity profile 144
Figure 4.49 Effect of Grashof number (Gr) on velocity profile 145
Figure 4.50 Effect of thermal radiation parameter (N) on velocity profile . 146
Figure 4.51 Effect of velocity slip parameter (γ) on temperature profile . . 148

Figure 4.52 Effect of temperature jump parameter (k_n) on temperature profile 149
Figure 4.53 Effect of thermal radiation parameter (N) on temperature profile 150
Figure 4.54 Effect of Grashof number (Gr) on temperature profile 151
Figure 4.55 Effect of velocity slip parameter (γ) on entropy generation rate 153
Figure 4.56 Effect of temperature jump parameter (k_n) on entropy generation rate 154
Figure 4.57 Effect of thermal radiation parameter (N) on entropy generation rate 155
Figure 4.58 Effect of Grashof number (Gr) on entropy generation rate . . . 156
Figure 4.59 Effect of velocity slip parameter (γ) on Bejan number 158
Figure 4.60 Effect of temperature jump parameter (k_n) on Bejan number . 159
Figure 4.61 Effect of thermal radiation parameter (N) on Bejan number . 160
Figure 4.62 Effect of Grashof number (Gr) on Bejan number 161

LIST OF SYMBOLS

Symbol	Units	Description
C_p	J/K	Specific heat capacity at constant pressure
CV	–	Control volume
h	m	Channel width
u	m/s	Velocity
p	N/m^2	Fluid pressure
ν_0	–	Uniform suction/injection
E_G	KJ/K	Volumetric entropy generation
g	m/s^2	Acceleration due to gravity
Re	–	Renolds number
Pr	–	Prandtl number
Br	–	Brinkman number
Be	–	Bejan number
T	–	Fluid temperature
T_0	–	Fluid initial temperature
T_f	–	Fluid final temperature
H^2	–	Magnetic field parameter
N_S	–	Dimensionless entropy generation
B_0	–	Uniform transverse magnetic field
b	–	Empirical constant in the second order (porous inertial) resistance
a	–	Couple stress inverse parameter
Bi_1	–	Lower wall Biot number
Bi_2	–	Upper wall Biot number
G	Pa/m	Pressure gradient
x, y	–	Cartesian coordinates
s	–	Dimensionless suction/injection parameter
u^*	–	axial velocity
T^a	K	absolute temperature
$T_{\cdot}^g$	–	geometry wall temperature
k	W/mK	thermal conductivity of the fluid
K	–	porous permeability of the medium
Q	kJ/mol	heat of reaction
A	M/s	rate constant
R	J/kgK	universal gas constant

C_0	–	initial concentration of the reactant species
U	–	fluid characteristic velocity
Da	–	Darcy number
l	–	Function of molecular dimension of the fluid
q_r	–	radiative heat flux
k^*	–	mean absorption coefficient for thermal radiation
k_n	–	Knusdsen number
N	–	thermal radiation parameter
v	Ns/m^2	Fluid viscosity

Greek Letters	**Units**	**Description**
μ	–	Coefficient of dynamic viscosity
ρ	kg/m^3	Fluid density
γ_1, γ_2	–	Slip parameters
η	–	fluid particle size effect due to couple stresses
ϕ	–	Irreversibility ratio
σ	S/m	Electrical conductivity
α	–	second order porous media resistance parameter
θ	–	Dimensionless temperature
Ω	–	Dimensionless temperature difference
ζ	–	volumetric expansion
	–	molecular mean free path
γ	–	Navier slip parameter
μ^c	–	combustible material dynamic viscosity coefficient
λ	–	Frank-Kameneskii parameter
$\in$	–	Activation energy parameter
δ	–	viscous heating parameter
β	–	porous media shape factor parameter
σ^c	–	Stefan-Boltman constant
σ_T	–	thermal accommodation coefficient intensity

ABSTRACT

The study of magnetohydrodynamics (MHD) flow has received much attention in the past years owing to its applications in MHD generators, plasma studies, nuclear reactor, geothermal energy extractions, purifications of metal from non-metal enclosures, polymer technology and metallurgy. In view of the above, theoretical analysis of the effects of buoyancy force, velocity slip, temperature jump and thermal radiation on entropy generation rate were investigated on electrically conducting couple stress fluid through porous channel and highly porous medium. Semi-analytical techniques of Adomian decomposition and differential transform were employed to solve the boundary value problems derived from the conservation of mass, momentum and energy balance. The velocity profile and temperature profile were used to compute the irreversibility ratio and Bejan number. Graphical representations were presented to explain the effects of various flow parameter variations. From the results, it was found that increase in magnetic field and buoyancy force increased entropy generation while increase in porosity, velocity slip and temperature jump parameters retarded entropy generation rate. Moreover, both irreversibility due to viscous dissipation and heat transfer contributed to entropy generation rate.

***K*eywords**: Magnetohydrodynmic; Entropy generation; Adomian decomposition method (ADM); Differential transform method (DTM); Bejan number.

CHAPTER ONE

INTRODUCTION

1.1 Background to the Study

The history of fluid flow is very old, one of the early studies is the work of Leonardo Da Vinci's which gave rapid advancement to the study of fluids mechanics about 500 years ago, but earlier than this time; prehistoric relics of irrigation canals have shown that the study of fluid behaviour were much more available by the time of ancient Egyptian (Nakayama and Boucher, 1999). Several centuries ago Johann (father) and Daniel (son) began more modern understanding of fluids motion known as Bernoulli's equation. Since then, many researchers have done numerous work on fluid mechanics.

Fluid Mechanics can be described as the study of the behaviour of fluid under the condition of rest and motion. It involves application of the fundamental laws encountered in Physics. The laws are Newton's laws of motion, conservation of mass, first law of thermodynamics and second law of thermodynamics. Studying the behaviour of fluids is an essential part in the analysis of fluid models, it is needed in order to understand various problems ranging from the study of blood flow in the capillaries to the flow of crude oil across Niger-Delta of Nigeria. Fluid mechanics principles are required to explain why airplanes are made streamlined with smooth surfaces for the most efficient flight, while in the other way golf balls are made with rough surfaces to improve their efficiency.

Fluids consist of liquid and gas (or vapour) phases of the physical forms in which matter exists. The distinguishing feature between a fluid and the solid state of matter is seen by comparing fluid and solid behaviour. When a shear stress is applied to a solid it deforms, but its deformation does not increase with time (Fox, McDonald and Pritchard, 2004) whereas a fluid deforms continuously when subjected to external shearing (Rajput, 2004). Fluid can be defined as a substance that offers negligible

resistance to a change of shape and is capable of flowing. Specifically, a fluid can be defined as a substance which deforms continuously when a shear stress of any magnitude is applied to it. A shear stress (that is force per unit area) occurs when a tangential force acts on a surface.

1.1.1 Couple Stress Fluid

In continuum mechanics, size effect of material particles within the flow is neglected. It therefore implies that rotational interaction among particles resulting to symmetrical nature of force-stress tensor is being ignored. However, in very important cases like fluid flowing with suspended particles, this is not true. Hence, a size-dependent couple stress theory is required. The spin field due to microrotation of freely suspended particles set up an antisymmetric stress, which is called couple-stress, and thus couple-stress fluid is formed.

Couple stress fluid was introduced by Stokes (1966), it has unique features like the presence of couple stress, body couples and non-symmetric stress tensor. The important feature of couple stress is the introduction of size-dependent effect. According to Sunil *et al.* (2002), couple stress appears in fluids with very large molecules. Examples of such fluids include various types of lubricants with small amount of polymer additives, blood, electro-rheological fluids, synthetic fluids, etc.

Several authors have discussed various aspects of couple stress fluid under different flow configurations. For example Srivastava (1985) investigated the flow of couple stress fluid through stenotic blood vessels. Zakaria (2002) investigated hydromagnetic fluctuating flow of a couple stress fluid through a porous medium. Rudraiah and Chandrashekara (2010) presented couple stress effects on the rate of growth of Rayleigh-Taylor instability at the interface in a finite thickness couple stress fluid. Devakar and Iyengar (2010) considered the run up flow of a couple stress fluid between parallel plates, while Srinivasacharya and Kaladhar (2012a) presented the analytical solution of free and forced convection couple stress fluid flowing between two circular

cylinders with the effects of Hall and ion-slip. Furthermore, Rani *et al.* (2011) investigated the numerical analysis of couple stress fluid between infinite vertical cylinder. Double diffusive mixed convection in couple stress fluids with variable fluid properties was analysed by Dinesh *et al.* (2015).

The analysis of couple stress fluids has many important applications in numerous processes that occur in industry like the extrusion of polymer fluids, solidification of liquid crystals, cooling of metallic plate in a bath, and colloidal solutions (Srinivasacharya and Kaladhar, 2012b). Application of couple stress fluids are equally found in synovial joints (shoulder, hip, knee and ankle), geophysics, chemical engineering and astrophysics. Walicki and Walicka (1999) and Kumar *et al.* (2015) modeled synovial fluids as couple stress fluids in human joints because of the long chain of lauronic acid molecules found as additives in synovial fluid.

1.1.2 Magnetohydrodynamic

The study of flows in which the fluid is electrically conducting is known as magnetohydrodynamics (MHD). Magneto means magnetic field; hydro means fluids; and dynamics mean forces and the laws of motion. Magnetohydrodynamics (MHD) is the mathematical model for the low frequency interaction that exists between electrically conducting fluids and electromagnetic fields (Schnack, 2009). In other words, magnetohydrodynamics can be described as the study of the interaction between magnetic fields and moving, conducting fluids (Dawson, 2001). Other terms used to describe MHD include magneto fluid dynamics or hydromagnetics. Examples are liquid metals (such as mercury, gallium, molten magnesium, molten antimony, liquid sodium etc.), plasmas (ionized gases or electrically conducting gases) such as the solar atmosphere and salt water or electrolyte.

The fundamental concept behind MHD is that the relative movement of a conducting fluid and a magnetic field causes an electromotive force to develop, this will induce electrical currents with density of order $\sigma(u\times \mathrm{B})$, where σ is the electrical conductivity,

B is the magnetic field and u is the velocity field. The currents will give rise to another induced magnetic field which is added to the original magnetic field and the fluid appears to flow along with magnetic field lines. The combined magnetic field (that is both the imposed and induced) then interacts with the induced current density, J, giving rise to a Lorentz force (per unit volume), $J \times B$. This acts on the conductor and it is directed so as to impede the relative movement of the magnetic field and the fluid. In the description above, it is observed that fluid can "drag" magnetic field lines while magnetic fields can pull on the conducting fluids, this partial "freezing together" of medium and the magnetic field is referred to as MHD. The drive to explore MHD came as a result of three technological innovations.

(i) Fast-breeder reactors which use liquid sodium as a coolant and this needs to be pumped,

(ii) Controlled thermonuclear fusion requires that the hot plasma be confined away from material surfaces by magnetic forces and

(iii) MHD power generation, in which ionized gas is propelled through magnetic field, was thought to offer improved power station efficiencies.

The governing equations of MHD in differential form are given as follows:
Navier-Stokes equations with Lorentz force

$$\rho\left(\frac{\partial u}{\partial t} + (u \cdot \nabla)u\right) = -\nabla p + j \times B + \mu_f \nabla^2 u + \rho g \tag{1.1}$$

Continuity equation:

$$\frac{\partial \rho}{\partial t} + \nabla \cdot \rho u = 0 \tag{1.2}$$

Faraday's equation:

$$\nabla \times E = -\frac{\partial B}{\partial t} \tag{1.3}$$

Ampere's law:

$$\nabla \times B = \mu_m j \tag{1.4}$$

Ohm's law:

$$j = \sigma(E + U \times B) \tag{1.5}$$

where μ_m is the magnetic permeability, σ fluid electrical conductivity, μ_f is the fluid dynamic viscosity, u is the fluid velocity, E is the electrical field, B is the magnetic field intensity and j is the current density. Implicit in equations (1.4)-(1.8) are these additional relations:

$\nabla \cdot B = 0$ and $\nabla \cdot j = 0$

Magnetohydrodynamics has applications in numerous engineering processes such as;

(i) the metallurgical industries where magnetic fields are routinely used to heat, pump, stir and levitate liquid metals,

(ii) electromagnetic stirring,

(iii) dampen the motion of liquid metal,

(iv) electrolysis cells where it is used to reduce aluminium oxide to aluminium (Dawson, 2001).

(v) Astrophysics (planetary magnetic field),

(vi) Ship propulsion where electric current is applied to create MHD propulsion force (see Figure 1.1),

(vii) MHD generators (as shown in Figure 1.2),

(viii) MHD flow meters,

(ix) Dispersion (granulation) of metals,

(x) MHD flow control (reduction of turbulent drag),

(xi) Magnetic filtration and separation,

(xii) Jet printers,

(xiii) Fusion reactors (Abdou, 2007).

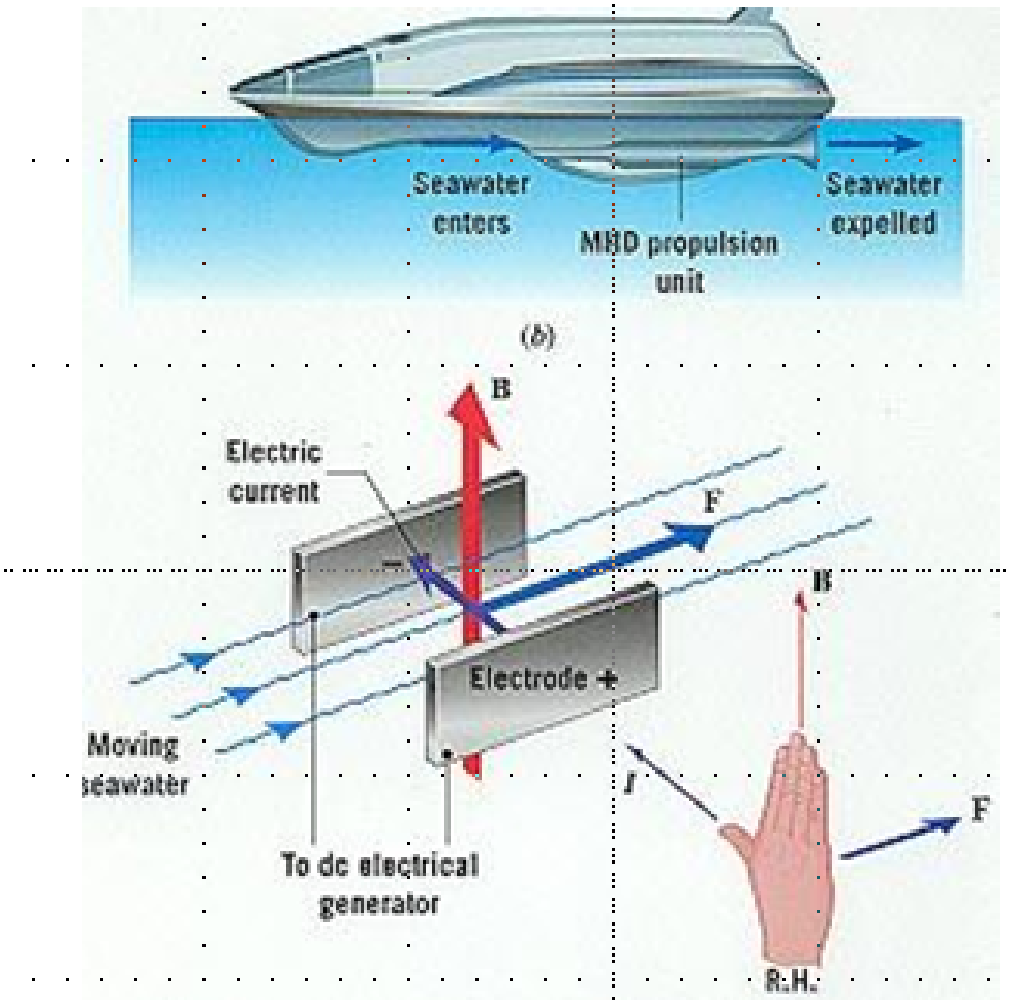

Figure 1.1: Magnetohydrodynamic Ship Propulsion (Abdou, 2007)

Figure 1.2: Magnetohydrodynamic Generator (Abdou, 2007)

1.2 Basic Equations of Flow

The three basic equations that govern the dynamic of fluid flow are the fundamental governing equations of fluid dynamics which are: the continuity equation, momentum equation and energy equation. These equations are mathematical statements of the three physical principles which are; conservation of mass, conservation of momentum (Newton's second law of motion) and conservation of energy (the first law of thermodynamics).

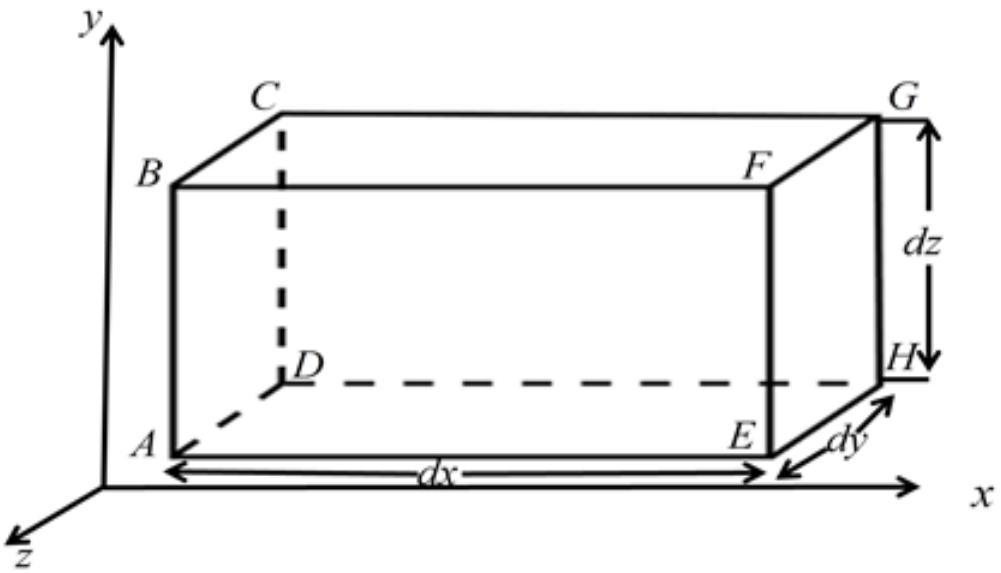

Figure 1.3: Fluid element in three-dimensional flow (Rajput, 2004)

1.2.1 Continuity Equation

Consider a small control volume (CV) as shown in Figure 1.3. Let ρ be mass density of the fluid at a particular instant and u, v, w are component of velocity of flow entering the three faces of the parallelepiped

Fluid influx (rate of mass of fluid entering the face ABCD) through ABCD = $\rho \times$ velocity (x-direction) $\times$ area of ABCD = $\rho \times$ u $\times\ dydz$

Fluid efflux (rate of mas of fluid leaving the face EFGH) through EFGH =

$$\rho\ u\ dydz + \frac{\partial}{\partial x}(\rho\ u\ dydz)dx \tag{1.6}$$

Gain in mass per unit time in x-direction = Fluid influx - Fluid efflux =

$$\rho\ u\ dydz - (\rho\ u\ dydz + \frac{\partial}{\partial x}(\rho\ u\ dx)dydz) \tag{1.7}$$

Y-direction

Fluid influx (rate of mas of fluid entering the face ADHE) through ADHE =

$\rho \times$ velocity (y-direction) $\times$ area of ADHE =$\rho \times$ v $\times\ dxdz$

Fluid efflux (rate of mas of fluid leaving the face BCGF) through BCGF =

$$\rho\ v\ dxdz + \frac{\partial}{\partial y}(\rho\ v\ dxdz)dy \tag{1.8}$$

Gain in mass per unit time in y-direction = Fluid influx - Fluid efflux =

$$\rho\ v\ dxdz - (\rho\ v\ dxdz + \frac{\partial}{\partial y}(\rho\ v\ dy)dxdz) \tag{1.9}$$

z-direction

Fluid influx (rate of mas of fluid entering the face CDHG) through CDHG =

$\rho \times$ velocity (z-direction) $\times$ area of CDHG = $\rho \times$ w $\times\ dxdy$

Fluid efflux (rate of mas of fluid leaving the face ABFE) through ABFE =

$$\rho\ w\ dxdy + \frac{\partial}{\partial z}(\rho\ w\ dxdy)dz \tag{1.10}$$

Gain in mass per unit time in z-direction = Fluid influx - Fluid efflux =

$$\rho\ w\ dxdy - (\rho\ w\ dxdy + \frac{\partial}{\partial z}(\rho\ w\ dz)dxdy) \tag{1.11}$$

Net mass gain in fluid along the three axes =

$$-\left[\frac{\partial \rho u}{\partial x} + \frac{\partial \rho v}{\partial y} + \frac{\partial \rho w}{\partial z}\right] dxdydz \tag{1.12}$$

The total mass gain must equal to the rate of mass decrease within the control volume, which is given as

$$\frac{\partial \rho}{\partial t} dxdydz \tag{1.13}$$

that is, equation (1.12) must be equal to equation (1.13), this yields

$$-\left[\frac{\partial \rho u}{\partial x} + \frac{\partial \rho v}{\partial y} + \frac{\partial \rho w}{\partial z}\right] dxdydz = \frac{\partial \rho}{\partial t} dxdydz \tag{1.14}$$

Simplifying, we have

$$\frac{\partial \rho u}{\partial x} + \frac{\partial \rho v}{\partial y} + \frac{\partial \rho w}{\partial z} + \frac{\partial \rho}{\partial t} = 0 \tag{1.15}$$

The equation above is a three dimensional continuity equation for both compressible and incompressible fluid. If the density is constant, that is $\frac{\partial \rho}{\partial t} = 0$, we obtain

$$\frac{\partial u}{\partial x} + \frac{\partial v}{\partial y} + \frac{\partial w}{\partial z} = 0 \tag{1.16}$$

which is the continuity equation for incompressible fluids. For 2-dimensional continuity equation (x and y directions where $w = 0$), we obtain

$$\frac{\partial u}{\partial x} + \frac{\partial v}{\partial y} = 0 \tag{1.17}$$

For one-dimensional continuity equation (x direction, $v = w = 0$), we have

$$\frac{\partial u}{\partial x} = 0 \tag{1.18}$$

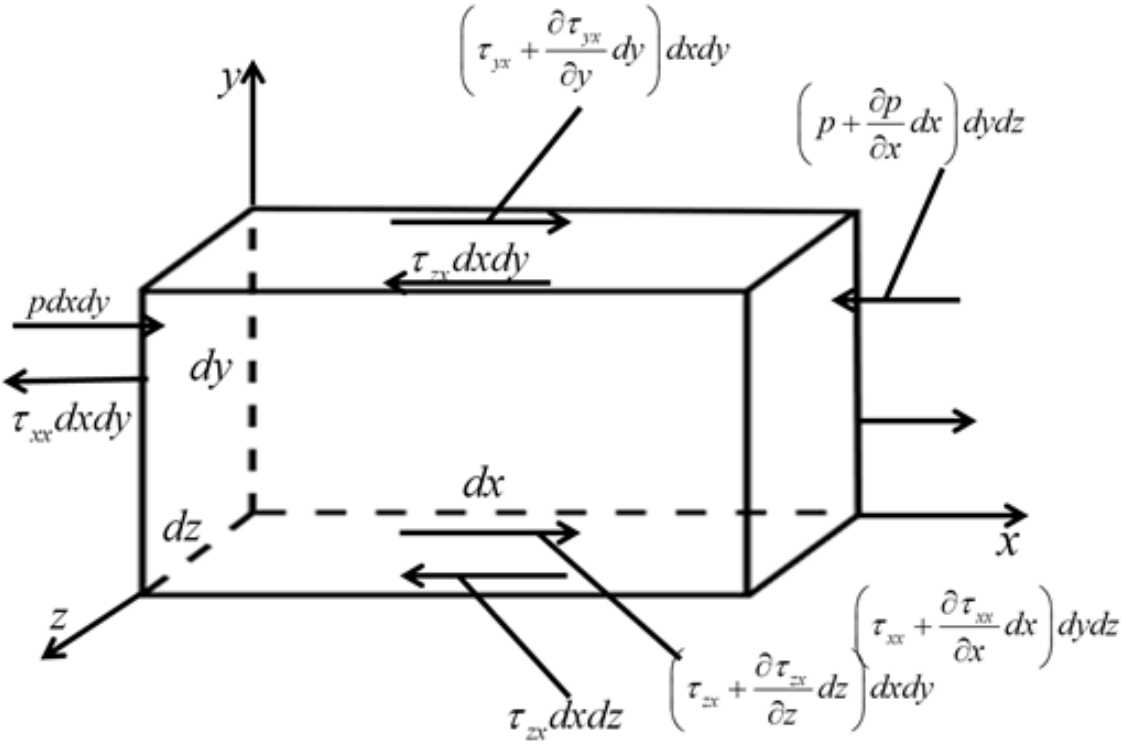

Figure 1.4: Infinitesimally small, moving fluid element(Wendt, 2009)

1.2.2 Momentum Equation

Navier-Stoke equations are non-linear partial differential equations with time and space dependency. The equations describe the flow of a fluid whose stress depends linearly on velocity and pressure. The principle of Newton's second law of motion is applied to derive the Navier-Stoke equation.

$$F = ma \tag{1.19}$$

where F = force, m = mass, a = acceleration. According to Newton's second law in equation (1.19) the net force on fluid element equals its mass times the acceleration of the element.

The x-component of equation (1.19) is given as:

$$F_x = ma_x \tag{1.20}$$

where F_x and a_x are the force and acceleration components in the x-direction. The force comprises the body forces and the surface forces. Body forces are forces like gravitational force which acts directly on the volumetric mass of the fluid element. If we denote the body force per unit mass acting on the fluid element by f and f_x as the components of this force in the x-direction, we get the body force on the fluid element acting in the x-direction as:

$$\rho\ f_x\ dxdydz \tag{1.21}$$

where $dxdydz$ is the volume of the fluid element. From this discussion and Figure 1.5. Net surface force in the x-direction =

$$\left[p - (p + \frac{\partial p}{\partial x}dx)\right]dydz + \left[(\tau_{xx} + \frac{\partial \tau_{xx}}{\partial x}dx - \tau_{xx}\right]dydz + \left[(\tau_{yx} + \frac{\partial \tau_{yx}}{\partial y}dy) - \tau_{yx}\right]dxdz + \left[(\tau_{zx} + \frac{\partial \tau_{zx}}{\partial z}dz) - \tau_{zx}\right]dxdy \tag{1.22}$$

Simplifying equation , we have

$$F_x = \left(-\frac{\partial p}{\partial x} + \frac{\partial \tau_{xx}}{\partial x} + \frac{\partial \tau_{yx}}{\partial y} + \frac{\partial \tau_{zx}}{\partial z} \right) dxdydz + \rho\, f_x\, dxdydz \tag{1.23}$$

Writing

$$m = \rho dxdydz \tag{1.24}$$

The substantial derivative is given as

$$a_x = \frac{Du}{Dt} \tag{1.25}$$

Using equations (1.23)-(1.25) in equation (1.20) gives

$$\rho \frac{Du}{Dt} = -\frac{\partial p}{\partial x} + \frac{\partial \tau_{xx}}{\partial x} + \frac{\partial \tau_{yx}}{\partial y} + \frac{\partial \tau_{zx}}{\partial z} + \rho f_x \tag{1.26}$$

In this way we can obtain y- and z-components as

$$\rho \frac{Du}{Dt} = -\frac{\partial p}{\partial y} + \frac{\partial \tau_{xy}}{\partial x} + \frac{\partial \tau_{yy}}{\partial y} + \frac{\partial \tau_{zy}}{\partial z} + \rho f_y \tag{1.27}$$

$$\rho \frac{Du}{Dt} = -\frac{\partial p}{\partial z} + \frac{\partial \tau_{xz}}{\partial x} + \frac{\partial \tau_{yz}}{\partial y} + \frac{\partial \tau_{zz}}{\partial z} + \rho f_z \tag{1.28}$$

Equations (1.26)-(1.28) are the x-, y- and z-components non-conservation forms of the momentum equations.

To derive the conservation form of the momentum equations, the left hand side of equation (1.26) is written using the definition of the substantial derivative:

$$\rho \frac{Du}{\partial t} = \rho \frac{\partial u}{Dt} + \rho V \cdot \nabla u \tag{1.29}$$

but

$$\frac{\rho(\partial u)}{\partial t} = \rho\frac{\partial u}{\partial t} + u\frac{\partial \rho}{\partial t} \Rightarrow \rho\frac{\partial u}{\partial t} = \frac{\partial(\rho u)}{\partial t} - u\frac{\partial \rho}{\partial t} \tag{1.30}$$

and

$$\nabla \cdot (\rho u V) = u\nabla \cdot (\rho V) + (\rho V) \cdot \nabla u \tag{1.31}$$

or

$$\rho V \cdot \nabla u = \nabla \cdot (\rho u V) - u\nabla \cdot (\rho V) \tag{1.32}$$

Then equation (1.29) becomes

$$\rho\frac{Du}{Dt} = \frac{\partial(\rho u)}{\partial t} - u\frac{\partial \rho}{\partial t} - u\nabla \cdot (\rho V) + \nabla \cdot (\rho u V) \tag{1.33}$$

$$\rho\frac{Du}{Dt} = \frac{\partial(\rho u)}{\partial t} - u\left|\frac{\partial \rho}{\partial t} + \nabla \cdot (\rho V)\right| + \nabla \cdot (\rho u V) \tag{1.34}$$

and from the continuity equation

$$\rho\frac{Du}{Dt} = \frac{\partial(\rho u)}{\partial t} + \nabla \cdot (\rho u V) \tag{1.35}$$

The momentum equations (1.26)-(1.28) can then be written in conservation form as

$$\frac{\partial(\rho u)}{\partial t} + \nabla \cdot (\rho u V) = -\frac{\partial p}{\partial x} + \frac{\partial \tau_{xx}}{\partial x} + \frac{\partial \tau_{yx}}{\partial y} + \frac{\partial \tau_{zx}}{\partial z} + \rho f_x \tag{1.36}$$

$$\frac{\partial(\rho p)}{\partial t} + \nabla \cdot (\rho u V) = -\frac{\partial p}{\partial y} + \frac{\partial \tau_{xy}}{\partial x} + \frac{\partial \tau_{yy}}{\partial y} + \frac{\partial \tau_{zy}}{\partial z} + \rho f_y \tag{1.37}$$

$$\frac{\partial(\rho u)}{\partial t} + \nabla \cdot (\rho u V) = -\frac{\partial p}{\partial z} + \frac{\partial \tau_{xz}}{\partial x} + \frac{\partial \tau_{yz}}{\partial y} + \frac{\partial \tau_{zz}}{\partial z} + \rho f_z \tag{1.38}$$

Suppose the fluid is Newtonian, that is, the shear stresses on the fluid element layer are directly proportional to the rate of shear strain. Then the shear stresses are written as

$$\tau_{xx} = \eta\nabla \cdot V + 2\mu\frac{\partial u}{\partial x}, \tau_{yy} = \eta\nabla \cdot V + 2\mu\frac{\partial v}{\partial x}, \tau_{zz} = \eta\nabla \cdot V + 2\mu\frac{\partial w}{\partial x} \tag{1.39}$$

$$\tau_{xy} = \tau_{yx} = \mu\left(\frac{\partial v}{\partial x}+\frac{\partial u}{\partial y}\right), \tau_{xz} = \tau_{zx} = \mu\left(\frac{\partial u}{\partial z}+\frac{\partial w}{\partial x}\right), \tau_{yz} = \tau_{zy} = \mu\left(\frac{\partial w}{\partial y}+\frac{\partial v}{\partial z}\right) \tag{1.40}$$

where μ is the molecular viscosity coefficient and $\eta = \frac{2}{3}\mu$ is the bulk viscosity coefficient. Using the above in equations (1.36)-(1.38) yields

$$\begin{aligned}\frac{\partial(\rho u)}{\partial t} + \frac{\partial(\rho u^2)}{\partial x} + \frac{\partial(\rho uv)}{\partial y} + \frac{\partial(\rho uw)}{\partial z} = -\frac{\partial p}{\partial x} + \\ \frac{\partial}{\partial x}\left(\eta\nabla \cdot V + 2\mu\frac{\partial u}{\partial x}\right) + \frac{\partial}{\partial y}\left|\mu(\frac{\partial v}{\partial x} + \frac{\partial u}{\partial y})\right| + \\ \frac{\partial}{\partial z}\left|\mu(\frac{\partial u}{\partial z} + \frac{\partial w}{\partial x})\right| + \rho f_x\end{aligned} \tag{1.41}$$

$$\begin{aligned}\frac{\partial(\rho v)}{\partial t} + \frac{\partial(\rho uv)}{\partial x} + \frac{\partial(\rho v^2)}{\partial y} + \frac{\partial(\rho vw)}{\partial z} = -\frac{\partial p}{\partial y} + \\ \frac{\partial}{\partial x}\left|\mu\left(\frac{\partial v}{\partial x} + \frac{\partial u}{\partial y}\right)\right| + \frac{\partial}{\partial y}\left(\eta\nabla \cdot V + 2\mu\frac{\partial v}{\partial x}\right) + \\ \frac{\partial}{\partial z}\left|\mu\left(\frac{\partial w}{\partial y} + \frac{\partial v}{\partial z}\right)\right| + \rho f_y\end{aligned} \tag{1.42}$$

$$\begin{aligned}\frac{\partial(\rho w)}{\partial t} + \frac{\partial(\rho uw)}{\partial x} + \frac{\partial(\rho vw)}{\partial y} + \frac{\partial(\rho w^2)}{\partial z} = -\frac{\partial p}{\partial z} + \\ \frac{\partial}{\partial x}\left|\mu\left(\frac{\partial u}{\partial z} + \frac{\partial w}{\partial x}\right)\right| + \frac{\partial}{\partial y}\left|\mu\left(\frac{\partial w}{\partial y} + \right.\right. \\ \left.\left.\frac{\partial v}{\partial z}\right)\right| \frac{\partial}{\partial z}\left(\eta\nabla \cdot V + 2\mu\frac{\partial w}{\partial x}\right) + \rho f_z\end{aligned} \tag{1.43}$$

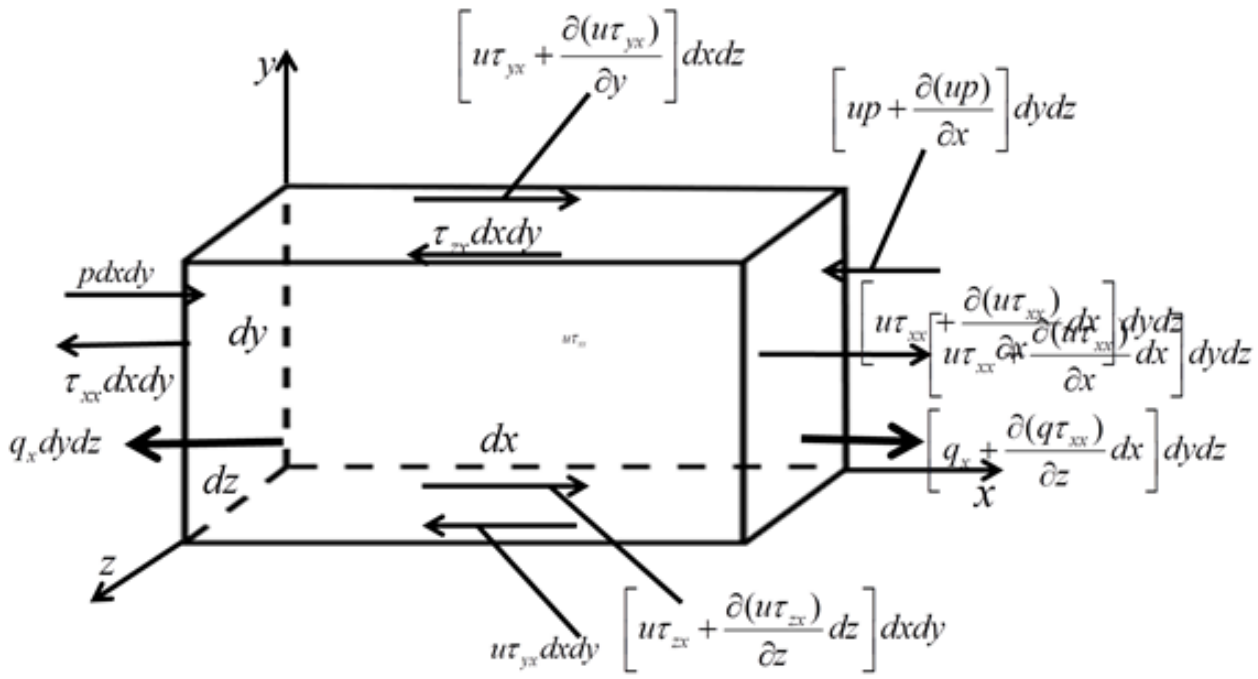

Figure 1.5: Energy fluxes associated with an infinitesimally small, moving fluid element (Wendt, 2009)

1.2.3 Energy Equation

The law of conservation of energy (the first law of thermodynamics) is applied here to derive energy equation. The law states that the sum of work and heat added to a system will always equal to the increase of energy,

{Rate of change of energy inside the fluid element} = {Net flux of heat into fluid element} + { Rate of work done on the element due to body and surface forces}

The rate of work done by the body force acting on the fluid element moving at a velocity V is given by ρ F $\cdot$ V dV = ρ F $\cdot$ V $dxdydz$

In Figure 1.6, the work done by pressure and shear stresses in the x-, y- and z-directions add up to

$$\left| -\frac{\partial(up)}{\partial x} + \frac{\partial(u\tau_{xx})}{\partial x} + \frac{\partial(u\tau_{yx}}{\partial y} + \frac{\partial(u\tau_{zx}}{\partial z} \right| dxdydz \tag{1.44}$$

$$\left| -\frac{\partial(vp)}{\partial y} + \frac{\partial(v\tau_{xy}}{\partial x} + \frac{\partial(v\tau_{yy}}{\partial y} + \frac{\partial(v\tau_{zy}}{\partial z)} \right| dxdydz \tag{1.45}$$

$$\left| -\frac{\partial(wp)}{\partial z} + \frac{\partial(w\tau_{xz})}{\partial x} + \frac{\partial(w\tau_{yz}}{\partial y} + \frac{\partial(w\tau_{zz})}{\partial z} \right| dxdydz \tag{1.46}$$

The total, net rate of work done on the moving fluid element is given as

$$\begin{aligned} &\left| -(\frac{\partial(up)}{\partial x} + \frac{\partial(vp)}{\partial y} + \frac{\partial(wp)}{\partial z}) + \frac{\partial(u\tau_{xx})}{\partial x} + \right. \\ &\frac{\partial(u\tau_{yx})}{\partial y} + \frac{\partial(u\tau_{zx})}{\partial z} + \frac{\partial(v\tau_{xy})}{\partial x} + \frac{\partial(v\tau_{yy})}{\partial y} + \frac{\partial(v\tau_{zy})}{\partial z} + \\ &\left. \frac{\partial(w\tau_{xz})}{\partial x} + \frac{\partial(w\tau_{yz})}{\partial y} + \frac{\partial(w\tau_{zz})}{\partial z} \right| dxdydz + \rho F \cdot V dxdydz \end{aligned} \tag{1.47}$$

The volumetric heating of the element is $\rho\, q\, dxdydz$, where q is the rate of volumetric heat addition per unit mass. The net heat transferred in the x-direction into the fluid

element by thermal conduction is given as

$$\left|(q_x(q_x + \frac{\partial q_x}{\partial x}dx)\right|dydz = -\frac{\partial q_x}{\partial x}dxdydz \tag{1.48}$$

Adding this to similar expressions for the y- and z-directions to give the total heat of the fluid element by thermal induction as

$$-\left(\frac{\partial q_x}{\partial x} + \frac{\partial q_y}{\partial y} + \frac{\partial q_z}{\partial z}\right)dxdydz \tag{1.49}$$

Combining this with volumetric heating of the fluid element, gives
Net flux of heat into the element =

$$\left|\rho q - \left(\frac{\partial q_x}{\partial x} + \frac{\partial q_y}{\partial y} + \frac{\partial q_z}{\partial z}\right)dxdydz\right| \tag{1.50}$$

substituting $q_x = -k\frac{\partial T}{\partial x}; q_y = -k\frac{\partial T}{\partial y}; q_z = -k\frac{\partial T}{\partial z}$ where k is the thermal conductivity, into equation (1.50), yields

Net flux of heat into the element =

$$\left[\rho q + \frac{\partial}{\partial x}\left(k\frac{\partial T}{\partial x}\right) + \frac{\partial}{\partial y}\left(k\frac{\partial T}{\partial y}\right) + \frac{\partial}{\partial z}\left(k\frac{\partial T}{\partial z}\right)\right]dxdydz \tag{1.51}$$

{ Rate of change of energy inside the fluid element } =

$$\rho\frac{D}{Dt}\left(E + \frac{V^2}{2}\right)dxdydz \tag{1.52}$$

where E is the internal energy per unit mass and $\frac{V^2}{2}(V^2 = u^2+v^2+w^2)$, is the kinetic energy per unit mass. The energy equation can then be written as

$$\rho\frac{D}{Dt}\Big(E+\frac{V^2}{2}\Big)=\rho q+\frac{\partial}{\partial x}\Big(k\frac{\partial T}{\partial x}\Big)+\frac{\partial}{\partial y}\Big(k\frac{\partial T}{\partial y}\Big)+\frac{\partial}{\partial z}\Big(k\frac{\partial T}{\partial z}\Big)-\left(\frac{\partial(up)}{\partial x}-\frac{\partial(vp)}{\partial y}-\frac{\partial(wp)}{\partial z}\right)+\frac{\partial(u\tau_{xx})}{\partial x}+\frac{\partial(u\tau_{yx})}{\partial y}+\frac{\partial(u\tau_{zx})}{\partial z}+\frac{\partial(v\tau_{xy})}{\partial x}+\frac{\partial(v\tau_{yy})}{\partial y}+\frac{\partial(v\tau_{zy})}{\partial z}+\frac{\partial(w\tau_{xz})}{\partial x}+\frac{\partial(w\tau_{yz})}{\partial y}+\frac{\partial(w\tau_{zz})}{\partial z}\rho F\cdot V \tag{1.53}$$

Replacing the viscous stress terms with their equivalent expression gives the energy equation (1.53) in terms of the flow field variables, to obtain

$$\rho\frac{D}{Dt}=\rho q+\frac{\partial}{\partial x}\Big(k\frac{\partial T}{\partial x}\Big)+\frac{\partial}{\partial y}\Big(k\frac{\partial T}{\partial y}\Big)+\frac{\partial}{\partial z}\Big(k\frac{\partial T}{\partial z}\Big)-p\left(\frac{\partial(u)}{\partial x}-\frac{\partial(v)}{\partial y}-\frac{\partial(w)}{\partial z}\right)+\eta\left(\frac{\partial(u)}{\partial x}-\frac{\partial(v)}{\partial y}-\frac{\partial(w)}{\partial z}\right)+\left|2\Big(\frac{\partial(u)}{\partial x}\Big)^2+2\Big(\frac{\partial(v)}{\partial y}\Big)^2+\Big(\frac{\partial(u)}{\partial y}+\frac{\partial(v)}{\partial x}\Big)^2+\Big(\frac{\partial(u)}{\partial y})+\frac{\partial(w)}{\partial x}\Big)^2+\Big(\frac{\partial(v)}{\partial z}+\frac{\partial(w)}{\partial y}\Big)^2\right| \tag{1.54}$$

The conservation form of the energy equation (1.54) can be written as

$$\rho\frac{\rho E}{Dt}+\nabla\cdot(\rho Ev)=\rho q+\frac{\partial}{\partial x}\Big(k\frac{\partial T}{\partial x}\Big)+\frac{\partial}{\partial y}\Big(k\frac{\partial T}{\partial y}\Big)+\frac{\partial}{\partial z}\Big(k\frac{\partial T}{\partial z}\Big)-p\left(\frac{\partial(u)}{\partial x}-\frac{\partial(v)}{\partial y}-\frac{\partial(w)}{\partial z}\right)+\eta\left(\frac{\partial(u)}{\partial x}-\frac{\partial(v)}{\partial y}-\frac{\partial(w)}{\partial z}\right)+\mu\left|2\Big(\frac{\partial(u)}{\partial x}\Big)^2+2\Big(\frac{\partial(v)}{\partial y}\Big)^2+\left(\frac{\partial(u)}{\partial y}+\frac{\partial(v)}{\partial x}\right)^2+\left(\frac{\partial(u)}{\partial y})+\frac{\partial(w)}{\partial x}\right)^2+\left(\frac{\partial(v)}{\partial z}+\frac{\partial(w)}{\partial y}\right)^2\right| \tag{1.55}$$

1.3 Statement of the Problem

Studies of electrically conducting fluids in porous channels are important areas of research due to their broad applications in Magnetohydrodynamic generators, ship propulsion, fusion reactors, electrolysis and astrophysics. Although several studies on electrically conducting fluids have been investigated in various fluid flows such as: second grade fluid (Olanrewaju *et al.*, 2016), third grade fluid (Hayat *et al.*, 2015), nanofluid (Das *et al.*, 2015), Jeffrey fluid (Noreen *et al.*, 2013), Eyring Powell fluid (Jawad *et al.*, 2015), Sisko fluid (Awaisa *et al.*, 2017), couple stress fluid and the likes, entropy generation of electrically conducting couples stress fluid has not been given due attention. It is worth pointing out that a few recent investigations in this area are channelled towards the effects of Brinkman number, Prandtl number, suction/injection and Biot numbers.

Consequently, this study considers entropy generation of MHD couple stress fluid which has been neglected. Furthermore, the analysis is carried out under the following flow configurations viz: porous channel, porous medium and vertical porous medium. In addition, the effects of other important parameters on the entropy generation of hydromagnetic couple stress fluid like velocity slip, temperature jump and thermal radiation are incorporated. Two semi-analytical techniques namely; Adomian Decomposition Method and Differential Transform Method are used for the analysis.

1.4 Aim and Objectives

The aim of this study is to investigate the influence of magnetohydrodynamic, Ohmic heating, porosity, buoyancy force, slip velocity, temperature jump and thermal radiation on entropy generation rate in the flow of couple stress fluid through porous channel and porous medium. The specific objectives are to:

(i) analyse the influence of magnetic field on couple stress flow through porous channel with entropy generation;

(ii) apply second law of thermodynamics for the analysis of hydromagnetic couple stress fluid through a channel filled with non-Darcian porous medium;

(iii) investigate the inherent irreversibiliy in a buoyancy induced MHD couple stress fluid;

(iv) investigate the combined effects of velocity slip and temperature jump on entropy generation of radiative reactive hydromagnetic couple stress fluid through vertical porous medium and

(v) compare the results with the existing method in literature.

1.5 Motivation

Heat transfer by convection process within the channel is irreversible, as a result, entropy generation is continuous due to energy and momentum exchange which occurs within the flow channel, and this can significantly alter the success of the desired goal in engineering processes. This is due to the fact that increased entropy generation rate translates into destruction of the available energy for work. According to Arikoglu *et al.* (2008) all processes that produce, convert and consume energy must be re-examined very carefully and all available-work destruction mechanisms be removed.

In view of the above, entropy generation analysis of electrically conducting couple stress fluid was considered in this study due to its enormous applications in engineering processes. This is to ensure all forms of exergy wastage involved in the application of MHD couple stress fluid are removed or reduced.

In addition, the rapidly convergent Adomian decomposition and differential transform techniques applied in this research have not been fully explored. However, few authors who have employed these techniques in solving boundary value problems arising from fluid flows are: Gbadeyan and Hassan (2012); Adesanya (2014); Adesanya *et al.* (2015); Hassan and Gbadeyan (2014) and Rashidi *et al.* (2011). Application of

these methods in other areas are noted in the works of Adesanya *et al.* (2013); Hassan (2008); Opanuga *et al.* (2015a); Opanuga *et al.* (2015b); Opanuga *et al.* (2016).

1.6 Justification for Research

The influence of magnetic field on the flow of thermal structure has received greater attention due to its important applications in numerous areas. This study will enhance safety of lives and properties during the application of reactive MHD couple stress fluids and reduce entropy production which arises due to Ohmic heating present in such flows.

In view of the foregoing, critical analysis of irreversibility associated with MHD couple stress fluid and reactive MHD couple stress fluid will assist in achieving such a goal.

1.7 Significance of the Study

There has been a renewed interest in the study of the factors responsible for entropy generation due to its destructive effect. This research will therefore provide insight into the causes of irreversibility on MHD couple stress fluid. Moreover, it will enable scientists and engineers to maximise the use of this type of fluid and hence reduce these losses.

1.8 Scope of Research

This study considered entropy generation of MHD couple stress fluid through porous channel, porous medium and vertical porous medium. The effect of convective heating, velocity slip, temperature jump boundary conditions as well as thermal radiation are analysed. Two semi-analytical techniques are applied in this analysis because of their rapid convergence and less computational involvement.

1.9 Limitation

Cylindrical and rotational flow geometries are not considered in this study due to time constraint.

1.10 Delimitation

This research is limited to the following:

(i) steady case of the models are considered;

(ii) the flow geometries include horizontal and vertical channels since these are the two broad categories of flow geometries due to the applications in ;

(iii) both porous and highly porous medium are analysed due to their applications in earth science, energy science, and many other areas.

1.11 Definition of Terms

In this section various terms used in this study are defined;

Definition 1.11.1 (**Viscosity**): Viscosity refers to fluid thickness. It is the resistance to the sliding motion of one fluid layer over the other (Sabersky *et al.*, 1999). Alternatively, it is defined as fluid property that determines its resistance to shearing stresses (Rajput, 2004). The relationship between viscosity and temperature differ from liquid to gas. In liquid, increase in temperature reduces the viscosity because molecules separate from each other, which decreases the attraction. In the case of gas, increase in temperature increases the molecular mixing, that is, it increases the cohesion and momentum exchange between the layers of gases, thereby increasing the viscosity of gaseous molecules (Nakayama and Boucher, 1999).

Definition 1.11.2 (**Newtonian Fluids**): These are fluids that obey the Newtonian's law which states that, "the shear stress (τ) on a fluid element layer is directly

proportional to the rate of shear strain". The constant of proportionality is referred to as the coefficient of viscosity that is,

$$\tau \alpha \frac{du}{dy} \Rightarrow \tau = \mu \frac{du}{dy} \tag{1.56}$$

where (μ) is the proportionality constant (Rajput, 2004). Examples of Newtonian fluids include water, gasoline, air, etc. Newtonian fluids do not change their viscosity when under stress. Fluid viscosity depends on temperature and pressure and not on the forces that act upon it.

Definition 1.11.3 (**Non-Newtonian Fluids**): These are fluids that do not follow the linearity between the shear stress and deformation rate. When non-Newtonian fluids are stressed their viscosity varies that is, they behave strangely either by becoming thicker or thinner. Some of these fluids behave either as a result of the applied stress or the length of time the stress is applied. They can be categorized into four viz:

(i) **Rheopetic**: These types of fluids become more viscous as they are stressed over a period of time. For example Cream (viscosity increases over a period of time).

(ii) **Thixotropic**: These fluids become less viscous as they are stressed over a period of time for example honey.

(iii) **Dilatant**: These fluids change their viscosity based on how much force is applied. They tend to become more viscous when more force is applied, for example Oobleck (viscosity increases with increased stress).

(iv) **Pseudoplastic**: They become less viscous when more force is applied for example Tomato ketchup (viscosity decreases with increase in stress)

Definition 1.11.4 (**Porous Channel**): Porous channel consists of a passage with permeable walls. They are built of solid matrix with pores. The walls are connected

together to allow the passage of fluids. Porous channel has applications in agriculture (irrigation, land drainage), geothermal system, microelectric heat transfer, grain storage and action of kidney.

Definition 1.11.5 (**Porous Medium**): This is a material that consists of a solid matrix with interconnected pores. The solid material is either rigid or it undergoes small deformation. Fluids flow through the material is due to the interconnectedness of the pores. Rye bread, beach sand, limestone, sandstone,wood and the human lung are some of the examples of natural porous media (Nield and Bejan, 2006) See Figure 1.6.

Definition 1.11.6 (**Thermal Diffusivity**): Thermal diffusivity is the ratio of a material thermal energy conduction to its thermal energy storage. Mathematically it can be expressed as in equation (1.57):

$$\alpha = \frac{k}{(\rho C_p)} \tag{1.57}$$

where α, k, ρ and C_p are the thermal diffusivity, thermal conductivity, density and the specific heat at a constant pressure respectively.

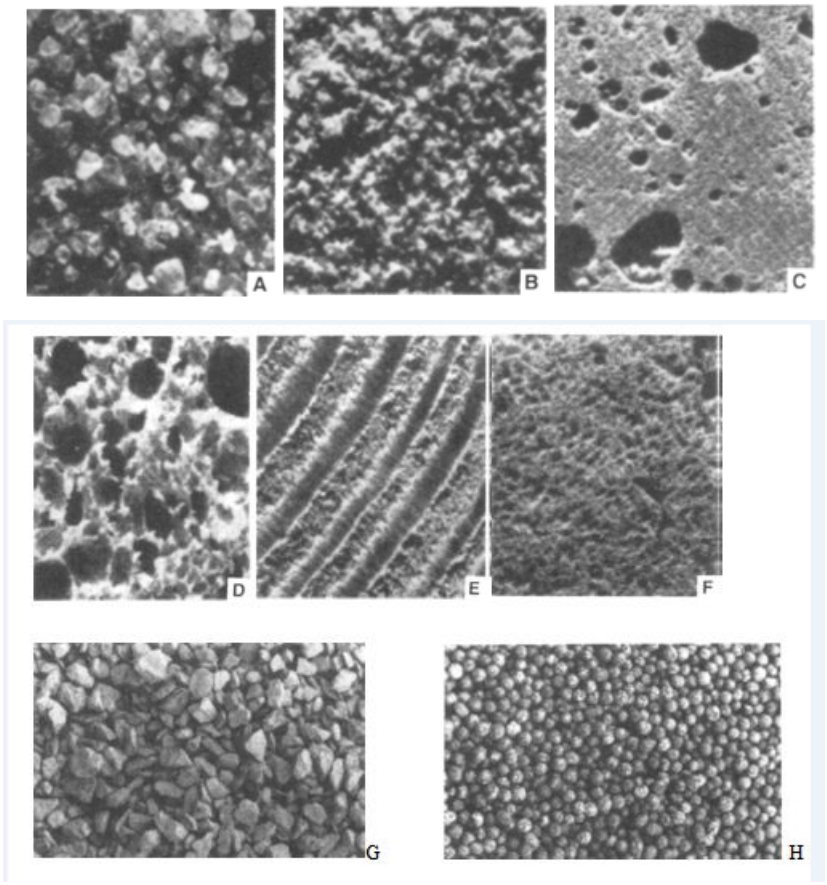

Figure 1.6: Application of Porous Medium, (Collins, 1961; Bejan, 1984)

(A) Beach Sand, (B) Sandstone, (C) Limestone, (D) Rye Bread, (E) Wood, (F) Human Lung, (G) Granular porous materials used in the construction and (H) Crushed Limestone

Definition 1.11.7 (**First Law of thermodynamics**): It is the statement of law of conservation of energy, that energy can neither be created nor destroyed but can be converted from one form to the other. First law of thermodynamics states that energy is conserved in all thermodynamic processes. It further states that the amount of work equals the product of the external force acting on the system and the component of the displacement parallel to the force (Schetz and Fuhs, 1999). The sum of work and heat added to a system will always equal to the increase of energy as given in equation (1.58).

$$\Delta U = q + w \tag{1.58}$$

where ΔU is the total change in internal energy of a system, q is the heat exchanged between a system and its surroundings and w is the work done by or on the system.

Definition 1.11.8 (**Second Law of Thermodynamics**): The second law states that during any reaction the total useful energy in the universe will decrease. It further states that a useful state variable called entropy S exists. The change in entropy delta S is equal to the ratio of heat transfer delta Q to the temperature T, that is,

$$\delta S = \frac{\delta Q}{T} \tag{1.59}$$

The second law is a statement of inequalities. It is also an expression of the impossibility of a process occurring. By first law such a process will possibly occur. Second law of thermodynamics can be stated that during the process of converting one form of energy into another, identical quantities of the energy are involved regardless of the feasibility of the process. In other form, second law states that in any irreversible physical process, there is an increase in both the entropy of the system and the environment. It has been experimentally confirmed that when energy (heat energy) is transferred to a system, only a portion of heat can be converted to work. The above definition leads to other two terms, entropy and exergy. The entropy of a system is

the degree of its disorderliness. It represents the unavailability of a system's thermal energy for conversion into mechanical work, while exergy is the available energy for conversion into work. The conclusion here is that a thorough knowledge of the irreversibility process will help in minimizing entropy and maximizing the conversion of energy to useful work in engineering processes (Noor *et al.*, 2012).

Definition 1.11.9 (**Entropy Generation**): Entropy production determines the performance of thermal machines such as power plants, heat engines, refrigerators, heat pumps, and air conditioners. It is the measure of the irreversibility that is associated with the real processes. As entropy generation occurs, the available energy (that is, exergy) reduces. To preserve the available energy in a fluid flow process or at least to reduce the irreversibility, it is necessary to investigate entropy generation distribution within the fluid volume. Minimizing entropy generation in systems is the only means by which optimal performance of machine can achieved. Many studies have been published to determine the factors responsible for irreversibility in components and systems. Bejan (1982) analysed the irreversibility for forced convective heat transfer due to temperature gradient and viscosity effect in a fluid. He equally presented some factors that cause entropy generation in applied thermal engineering. According to Bejan (1996), the general equation for the entropy generation per unit volume is given by:

$$S^m = \frac{k}{T_w^2}(\nabla T)^2 + \frac{\mu}{T_w}\Phi \tag{1.60}$$

the first term in the equation is the entropy generation due to heat transfer while the second term is the viscous dissipation irreversibility. k is thermal conductivity, T is fluid temperature, μ is the dynamic viscosity and Φ is the irreversibility ratio.

Definition 1.11.10 (**Buoyancy Force**): An object is submerged when a fluid exerts a force on it. Such a force due to a fluid in equilibrium is known as the buoyancy or the upthrust. Buoyancy forces occur due to variations of density in a fluid subject to

gravity (Turner, 1973). The weight of the displaced volume of fluid and the buoyance has the same magnitude. Buoyancy is very important in many engineering application such as in the designing of ships, boats, buoys and so on.

Definition 1.11.11 (**No-Slip Condition**): In fluid dynamics, the no-slip condition for all viscous fluids states that at a solid boundary, fluid assumes the velocity of the boundary. Velocity of fluid at all fluid-solid boundaries is equal to that of the solid boundary (Michael, 1990). Particles that are close to a surface do not flow along with other fluid, this occurs when the forces of adhesion is stronger than forces of cohesion. At the fluid-solid interface, the attractive force between the fluid particles and solid particles (that is forces of adhesion) is greater than the forces between the particles of fluid (forces of cohesion). The imbalance between the two forces reduces the fluid velocity to zero. A common approximation for fluid slip is:

$$u - u_{wall} = \beta \frac{\partial u}{\partial \eta} \tag{1.61}$$

where η is the coordinate normal to the wall and β is called the slip length. For an ideal gas, the slip length is often approximated as $\beta \approx 1.15l$ where l is the mean free path (David *et al.*, 1992).

Definition 1.11.12 (**Prandlt Number**): The Prandtl number (Pr) is the measure of the momentum diffusivity (kinematic viscosity) divided by the thermal diffusivity. Low Pr indicates strong conductive transfer whereas high Pr indicates strong convective transfer (Chandra and Chhabra, 2012).

Mathematically,

$$Pr = \frac{v}{k} = \frac{\frac{\eta}{\rho}}{\frac{\lambda}{\rho C_p}} = \frac{\eta C_p}{\lambda} \tag{1.62}$$

where v is kinematic viscosity and k is thermal diffusivity

Definition 1.11.13 (**Frank-Kamenetskii Parameter**): The Frank-Kamenetskii parameter (λ) is a measure of how reactive the gases or reactants are, what the dimensions of the system involved, and the effect of ambient temperature on the

Table 1.1: Typical values of Prandtl number

Material	Pr
Gases	0.7-1.0
Air 20°C	0.71
Water	1.7-13.7
Oils	50-100,000

system.

Definition 1.11.14 (**Ohmic Heating**): Ohmic heating, also known as Joule heating and resistive heating, is the process by which heat is released during the passage of an electric current through a conductor. The amount of heat released is in direct proportion to the square of the current such that.

$$H \propto I^2 \cdot R \cdot t \tag{1.63}$$

Equation (1.63) represents Joule's first law or Joule-Lenz law. Joule heating affects the whole electric conductor, unlike the Peltier effect which transfers heat from one electrical junction to another (Singh and Kumar, 1996).

1.12 Organisation of the Study

The rest of the thesis is organised as follows: Chapter two focuses on the review of related literature. The review examines previous studies with the view to identifying gaps and determining the gaps this current study would fill. In chapter three, analysis of the two methods applied in this study are presented together with model formulation and solution procedure. Chapter four presents the results as well as the detailed discussion of results. Finally, chapter five concludes the study, while summarising and offering recommendations for further study.

CHAPTER TWO

LITERATURE REVIEW

2.1 Introduction

The study of magnetohydrodynamics flow has received much attention in the past years owing to its applications in MHD generators, plasma studies, nuclear reactor, geothermal energy extractions, purifications of metal from non-metal enclosures, polymer technology and metallurgy. Magnetic fields produce many complex phenomena in magnetohydrodynamic flows such as Hall currents, ion slip effects (at higher strength magnetic fields), Joule (Ohmic) heating, Alfven waves in plasma flows, etc. (Cramer and Pai, 1973). Such effects can have a significant effect on heat transfer and flow dynamics. For instance in ionized gases having low density and strong magnetic field, the electrical conductivity perpendicular to the magnetic field is reduced due to free spiraling of electrons and ions about the magnetic lines of force prior to collisions; a current is thereby induced which is mutually perpendicular to both electrical and magnetic fields, constituting the Hall current effect. (Beg *et al.*, 2009).

One of the earliest attempts to understand MHD was the Faraday's famous experiment of 1832 on Waterloo Bridge, which was intended to detect tidal motion in River Thames by electromagnetic induction. Such experiment is not an MHD experiment, since the dynamical effect of the field on the motion is negligible and is not included. The main origin of MHD dates back to pioneering discoveries of Northrup, Hartmann, Alfven, and others in the early twentieth century. After 1950, the subject witnessed rapid development and soon became a well established field of scientific endeavour in various contexts: These include geomagnetism and planetary magnetism, astrophysics, nuclear fusion (plasma) physics, liquid metal technology and so on (Molokov *et al.*, 2007).

2.2 Review of Related Literature

2.3 Magnetohydrodynamic

Batchelor (1949) investigated on the spontaneous magnetic field in a conducting liquid in turbulent motion. Alfven (1956) presented the Sun's general magnetic field, submitting that all the fine structure of the corona is given by the magnetic field, Chang and Lundgren (1961) studied the duct flow in magnetohydrodynamics, (Moffatt, 1970) considered the Turbulent dynamo action at low magnetic Reynolds number while Hunt and Shercliff (1971) investigated magnetohydrodynamics at high Hartmann number. Some extremum principles for pipe flow in magnetohydrodynamics was presented by Smith (1972), who argued that with appropriate choices for the extrema, an asymptotic expansion for the mass-flow rate at large Hartman number can be constructed. Later, Sloan (1973) extended it to extremum principles for magnetohydrodynamic channel flow. In the work of Gupta (1972), effect of uniform magnetic field on the Eckman layer over an infinite horizontal plate at rest relative to an electrically conducting liquid rotating with uniform angular velocity about a vertical axis was considered. Rao *et al.* (1982) analyzed the combined effect of free and forced convection on MHD flow in a rotating porous channel. Seth *et al.* (1982) investigated unsteady hydromagnetic Couette flow in a rotating system. Chandran *et al.* (1992) further reported the effect of rotation on unsteady electrically conducting Couette flow, showing that increase in magnetic field increases the velocity of the fluid. Singh *et al.* (1994) considered transient effects on electrically conducting Couette flow with rotation. Singh (2000) investigated an oscillatory hydromagnetic Couette flow with transpiration. Gbadeyan *et al.* (2005) analyzed the radiative effect on electrohydrodynamic froth flow in vertical channel. Also, Gbadeyan *et al.* (2006) investigated the radiation effect of magnetohydrodynamics flow of gas between concentric spheres.

Furthermore, Patel and Kassegne (2007) considered electroosmosis and thermal effects in magnetohydrodynamic (MHD) micropumps using 3D MHD equations, Akyildiz

and Vajravelub (2008) used homotopy analysis method (HAM) to investigate MHD flow of a viscoelastic fluid and showed that magnetic field acts as an aiding force in increasing the velocity of the fluid. Beg *et al.* (2009) reported on the unsteady electrically conducting Hartmann-Couette flow and heat transfer in a Darcian channel with Hall current, ionslip, viscous and Joule heating effects, using Network Numerical Solutions (NMS), it was reported that Primary velocity decreased with a rise in Hartmann number (Ha), whereas the secondary velocity (w*) is enhanced. Furthermore, temperature (T*) is reduced significantly with the rising values of Hartmann number (Ha) which indicates that the system is cooled with stronger magnetic fields. Also, Beg *et al.* (2009) presented the numerical study of free convective MHD heat and mass transfer from a stretching surface to a saturated porous medium with soret and Dufour effects. Gbadeyan *et al.* (2010) considered the radiative effect on velocity, magnetic and temperature fields of a magnetohydrodynamic oscillatory flow past a limiting surface with variable suction. Chauhan and Rastogi (2010) researched on the radiation effects on free convection of electrically conducting fluid through a rotating vertical porous medium. Turkyilmazoglu (2011) documented some findings on the existence and limit of solutions of heat and mass transfer of MHD slip flow for the viscoelastic fluid over a stretching sheet. Also, Fang *et al.* (2009) obtained a closed form solution for slip MHD viscous fluid over a stretching sheet. Noor *et al.* (2012) used shooting method to assess the heat and mass transfer of electrically conducting thermophoretic flow over an inclined radiate isothermal permeable surface with heat source/sink, it was observed that increase in thermophoretic parameter corresponds to lower fluid flow concentration on the inclined surface. Rashidi *et al.* (2011) reported on the application of modified differential transform method (DTM) to simulate electrically conducting multi-physical flow phenomena from a rotating disk. The results showed that increase in magnetic parameter (M) suppresses radial velocity, decreases tangential velocity and elevates axial velocity.

Other studies are (Hamad and Pop, 2011) in unsteady hydromagnetic free convection flow through a vertical permeable flat plate in a rotating frame of reference with con-

stant heat source in a nanofluid. Adesanya and Makinde (2012) used Erying-Powel model to analyze heat transfer to MHD non-Newtonian couple stress pulsatile flow between two parallel porous plates. Thermal radiation effects on magnetohydrodynamic free convection heat and mass transfer from a sphere in a variable porosity regime was examined by Prasad, Vasu, Beg and Parshad (2012), they concluded that increasing porosity accelerated the flow but decreased temperatures. Mutuku-Njane and Makinde (2013) employed fourth-order Runge-Kutta together with shooting technique to study the effects of Navier slip on MHD flow of a Nanofluid through vertical porous plates with convective heating, it was submitted that increase in Grashof number decreases the fluid velocity. Singh (2013) considered the exact solution of hydromagnetic mixed convection periodic flow in a rotating vertical channel with heat radiation. Khan *et al.* (2014) studied electrically conducting boundary layer radiative, heat generating and chemical reacting flow of nanofluid. Hassan and Gbadeyan (2014) investigated thermal stability of a reactive hydromagnetic Poiseuille fluid flow through a channel. Hassan and Gbadeyan (2015) examined a reactive hydromagnetic internal heat generating fluid flow through a channel. Shehzad *et al.* (2015) considered influence of convective heat and mass conditions in MHD flow of nanofluid. Hayat *et al.* (2015) examined the effect of inclined magnetic field in flow of third grade fluid with variable thermal conductivity and submitted that higher values of magnetic field enhances the skin-friction, the temperature and concentration profiles of the fluid.

2.4 Flow through Porous Medium

Fluid flows through non-Darcian porous medium abound in many real life scenarios such as geophysical and petrochemical flows. In the recent times the application of porous media to improve convection heat transfer has been studied by many authors like Chauhan and Kumar (2009) in which the effects of slip conditions on forced convection and entropy generation in a circular channel occupied by a highly porous medium was investigated. In a related study, Jha *et al.* (2015) investigated mixed

convection in a vertical annulus filled with porous material having time-periodic thermal boundary conditions. Barletta, Magyari, Pop and Storesletten (2007) studied mixed convection with viscous dissipation in a vertical channel filled with a porous medium while Al-nimr and Khadrawl (2003) analysed transient free convection fluid flow in domains partially filled with porous media.

2.5 Flow through Vertical Channel

The study of fluid flow and heat transfer in a vertical porous channel have been given considerable attention in the past few decades due to its wide applications in areas such as the design of cooling systems for electronic devices, chemical processing equipment, microelectronic cooling and solar energy (Jamalabadi *et al.*, 2015). Numerous authors who conducted investigations on such flow include: Mutuku-Njane and Makinde (2013) who investigated the combined effects of buoyancy force and Navier slip on MHD flow of a Nanofluid over a convectively heated vertical porous plate and submitted that increase in Grashof number decreases the fluid velocity. In the work of Jamalabadi *et al.* (2015), in which optimal design of Magnetohydrodynamic mixed convection flow in a vertical channel with slip boundary conditions and thermal radiation effects was analysed by using an entropy generation minimization method. It was concluded that Grashof numbers to Reynolds number ratio are better for maximizing the exergy of the system. Adesanya and Falade (2015) presented the study on thermodynamic analysis for a third grade fluid through a vertical channel with internal heat generation, among the submissions was that increase in the Grashof number depletes the exergy level of the thermal system. In addition, heat transfer dominates the channel with increase in Grashof number. Also, Sharma *et al.* (2014) investigated radiative and free convective effects on MHD flow through a porous medium with periodic wall temperature and heat generation or absorption with the conclusion that increase in Grashof number increases the skin-friction coefficient at the wall.

2.6 Boundary Layers Flows

Boundary layers flows due has numerous applications in various industries and manufacturing processes, for example polished heart valves, polishing of internal civilities, micro-electronic mechanical systems (MEMS). Researchers have found that $Kn = 0$ which means the non-slip condition and the continuum flow assumption is valid for $Kn < 0.001$. For the range of $0.001 < Kn < 0.1$, the flow is called slip flow where Kn is the ratio of molecular mean free path λ to macrolength scale and it is given as $Kn = \frac{\lambda}{H}$. In the slip region, the standard Navier-Stokes and energy equations can still be applied by taking into account velocity slip and temperature jump at the walls (Renksizbulut *et al.*, 2006; Hooman, 2007). Navier (1823) was the first to introduce the linear slip boundary condition, it was later proposed by Maxwell (1879), which is the standard characterization of slip used in contemporary time.

Interesting research work on slip velocity and temperature jump include the following; Adesanya (2015) studied free convective flow of heat generating fluid through a porous vertical channel with velocity slip and temperature jump. Fang *et al.* (2009) gave an exact solution of Slip MHD viscous flow over a stretching sheet. Jha and Ajibade (2009) investigated free convective flow of heat generating/absorbing fluid between vertical porous plates with periodic heat input. Zhenga *et al.* (2012) discussed MHD flow and heat transfer over a porous shrinking surface with velocity slip and temperature jump. Hayat *et al.* (2010) considered simultaneous effects of slip and heat transfer on the peristaltic flow.

2.7 Reactive Flows

Reactive fluid flow problems has application in many reservoir and automobile engineering such as; fuel combustion during industrial and engineering processes, bush burning, releases from automobile engines, waste burning, production of liquid steel, burning of crude oil leakages on high sea, thermal explosions, nuclear reactor, bomb

detonation, petro-chemical fluid flows in refineries etc. (Adesanya, 2013). Reactive viscous fluid was first introduced by Frank-Kamenetskii (1969), thereafter Chao *et al.* (1996) examined theoretically the heat transfer and reaction characteristics of a chemically reactive forced convection flow near the stagnation point of a catalytic porous bed with finite thickness. Ayeni (1982) reported on the explosion of chain-thermal reaction while Dainton (1960) presented an introduction to chain reaction, by including the effects of Arrhenius temperature dependence with variable pre-exponential factor. Okoya (2006) presented the thermal stability for a reactive viscous flow of a third – grade fluid between two parallel plates with a uniform pressure gradient (Plane – Poiseuille flow). Jha *et al.* (2011) investigated a transient natural convection flow of a reactive viscous flow in a vertical channel formed by two infinite vertical parallel plates. Jha *et al.* (2013) studied unsteady/steady natural convection flow of reactive viscous fluid in a vertical annulus.

2.8 Entropy Generation

The current trend of entropy generation analysis is the application of second law of Thermodynamics, and its design-related concept of entropy generation minimization (EGM). After the pioneering work of (Bejan, 1980; Bejan, 1982; Bejan, 1996), several investigations on the factors responsible for the entropy generation under various physical situations have been carried out. Yapici, Basturk, Kayatas and Yalcin (2005) investigated the transient local entropy generation in pulsating turbulent flow through an externally heated pipe, it was concluded that entropy generation rates increased in the case of sinusoidal and saw-down flow. Pakdemirli and Yilbass (2006)investigated entropy generation in a pipe due to non-Newtonian fluid flow, it was submitted that increase in the non-Newtonian parameter reduces the fluid friction in the region close to the pipe wall which in turn results in low entropy generation. Hooman (2007) presented entropy generation for microscale forced convection with focus on the effects of different thermal boundary conditions, velocity slip, temperature jump, viscous dissipation, and duct geometry. Sahiti, Krasniqi, Fejzullahu, Bunjaku and Muriqi (2008)

studied entropy generation minimization of a double-pipe pin fin heat exchanger, it was concluded that larger pin lengths are accompanied with larger entropy production rates. Arikoglu *et al.* (2010) investigated combined effects of temperature and velocity jump on the heat transfer, fluid flow, and entropy generation over a single rotating disk. Jery *et al.* (2010) studied the effect of an inclined magnetic field on the entropy generation rate by considering only the natural convention flow. Maghrbi, Jery, Hidouri and Brahim (2010) studied the evanescent magnetic field effects on entropy generation at the onset of natural convection, the results show that increase in relaxation time decreased entropy generation. Bouabid *et al.* (2011) studied entropy generation by free convection in an inclined rectangular channel.

Furthermore, Ajibade *et al.* (2011) obtained a closed form solution on the effect of entropy generation in a steady flow of viscous incompressible fluids between two infinite parallel porous plates. Two flow geometries were considered: Couette and Poiseuille flow with suction/injection; it was noted that entropy generation number increases on one porous plate with suction while it decreases on the other porous plate with injection. Karamallah, Mohammad and Khalil (2011) studied the entropy generation in a vertical square channel packed with saturated porous media, it was shown that entropy generation reduced as Reynold, Darcy number and Eckert numbers decreased. Rashidi and Freidoomehr (2012) considered the effects of velocity slip and temperature jump on the entropy generation in MHD flow over a porous rotating disk. Eegunjobi and Makinde (2012) considered the effects of Navier slip on steady flow of an incompressible viscous fluid through a porous channel with suction/injection. It was submitted that increase in asymmetric slip parameters increases the dominance effects of heat transfer irreversibility at the lower wall and fluid friction irreversibility at the upper wall. Later, Makinde and Eegunjobi (2013) employed Runge-kutta fourth-order integration scheme to study the effects of convective heating and suction/injection on the entropy generation in a steady flow of a viscous fluid through a channel with permeable walls. The results indicated that entropy generation rate increases with increase in the value of Biot numbers at both walls while heat transfer

irreversibility dominates the centreline region of the channel. Adesanya and Makinde (2014) discussed the effects of couple stresses and Navier slip on the entropy generation. Furthermore, Das and Jana (2014) investigated the effects of magnetic field and Navier slip on the entropy generation in a flow of viscous incompressible hydromagnetic fluid flowing between two infinite horizontal parallel porous plates. It was stated that entropy generation rises with an increase in magnetic field parameter, heat transfer irreversibility dominates the flow process within the channel centreline region, while the influence of fluid friction irreversibility is observed at the channel walls from the conclusion. Basak *et al.* (2012) investigated entropy generation during natural convection in a porous cavity considering the effect of thermal boundary conditions and reported that entropy generation is mainly contributed by heat transfer irreversibility.

The effect of entropy generation on third grade fluid has also been investigated by several authors, these include Makinde (2009) who conducted an investigation on the thermal stability effect of a reactive third-grade fluid in a channel with convective cooling. Irreversibility analysis of third-grade fluid with variable properties was analysed by Adesanya, (2014), and it was explained that increase in the internal heat generation parameter corresponds to a rise in the entropy generation rate in the centerline of the channel only. Moreover, Adesanya and Makinde (2015a) utilised the rapidly convergent ADM to study the effect of buoyancy force on the entropy generation of a third grade fluid through a vertical channel with internal heat generation. The reactive case induced by chemical reaction was considered and it was reported that the available energy of the system rises with an increase in the non-Newtonian parameter while buoyancy force, internal heat generation and viscous heating of the fluid reduced the exergy level of the thermal system. Adesanya and Falade (2015) further extended the work to hydromagnetic case of third grade fluid flowing through porous medium, it was argued that fluid irreversibility increases at the centreline with increased magnetic field intensity which was attributed to the imbalance in the Lorentz force that acted as a resistance to the flow and increased the fluid temperature.

Irreversibility associated with couple stress fluid was also investigated by Adesanya and Makinde (2015b) where the effects of entropy generation of couple stress fluid through porous channel with convective heating was analysed, it was discovered that increase in couple stresses reduces the entropy generation rate within the channel except at the heated wall. Also, Adesanya and Makinde (2015c) studied irreversibility analysis in a couple stress film flow along an inclined heated plate with adiabatic free surface using regular perturbation method. The study revealed that there is an increase in entropy generation rate along the heated inclined plate as viscosity variation, viscous heating and couple stress inverse parameters increased.

Most of the studies presented above either considered the entropy generation of some electrically conducting fluids or the entropy generation of couple stress fluid under various flow configurations. The literature survey reveals that adequate attention has not been paid to entropy generation of electrically conducting couple stress fluid. Meanwhile it has been discovered that applying magnetic field to lubricants can increase its load carrying capacity and improve its lubrication capacity as well as the performance of squeeze film (Hughes and Elco, 1962; Rajashekar and Kashinath, 2012). Furthermore, Gerbeth *et al.* (2013) submitted that the magnetic field produced by a simple magnet placed across the channel usually interact with the flow of fluid and this plays very important role in the control of motion of hot fluid in many metallurgical engineering applications, crystal growth, electrochemistry and other thermal processes which occurs at very high temperature. This explains why the research is worthwhile.

CHAPTER THREE

METHODOLOGY

3.1 Introduction

Analysis of the two methods applied in this study and the mathematical models are presented in this chapter. The procedure for the implementation of Adomian decomposition and differential transform techniques are discussed in details. The choice of the two semi-analytical techniques employed in this work is due to unavailability of analytical solution to the non-linear governing equations derived from the models. In subsequent sections, the mathematical formulation and solution procedure are presented.

3.2 Description of Methods

In literature, different types of numerical and analytical procedures such as: finite element method, Galerkin method, the Laplace transformation, Finite Difference Approach, Perturbation Technique, Homotopy Perturbation Technique, Variational Iteration Method, Shooting Quadrature Method, Runge-Kutta -Fehlberg method etc., are available. Some of these existing techniques have difficulties in relation to the size of computational work and convergence. In this study, the Adomian Decomposition Method (ADM) and Differential Transform Method (DTM) applied have advantage over other methods because of their simplicity in handling boundary value problems, high accuracy and rapid convergence. The computations are done by developing numerical codes that incorporate the methods described below in Mathematica and Maple software. Detailed solution are in the appendix section.

3.2.1 Adomian Decomposition Method

In the 1980s, George Adomian (1923-1996) proposed this powerful technique for solving linear and nonlinear ordinary and partial differential equations. The method has since then been called Adomian Decomposition Method (ADM) (Adomian, 1989; Adomian, 1994). To apply ADM the given equation is split into linear and non-linear parts, the highest-order derivative operator in the linear operator is inverted on both sides. The initial/boundary conditions together with the source term constitute the zeroth component while any nonlinear term in the equation is decomposed as Adomian polynomials and the successive terms as series solution by recurrent relation using Adomian polynomials. Later, Wazwaz (1999) developed the modified version of the Adomian decomposition method. The modified technique provides a qualitative improvement over standard Adomian method, although it introduces a slight change in the formulation of Adomian recursive relation. The reason for this improvement rests on the fact that the technique accelerates the convergence of the solution and facilitates the formulation of Adomian polynomials.

Consider the generalized differential equation of the form

$$Ly + Ry + Ny = g \tag{3.1}$$

L is the highest order derivative (L is invertible), R is a linear differential operator, N is the nonlinear term and g is the source term.
Applying L^{-1} on both sides of equation (3.1) to obtain

$$y = L^{-1}(g) - L^{-1}(Ry) - L^{-1}(Ny) \tag{3.2}$$

Equation (3.2) can be written as

$$y = h - L^{-1}(Ry) - L^{-1}(Ny) \tag{3.3}$$

Note that h represents the terms arising from integrating the source term g that is,

$(L^{-1}(g))$ and from the given conditions.

Using the standard Adomian decomposition method, the zeroth component is written as

$$y_0 = h \tag{3.4}$$

and the recursive relation is

$$y_{n+1} = -L^{-1}(Ry_n) - L^{-1}(Ny_n), n \geq 0 \tag{3.5}$$

$$y_1 = -L^{-1}(Ry_0) - L^{-1}(Ny_0) \tag{3.6}$$

$$y_2 = -L^{-1}(Ry_1) - L^{-1}(Ny_1) \tag{3.7}$$

$$y_3 = -L^{-1}(Ry_2) - L^{-1}(Ny_2) \tag{3.8}$$

Then the solution will be of the form

$$y(t) = \sum_{n=0}^{\infty} y_n(t) \tag{3.9}$$

The non-linear term can be determined by an infinite series of Adomian polynomials

$$Ny = \sum_{n=0}^{\infty} A_n \tag{3.10}$$

where $A_n^{'}s$ are calculated by the relation

$$A_n = \frac{1}{n!}\frac{d^n}{dt^n}[N(\sum_{i=0}^{n} t^i y_i)]_{t=0}, n = 0, 1, 2, 3 \cdots \tag{3.11}$$

3.2.2 Differential Transform Method

The concept of the differential transform method was first introduced by Zhou (1986), and it was applied to solve both linear and nonlinear initial value problems in electric circuit analysis. Chen and Ho (1999) later developed this method for the solution of partial differential equations. To apply this method for the solution of differential equations, a semi-analytical numerical technique that uses Taylor series in the form of a polynomial is constructed. The advantage of this method over high-order Taylor series method is that it does not require symbolic computation of the necessary derivatives of the data functions. Furthermore, Taylor series method is computationally time-consuming especially for higher order equation while differential transform is an iterative procedure for obtaining analytic Taylor series solutions of differential equations.The basic definition and the fundamental theorems of DTM and its applicability are well addressed in Arikoglu and Ozkol (2005), Liu and Song (2007) and Hassan (2008). However, the basic principles of the differential transformation method are described as follows.

Let the differential transformation of the kth derivative of the function $u(t)$ about a point $t = t_0$ be defined as

$$U(k) = \frac{1}{k!}[\frac{d^k u(t)}{dt^k}]_{t=t_0} \tag{3.12}$$

where $u(t)$ is the original function and $U(k)$ is the transformed function. The inverse differential transform $U(k)$ can be written as

$$u(t) = \sum_{i=0}^{\infty} U(k)(t - t_0)^k \tag{3.13}$$

Function $u(t)$ can then be written as a finite series with equation (3.12) stated as

$$u(t) = \sum_{i=0}^{n} U(k)(t - t_0)^k \tag{3.14}$$

Relevant theorems for the differential equations to be solved can then be derived from equations (3.12) and equation (3.13)

If

(i) $u(t) = v(t) \pm w(t)$, then $U(k) \pm W(K)$

(ii) $u(t) = \alpha v(t)$, then $U(k) = \alpha V(k)$

(iii) $u(t) = \frac{dv(t)}{dt}$, then $U(k) = (k+1)V(k+1)$

(iv) $u(t) = \frac{d^r v(t)}{dt^r}$, then $U(k) = (k+1)\cdots(k+r)V(k+r)$

(v) $u(t) = t^r$, then $U(k) = \delta(k-r) = \begin{cases} 1, & k=r \\ 0, & k \neq r \end{cases}$

(vi) $u(t) = v(t)w(t)$, then $U(k) = \sum_{n=0}^{k} V(k)W(k-n)$

(vii) $u(t) = v^3(t)$, then $U(k) = \sum_{k_1}^{k} \sum_{r}^{k_1} V(r)V(k_1 - r)V(k-r)$

(viii) $u(t) = (\frac{dv(t)}{dt})^2$, then $V(k) = \sum_{r}^{k}(k+1)(k-r+1)V(r+1)V(k-r+1)$

(ix) $u(t) = \frac{d^2 v(t)}{dt^2}$, then $V(k) = \sum_{r}^{k}(r+1)(r+2)(k-r+2)(k-r+1)V(r+2)V(k-r+2)$

The procedure for the solution of the model equations is organized into the following stages:

(i) The governing equations of motion were derived,

(ii) the equations were non-dimensionalised to obtain the required boundary value problems,

(iii) the boundary value problems were solved by Adomian decomposition and differential transform techniques,

(iv) the obtained velocity and temperature profiles were utilised to compute the entropy generation rate, irreversibility distribution ratio and Bejan number and

(v) finally, the graphs for the velocity profile, temperature profile , entropy generation rate and Bejan number were plotted

3.3 Mathematical Models

3.3.1 Model 1: Influence of Magnetic Field on Couple Stress Flow Through Porous Channel with Entropy Generation

In this model, emphasis is on the control of heat irreversibility which could arise from viscous dissipation or heat transfer. This is because heat irreversibility is generated continuously with temperature difference across the heated channel. This all-important effect has been neglected in the recent work by Adesanya and Makinde (2015b). This is in spite of various magnetohydodynamic applications in industrial and engineering systems involving heat transfer in industries and systems involving thermal engineering.

3.3.2 Formulation of Model 1

Consider the steady flow and heat transfer of hydromagnetic couple stress fluid flowing steadily through a porous channel taking Ohmic heating of the fluid into consideration. A uniform transverse magnetic field B_0 is applied perpendicularly to the channel plates. It is assumed that the fluid exchanges heat with the ambient in an axi-symmetrical manner. Due to wall porosity, fluid is injected with a constant velocity at the lower plate and sucked off at the upper plate with the same velocity. Under this configuration (see Figure 3.1), the momentum and energy balance equations governing the fluid flow can be written as follows (Adesanya and Makinde, (2015b))

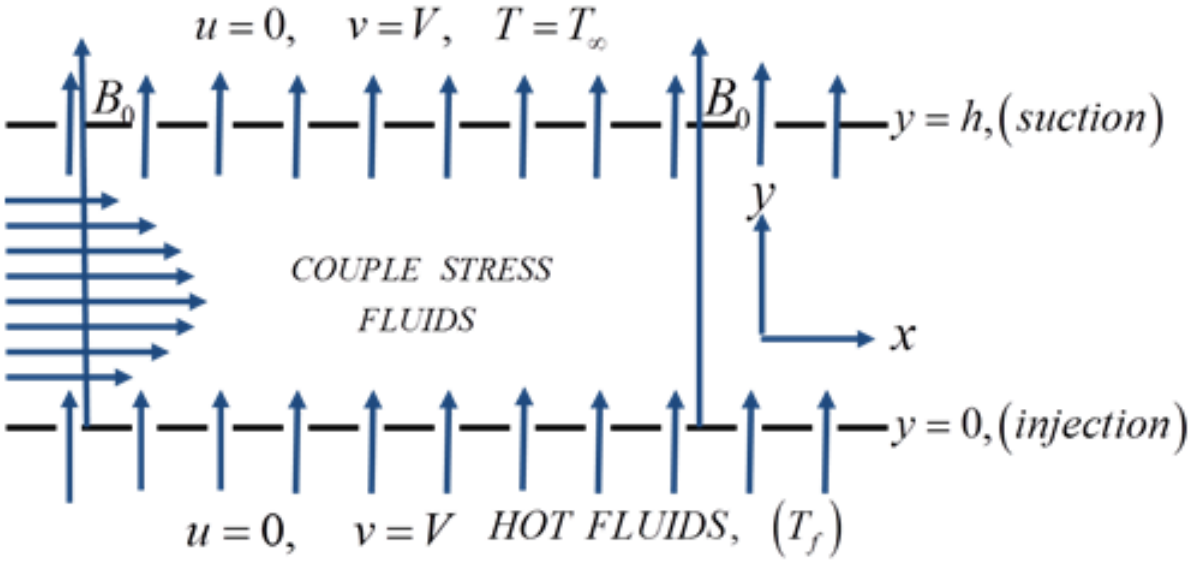

Figure 3.1: Schematic diagram for Model 1

$$\rho V_0 \frac{du^{'}}{dy^{'}} = -\frac{dp}{dx^{'}} + \mu \frac{d^2u^{'}}{dy^{'2}} - \eta \frac{d^4u^{'}}{dy^{'4}} - \sigma B_0^2 u^{'} \tag{3.15}$$

$$\rho C_p v_0 \frac{dT}{dy^{'}} = k \frac{d^2T^{'}}{dy^{'2}} + \mu \Big(\frac{du^{'}}{dy^{'}}\Big)^2 + \eta \Big(\frac{d^2u^{'}}{dy^{'2}}\Big)^2 + \sigma B_0^2 u^{'2} \tag{3.16}$$

The last terms in equations (3.15)-(3.16) are due to the magnetic field arising from interactions with the fluid. The thermal boundary conditions are

$$k\frac{dT^{'}}{dy^{'}}(0) = -\gamma_1(T_f - T^{'}), k\frac{dT^{'}}{dy^{'}}(h) = -\gamma_2(T_f - T_0^{'}) \tag{3.17}$$

while the no-slip and stress-free conditions are

$$u^{'}(0) = \frac{d^2u^{'}}{dy^2}(0) = 0 = u^{'}(h) = \frac{d^2u^{'}}{dy^2}(h) \tag{3.18}$$

Introducing the following dimensionless parameters

$$y = \frac{y^{'}}{h}, u = \frac{u^{'}}{v_0}, \theta = \frac{T^{'} - T_0}{T_f - T_0}, s = \frac{v_0 h}{v}, G = -\frac{h^2 dp}{\mu v_0 dx}, a^2 = \mu\frac{h^2}{\eta}, Pr = \frac{v\rho C_p}{k},$$
$$Br = \frac{\mu v_0}{k(T_f - T_0)}, Bi_1 = \frac{\gamma_1 h}{k}, Bi_2 = \frac{\gamma_2 h}{k}, Ns = \frac{T_0^2 h^2 E_G}{k(T_f - T_0)^2}, \Omega = \frac{T_f - T_0}{T_0},$$
$$v = \frac{\mu}{\rho}, H^2 = \frac{\sigma B_0^2 h^2}{\mu} \tag{3.19}$$

into equations (3.15)-(3.18) to obtain the following boundary-value problems

$$s\frac{du}{dy} = G + \frac{d^2u}{dy^2} - \frac{1}{a^2}\frac{d^4u}{dy^4} - H^2u; u(0) = \frac{d^2u}{dy^2}(0) = 0 = u(1) = \frac{d^2u}{dy^2}(1) \tag{3.20}$$

$$\frac{d^2\theta}{dy^2} = sPr\frac{d\theta}{dy} - Br\left\{\Big(\frac{du}{dy}\Big)^2 + \frac{1}{a^2}\Big(\frac{d^2u}{dy^2}\Big)^2 + H^2u^2\right\};$$
$$\frac{d\theta(0)}{dy} = Bi_1(\theta(0) - 1); \frac{d\theta(1)}{dy} = -Bi_2(\theta(1)) \tag{3.21}$$

Other quantities of interest in this work include the skin friction coefficient C_f and

heat transfer rate Nu at the channels wall respectively:

$$C_f = \frac{du(y)}{dy}\bigg|_{y=0,1} ; Nu = -\frac{d\theta(y)}{dy}\bigg|_{y=0,1} \tag{3.22}$$

3.3.3 Solution by Adomian Decomposition Method (ADM)

Writing equations (3.20) and (3.21) in the integral form yields

$$u(y) = b_1 y + \frac{b_2}{3!}y^3 + a^2 \int_0^y \int_0^y \int_0^y \int_0^y \Big\{ G + \frac{d^2u}{dY^2} - s\frac{du}{dY} - H^2 u \Big\} dY dY dY dY \tag{3.23}$$

and

$$\theta(y) = b_3 + b_4(y) + \int_0^y \int_0^y \Big\{ sPr\frac{d\theta}{dY} - Br\Big(\frac{du}{dY}\Big)^2 - \frac{Br}{a^2}\Big(\frac{d^2u}{dY^2}\Big)^2 - BrH^2u^2 \Big\} dY dY \tag{3.24}$$

where b_1 ,b_2 ,b_3 , b_4 are the parameters to be determined later.

By ADM, an infinite series solution is defined as

$$u(y) = \sum_{n=0}^{\infty} u_n(y), \theta(y) = \sum_{n=0}^{\infty} \theta_n(y) \tag{3.25}$$

Now using equation (3.25) in equations (3.23)-(3.24) yields

$$\sum_{n=0}^{\infty} u_n(y) = b_1 y + \frac{b_2}{3!}y^3 + a^2 \int_0^y \int_0^y \int_0^y \int_0^y \Big\{ G + \sum_{n=0}^{\infty}\frac{d^2u_n}{dY^2} - sPr\sum_{n=0}^{\infty}\frac{du_n}{dY} - H^2\sum_{n=0}^{\infty}u_n \Big\} dY dY dY dY \tag{3.26}$$

and

$$\sum_{n=0}^{\infty} \theta_n(y) = b_3 + b_4 y + \int_0^y \int_0^y \Big\{ sPr\sum_{n=0}^{\infty}\frac{d\theta_n}{dY} - Br\Big(\sum_{n=0}^{\infty}\frac{du}{dY}\Big)^2 - \frac{Br}{a^2}\Big(\sum_{n=0}^{\infty}\frac{d^2u}{dY^2}\Big)^2 - BrH^2\sum_{n=0}^{\infty}u^2 \Big\} dY dY \tag{3.27}$$

In view of (3.26)-(3.27), the zeroth order terms can be written as

$$\sum_{n=0}^{\infty} u_0(y) = b_1 y + \frac{b_2}{3!} y^3 + a^2 \int_0^y \int_0^y \int_0^y \int_0^y \Big\{G\Big\} dY\, dY\, dY\, dY \tag{3.28}$$

$$\sum_{n=0}^{\infty} \theta_0(y) = b_3 + b_4 y \tag{3.29}$$

while other terms can be determined using the recurrence relations

$$\sum_{n=0}^{\infty} u_{n+1}(y) = a^2 \int_0^y \int_0^y \int_0^y \int_0^y \Bigg\{ \sum_{n=0}^{\infty} \frac{d^2 u_n}{dY^2} - s \sum_{n=0}^{\infty} \frac{du_n}{dY} - H^2 \sum_{n=0}^{\infty} u_n \Bigg\} dY\, dY\, dY\, dY \tag{3.30}$$

and

$$\sum_{n=0}^{\infty} \theta_{n+1}(y) = \int_0^y \int_0^y \Bigg\{ sPr \sum_{n=0}^{\infty} \frac{d\theta_n}{dY} - Br \left(\sum_{n=0}^{\infty} \frac{du}{dY} \right)^2 - \frac{Br}{a^2} \left(\sum_{n=0}^{\infty} \frac{d^2 u}{dY^2} \right)^2 - BrH^2 \sum_{n=0}^{\infty} u^2 \Bigg\} dY\, dY \tag{3.31}$$

The nonlinear term in equation (3.31) is written as

$$B_n = u^2 \tag{3.32}$$

while the Adomian polynomials are computed as

$$B_0 = u_0^2,\ B_1 = 2u_0 u_1,\ B_2 = 2u_0 u_2 + u_1^2, \ldots \tag{3.33}$$

Substituting equation (3.32) in (3.31) yields

$$\sum_{n=0}^{\infty} \theta_{n+1}(y) = \int_0^y \int_0^y \Bigg\{ sPr \sum_{n=0}^{\infty} \frac{d\theta_n}{dY} - Br \left(\sum_{n=0}^{\infty} \frac{du}{dY} \right)^2 - \frac{Br}{a^2} \left(\sum_{n=0}^{\infty} \frac{d^2 u}{dY^2} \right)^2 - BrH^2 \sum_{n=0}^{\infty} B_n \Bigg\} dY\, dY \tag{3.34}$$

Solving equations (3.28)-(3.30) and (3.34) yields the solution of the boundary value problems.

3.3.4 Solution by Differential Transform Method (DTM)

To solve the boundary value problems by DTM, equations (3.20)-(3.21) are transformed as

$$U(k+4) = \frac{a}{(k+4)!}\Big[(k+1)(k+2)U(k+2) - s(k+1)U(k+1) + G\delta(k) - H^2U(k)\Big] \tag{3.35}$$

$$\theta(k+2) = \frac{1}{(k+2)!}\Big[sPr(k+1)\theta(k+1) - Br\sum_{r=0}^{k}(r+1)(k-r+1)U(k-r+1) - \frac{Br}{a^2}\sum_{r=0}^{k}(r+1)(r+2)(k-r+2)(k-r+1)U(k-r+2) - H^2\sum_{r=0}^{k}U(r)U(k-r)\Big] \tag{3.36}$$

$$U(0) = 0, U(1) = A, U(2) = 0, U(3) = \frac{B}{3!} \tag{3.37}$$

$$\theta(0) = C, \theta(1) = Bi_1(\theta(1) - 1) \tag{3.38}$$

Using equation (3.37) in equation (3.35) and equation (3.38) in equation (3.36), the solution of the boundary value problem is obtained. To verify the accuracy of the computations, the approximate solution obtained by ADM is compared with DTM solution in Table 3.1. In the result section, the obtained velocity and temperature

profiles are used to compute the entropy generation rate.

Table 3.1: Comparison between ADM and DTM for $G = H = a = 1, s = 0.1$

y	U_{ADM}	U_{DTM}	**Abs Error**
0.1	0.003680317	0.003680317	2.99999×10^{-12}
0.2	0.006959623	0.006959623	5.99968×10^{-12}
0.3	0.009523962	0.009523962	8.99757×10^{-12}
0.4	0.011151328	0.011151328	1.19898×10^{-11}
0.5	0.011709275	0.011709275	1.49687×10^{-11}
0.6	0.011153527	0.011153527	1.79222×10^{-11}
0.7	0.009527596	0.009527596	2.08318×10^{-11}
0.8	0.006963372	0.006963372	2.3672×10^{-11}
0.9	0.003682714	0.003682714	2.64088×10^{-11}
1	2.52325×10^{-12}	-2.6475×10^{-11}	2.89982×10^{-11}

3.3.5 Entropy Generation Analysis

The local entropy generation rate according to Bejan (1996), for the problem under discussion can be written as:

$$E_G = \frac{k}{T_0^2}\left(\frac{dT^{'}}{dy^{'}}\right)^2 + \frac{\mu}{T_0}\left(\frac{du^{'}}{dy}\right)^2 + \frac{\eta}{T_0}\left(\frac{d^2u^{'}}{dy^{'2}}\right)^2 + \frac{\sigma B_0^2 u^2}{T_0} \tag{3.39}$$

Using the dimensionless variables (3.19) in equation (3.39) gives

$$Ns = \left(\frac{d\theta}{dy}\right)^2 + \frac{Br}{\Omega}\left\{\left(\frac{du}{dy}\right)^2 + \frac{1}{a^2}\left(\frac{d^2u}{dy^2}\right)^2 + H^2u^2\right\} \tag{3.40}$$

The first term of equation (3.39) is the irreversibility due to heat transfer, the second and the third terms are entropy generation due to fluid friction and couple stresses respectively while the fourth term is the irreversibility due to the effect of magnetic field. Setting N_1 as irreversibility due to heat transfer and N_2 as hydromagnetic fluid friction irreversibility

$$N_1 = \left(\frac{d\theta}{dy}\right)^2, N_2 = \frac{Br}{\Omega}\left\{\left(\frac{du}{dy}\right)^2 + \frac{1}{a^2}\left(\frac{d^2u}{dy^2}\right)^2 + H^2u^2\right\} \tag{3.41}$$

then the Bejan number (Be) for the irreversibility ratio can be written as:

$$Be = \frac{N_1}{Ns} = \frac{1}{1+\Phi}, \Phi = \frac{N_2}{N_1} \tag{3.42}$$

Observe $Be = 0$ corresponds to the special case when heat irreversibility due to magnetic fluid friction dominates over heat transfer irreversibility. Similarly, as N_1 takes preeminence over N_2 the numerical value of Be is expected to be unity and $Be = \frac{1}{2}$ when both contribute equally.

Table 3.2: Comparison between Adesanya and Makinde (2015b), ADM and DTM solution of velocity profile for G = a = 1, s = 0.1, H = 0

y	**Adesanya and Makinde (2015b)**	U_{ADM}	U_{DTM}
0	0.000000000	0.000000000	0.000000000
0.1	0.003714182	0.003714182	0.003714182
0.2	0.007024039	0.007024039	0.007024039
0.3	0.009612623	0.009612623	0.009612623
0.4	0.011255559	0.011255559	0.011255559
0.5	0.011818879	0.011818879	0.011818879
0.6	0.011257781	0.011257781	0.011257781
0.7	0.009616293	0.009616293	0.009616293
0.8	0.007027825	0.007027825	0.007027825
0.9	0.003716603	0.003716603	0.003716603
1	2.02478×10^{-11}	1.92488×10^{-11}	3.71469×10^{-11}

3.3.6 Model 2: Second Law Analysis of Hydromagnetic Couples Stress Fluid Embedded in a Non-Darcian Porous Medium

Analysis of hydromagnetic couples stress fluid embedded in a non-Darcian porous medium is useful and important basically for (i) gaining fundamental understanding of such flows, (ii) the need to ensure entropy minimization in a hydromagnetic couple stress fluid flow and (iii) possible application of such non-Newtonian fluids in petroleum production, power engineering, movement of biological fluids and food, and construction engineering. The primary motivation for this problem is derived from the above issues which is very important yet un-addressed in the previous works on the subject (Adesanya, 2014; Adesanya and Makinde, 2015b). In particular, the objective of this model is second law analysis of hydromagnetic couples stress fluid embedded in a non-Darcian porous medium.

3.3.7 Formulation of Model 2

Consider the steady flow of electrically conducting couple stress non-Newtonian fluid through non-Darcian porous medium. The flow is subjected to injection of the fluid at the lower plate and suction at the upper plate with constant velocity. A uniform transverse magnetic field is applied in the direction of flow and the interaction of the induced magnetic field is considered negligible compared to the interaction of the applied magnetic field. The wall plates are assumed to exchange heating in an axi-symmetrical manner with the ambient temperature. Under the configuration shown in Figure 3.2, the governing equations for the momentum, heat balance and entropy generation rate can be written as Adesanya and Makinde, (2015b)

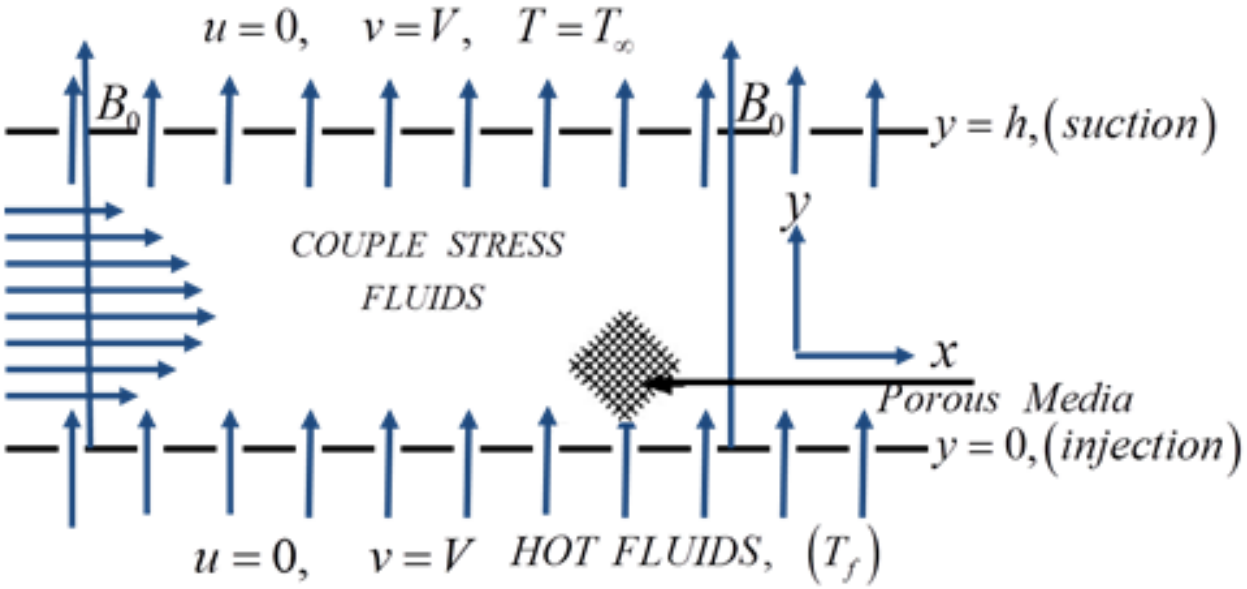

Figure 3.2: Schematic diagram for Model 2

$$\rho V_0 \frac{du^{'}}{dy^{'}} = -\frac{dp}{dx^{'}} + \mu \frac{d^2u^{'}}{dy^{'2}} - \eta \frac{d^4u^{'}}{dy^{'4}} - \sigma B_0^2 u^{'} - \frac{\mu u^{'}}{K} - \frac{bu^{'2}}{\sqrt{K}} \tag{3.43}$$

$$\rho C_p v_0 \frac{dT}{dy^{'}} = k \frac{d^2T^{'}}{dy^{'2}} + \mu \Big(\frac{du^{'}}{dy^{'}}\Big)^2 + \eta \Big(\frac{d^2u^{'}}{dy^{'2}}\Big)^2 + \sigma B_0^2 u^{'2} + \frac{\mu u^{'2}}{K} + \frac{bu^{'3}}{\sqrt{K}} \tag{3.44}$$

$$E_G = \frac{k}{T_0^2}\Big(\frac{dT^{'}}{dy^{'}}\Big)^2 + \frac{\mu}{T_0}\Big(\frac{du^{'}}{dy^{'}}\Big)^2 + \frac{\eta}{T_0}\Big(\frac{d^2u^{'}}{dy^{'2}}\Big)^2 + \frac{\sigma B_0^2 u^2}{T_0} + \frac{\mu u^{'2}}{T_0 K} + \frac{bu^{'3}}{T_0\sqrt{K}} \tag{3.45}$$

The boundary conditions are

$$\begin{aligned} u^{'}(0) = 0 = \frac{d^2u^{'}(0)}{dy^2}, k\frac{dT^{'}(0)}{dy^{'}} = -\gamma_1(T_f - T^{'}); \\ u^{'}(h) = 0 = \frac{d^2u^{'}(h)}{dy^2}, k\frac{dT^{'}(h)}{dy^{'}} = -\gamma_2(T^{'} - T_0) \end{aligned} \tag{3.46}$$

The following dimensionless variables are introduced

$$\begin{aligned} y = \frac{y^{'}}{h}, u = \frac{u^{'}}{v_0}, \theta = \frac{T^{'} - T_0}{T_f - T_0}, s = \frac{v_0 h}{v}, G = -\frac{h^2 dp}{\mu v_0 dx}, a^2 = \mu\frac{h^2}{\eta}, \\ Pr = \frac{v\rho C_p}{k}, Br = \frac{\mu v_0}{k(T_f - T_0)}, Bi_1 = \frac{\gamma_1 h}{k}, Bi_2 = \frac{\gamma_2 h}{k}, \\ N_S = \frac{T_0^2 h^2 E_G}{k(T_f - T_0)^2}, \Omega = \frac{T_f - T_0}{T_0}, v = \frac{\mu}{\rho}, H^2 = \frac{\sigma B_0^2 h^2}{\rho}, \\ \beta^2 = \frac{h^2}{K}, \alpha^2 = \frac{bh^2 v_0}{\mu\sqrt{K}} \end{aligned} \tag{3.47}$$

Substituting equation (3.47) into equations (3.43)-(3.46), the following dimensionless equations are obtained

$$s\frac{du}{dy} = G + \frac{d^2u}{dy^2} - \frac{1}{a}\frac{d^4u}{dy^4} - H^2u - \beta^2 u - \alpha^2 u^2 \tag{3.48}$$

$$\frac{d^2\theta}{dy^2} = sPr\frac{d\theta}{dy} - Br\left\{\Big(\frac{du}{dy}\Big)^2 + \frac{1}{a^2}\Big(\frac{d^2u}{dy^2}\Big)^2 + H^2u^2 + \beta^2u^2 + \alpha^2u^3\right\}, \tag{3.49}$$

$$Ns = \left(\frac{d\theta}{dy}\right)^2 + \frac{Br}{\Omega}\left\{\left(\frac{du}{dy}\right)^2 + \frac{1}{a^2}\left(\frac{d^2u}{dy^2}\right)^2 + H^2u^2 + \beta^2u^2 + \alpha^2u^3\right\} \tag{3.50}$$

with the boundary conditions

$$\begin{aligned} u(0) = 0 = \frac{d^2u(0)}{dy^2}, \frac{d\theta(0)}{dy} = Bi_1(\theta(0) - 1); \\ u(1) = 0 = \frac{d^2u(1)}{dy^2}, \frac{d\theta(1)}{dy} = -Bi_2(\theta(1)) \end{aligned} \tag{3.51}$$

3.3.8 Solution by Adomian Decomposition Method (ADM)

Writing equations (3.48)-(3.49) in the integral form gives

$$\begin{aligned} u(y) = f_1 y + \frac{f_2}{3!}y^3 + a^2 \int_0^y \int_0^y \int_0^y \int_0^y \Bigg\{G + \frac{d^2u}{dY^2} - \\ s\frac{du}{dY} + BrH^2u - Br\beta^2u - Br\alpha^2u\Bigg\} dY dY dY dY \end{aligned} \tag{3.52}$$

and

$$\begin{aligned} \theta(y) = f_3 + f_4(y) + \int_0^y \int_0^y \Bigg\{sPr\frac{d\theta}{dY} - Br\Bigg\{\left(\frac{du}{dY}\right)^2 + \frac{Br}{a^2}\left(\frac{d^2u}{dY^2}\right)^2 + \\ BrH^2u^2 + Br\beta^2u^2 + Br\alpha^2u^3\Bigg\}\Bigg\} dY dY \end{aligned} \tag{3.53}$$

Note that f_1, f_2, f_3, f_4 are the parameters to be determined later.

ADM solutions in the form of an infinite series are stated as

$$u(y) = \sum_{n=0}^{\infty} u_n(y), \theta(y) = \sum_{n=0}^{\infty} \theta_n(y) \tag{3.54}$$

Now, substituting equation (3.54) in equations (3.52)-(3.53) to obtain

$$\sum_{n=0}^{\infty} u_n(y) = f_1 y + \frac{f_2}{3!}y^3 + a^2 \int_0^y \int_0^y \int_0^y \int_0^y \Bigg\{ G + \sum_{n=0}^{\infty} \frac{d^2 u_n}{dY^2} - s \sum_{n=0}^{\infty} \frac{du_n}{dY} - H^2 \sum_{n=0}^{\infty} u_n - \beta^2 \sum_{n=0}^{\infty} u_n - \alpha^2 \sum_{n=0}^{\infty} u_n \Bigg\} dY dY dY dY \tag{3.55}$$

and

$$\sum_{n=0}^{\infty} \theta_n(y) = f_3 + f_4 y + \int_0^y \int_0^y \Bigg\{ sPr \sum_{n=0}^{\infty} \frac{d\theta_n}{dY} - Br \Bigg\{ \left(\sum_{n=0}^{\infty} \frac{du}{dY} \right)^2 + \frac{Br}{a^2} \left(\sum_{n=0}^{\infty} \frac{d^2 u}{dY^2} \right)^2 + BrH^2 \sum_{n=0}^{\infty} u^2 + Br\beta^2 \sum_{n=0}^{\infty} u^2 + Br\alpha^2 \sum_{n=0}^{\infty} u^3 \Bigg\} \Bigg\} dY dY \tag{3.56}$$

In view of (3.55)-(3.56), the zeroth order term can be written as

$$\sum_{n=0}^{\infty} u_0(y) = f_1 y + \frac{f_2}{3!}y^3 + a^2 \int_0^y \int_0^y \int_0^y \int_0^y \Big\{ G \Big\} dY dY dY dY \tag{3.57}$$

$$\sum_{n=0}^{\infty} \theta_0(y) = f_3 + f_4 y \tag{3.58}$$

while other terms are determined using the recurrence relations

$$\sum_{n=0}^{\infty} u_{n+1}(y) = a^2 \int_0^y \int_0^y \int_0^y \int_0^y \Bigg\{ \sum_{n=0}^{\infty} \frac{d^2 u_n}{dY^2} - s \sum_{n=0}^{\infty} \frac{du_n}{dY} - H^2 \sum_{n=0}^{\infty} u_n - \beta^2 \sum_{n=0}^{\infty} u_n - \alpha^2 \sum_{n=0}^{\infty} u_n \Bigg\} dY dY dY dY \tag{3.59}$$

$$\sum_{n=0}^{\infty} \theta_{n+1}(y) = a^2 \int_0^y \int_0^y \Bigg\{ sPr \sum_{n=0}^{\infty} \frac{d\theta_n}{dY} - Br \Bigg\{ \left(\sum_{n=0}^{\infty} \frac{du}{dY} \right)^2 + \frac{Br}{a^2} \left(\sum_{n=0}^{\infty} \frac{d^2 u}{dY^2} \right)^2 + BrH^2 \sum_{n=0}^{\infty} u^2 + Br\beta^2 \sum_{n=0}^{\infty} u^2 + Br\alpha^2 \sum_{n=0}^{\infty} u^3 \Bigg\} \Bigg\} dY dY \tag{3.60}$$

The nonlinear terms in equation (3.60) can be represented as

$$B_n = u^2, C_n = u^3 \tag{3.61}$$

Adomian polynomials of the nonlinear terms are computed as

$$B_0 = u_0^2,\ B_1 = 2u_0u_1,\ B_2 = 2u_0u_2 + u_1^2, \ldots;\ C_0 = u_0^3,\ C_1 = 3u_0^2u_1, \tag{3.62}$$
$$C_2 = 3u_0^2u_2 + 3u_0u_1^2, \ldots$$

Substituting equation (3.61) in (3.60) yields

$$\sum_{n=0}^{\infty}\theta_{n+1}(y) = a^2\int_0^y\int_0^y\left\{sPr\sum_{n=0}^{\infty}\frac{d\theta_n}{dY} - Br\left\{\left(\sum_{n=0}^{\infty}\frac{du}{dY}\right)^2 + \frac{Br}{a^2}\left(\sum_{n=0}^{\infty}\frac{d^2u}{dY^2}\right)^2 + BrH^2\sum_{n=0}^{\infty}B_n + Br\beta^2\sum_{n=0}^{\infty}B_n + Br\alpha^2\sum_{n=0}^{\infty}C_n\right\}\right\}dY\,dY \tag{3.63}$$

Solution to equations (3.57)-(3.58) and (3.63) are obtained at $n = 0, 1, 2, 3, \ldots$

3.3.9 Solution by Differential Transform Method (DTM)

To solve the boundary value problems by DTM, equations (3.48)-(3.49) and equation (3.51) are transformed as

$$U(k+4) = \frac{a}{(k+4)!}\Big[(k+1)(k+2)U(k+2) - s(k+1)U(k+1) + G\delta(k) - H^2U(k) - \beta^2U(k) - \alpha^2\sum_{r=0}^{k}U(k)U(k-r)\Big] \tag{3.64}$$

$$\theta(k+2) = \frac{1}{(k+2)!}\Bigg[sPr(k+1)\theta(k+1) - Br\sum_{r=0}^{k}(r+1)(k-r+1)U(k-r+1) + \frac{Br}{a^2}\sum_{r=0}^{k}(r+1)(r+2)(k-r+2)(k-r+1)U(k-r+2) - H^2\sum_{r=0}^{k}U(r)U(k-r) + \beta^2\sum_{r=0}^{k}U(r)U(k-r) - \alpha^2\sum_{r}^{k}\sum_{s}^{r}U(s)U(r-s)U(k-r)\Bigg] \tag{3.65}$$

$$U(0) = 0, U(1) = A, U(2) = 0, U(3) = \frac{B}{3!} \tag{3.66}$$

$$\theta(0) = C, \theta(1) = Bi_1(\theta(1) - 1) \tag{3.67}$$

Using equation (3.66) in equation (3.64) and equation (3.67) in equation (3.65), the solution of the boundary value problem is obtained.

The accuracy of the results of these computations can be verified by comparing the approximate solutions obtained by ADM and DTM in Table 3.3.

Table 3.3: Comparison between ADM and DTM solutions for $s = 0.1, H = a = Br = \beta = \alpha = Bi_1 = Bi_2 = G = 1$

y	U_{ADM}	U_{DTM}	$AbsError$
0	0.000000000	0.000000000	0.000000000
0.1	0.0036467	0.0036468	1.42433×10^{-08}
0.2	0.0068958	0.0068958	2.76217×10^{-08}
0.3	0.0094361	0.0094361	3.92577×10^{-08}
0.4	0.011048	0.011048	4.82496×10^{-08}
0.5	0.0116006	0.0116007	5.36641×10^{-08}
0.6	0.0110502	0.0110502	5.45404×10^{-08}
0.7	0.0094397	0.0094397	4.99391×10^{-08}
0.8	0.0068995	0.0068995	3.91091×10^{-08}
0.9	0.0036491	0.0036491	2.19351×10^{-08}
1	3.879×10^{-11}	1.529×10^{-11}	2.34932×10^{-11}

3.3.10 Entropy Generation

Investigating entropy generation within the flow, according to Bejan (1996) the local entropy generation rate as shown in (3.45) is

$$E_G = \frac{k}{T_0^2}\left(\frac{dT^{'}}{dy^{'}}\right)^2 + \frac{\mu}{T_0}\left(\frac{du^{'}}{dy^{'}}\right)^2 + \frac{\eta}{T_0}\left(\frac{d^2u^{'}}{dy^{'2}}\right)^2 + \frac{\sigma B_0^2 u^2}{T_0} + \frac{\mu u^{'2}}{T_0 K} + \frac{bu^{'3}}{T_0\sqrt{K}}$$

The first term in the above equation is the irreversibility due to heat transfer, the second and the third terms account for entropy generation due to fluid friction and couple stress respectively while the last three terms represent irreversibility due to the effect of magnetic field and porosity.

The dimensionless form as shown in equation (3.50) is given as

$$Ns = \left(\frac{d\theta}{dy}\right)^2 + \frac{Br}{\Omega}\left\{\left(\frac{du}{dy}\right)^2 + \frac{1}{a^2}\left(\frac{d^2u}{dy^2}\right)^2 + H^2u^2 + \beta^2u^2 + \alpha^2u^3\right\}$$

Investigating entropy generation within the flow, let

$$N_1 = \left(\frac{d\theta}{dy}\right)^2, N_2 = \frac{Br}{\Omega}\left\{\left(\frac{du}{dy}\right)^2 + \frac{1}{a^2}\left(\frac{d^2u}{dy^2}\right)^2 + H^2u^2 + \beta^2u^2 + \alpha^2u^3\right\} \tag{3.68}$$

The Bejan number $Be = 0$ is the irreversibility due to viscous dissipation, couple stress effect, The Bejan number can be written as in equation (3.42)

3.3.11 Model 3: Inherent Irreversibility Analysis in Buoyancy Induced Magnetohydrodynamic Couple Stress Fluid

In this present section, the objective is to analyze the inherent irreversibiliy analysis in a buoyancy induced MHD couple stress fluid.

3.3.12 Formulation of Model 3

The following assumptions are made:

(i) The flow is steady, electrically conducting and incompressible,

(ii) the fluid is viscous and flow through vertical porous medium,

(iii) the channel walls exchange heat with the ambient surrounding following the Newton's cooling law,

(iv) a uniform magnetic field of strength (B_0) is applied,

(v) hall effect and induced magnetic field (since magnetic Reynolds number is very small for most fluid used in industrial applications) will be neglected and

(vi) there is injection at the plate where $y = 0$ and suction at the plate where $y =$ h at the same velocity v_0

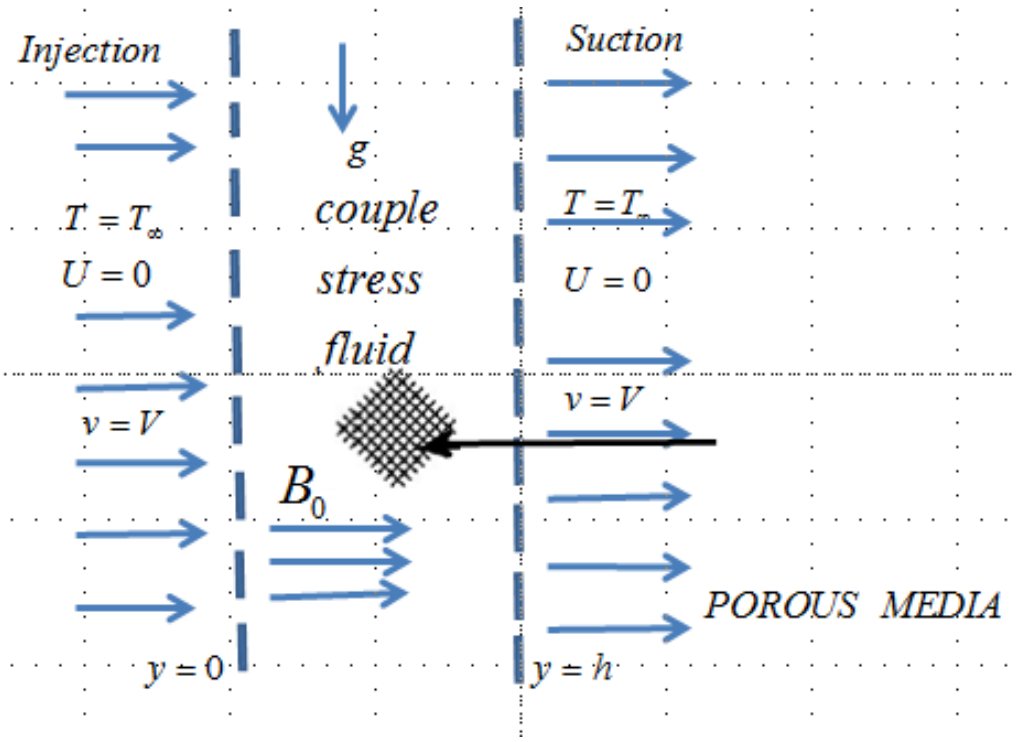

Figure 3.3: Schematic diagram for Model 3

Then the governing equations for the momentum, heat balance and entropy generation rate can be written as Adesanya and Makinde, (2015b)

$$\rho V_0 \frac{du^{'}}{dy^{'}} = -\frac{dp}{dx^{'}} + \mu \frac{d^2u^{'}}{dy^{'2}} - \eta \frac{d^4u^{'}}{dy^{'4}} - \sigma B_0^2 u^{'} - \frac{\mu u^{'}}{K} - \frac{bu^{'2}}{\sqrt{K}} + g\zeta(T - T_0) \tag{3.69}$$

$$\rho C_p v_0 \frac{dT}{dy^{'}} = k\frac{d^2T^{'}}{dy^{'2}} + \mu\left(\frac{du^{'}}{dy^{'}}\right)^2 + \eta\left(\frac{d^2u^{'}}{dy^{'2}}\right)^2 + \sigma B_0^2 u^{'2} + \frac{\mu u^{'2}}{K} + \frac{bu^{'3}}{\sqrt{K}} \tag{3.70}$$

$$E_G = \frac{k}{T_0^2}\left(\frac{dT^{'}}{dy^{'}}\right)^2 + \frac{\mu}{T_0}\left(\frac{du^{'}}{dy^{'}}\right)^2 + \frac{\eta}{T_0}\left(\frac{d^2u^{'}}{dy^{'2}}\right)^2 + \frac{\sigma B_0^2 u^2}{T_0} + \frac{\mu u^{'2}}{T_0 K} + \frac{bu^{'3}}{T_0\sqrt{K}} \tag{3.71}$$

The boundary conditions are

$$\begin{aligned} u^{'}(0) = 0 = \frac{d^2u^{'}(0)}{dy^2}, k\frac{dT^{'}(0)}{dy^{'}} = -\gamma_1(T_f - T^{'}), \\ u^{'}(h) = 0 = \frac{d^2u^{'}(h)}{dy^2}, k\frac{dT^{'}(h)}{dy^{'}} = -\gamma_2(T^{'} - T_0) \end{aligned} \tag{3.72}$$

Introducing the following dimensionless variables

$$\begin{aligned} y = \frac{y^{'}}{h}, u = \frac{u^{'}}{v_0}, \theta = \frac{T^{'} - T_0}{T_f - T_0}, s = \frac{v_0 h}{v}, G = -\frac{h^2 dp}{\mu v_0 dx}, a^2 = \mu\frac{h^2}{\eta}, \\ Pr = \frac{v\rho C_p}{k}, Br = \frac{\mu v_0^2}{k(T_f - T_0)}, Bi_1 = \frac{\gamma_1 h}{k}, Bi_2 = \frac{\gamma_2 h}{k}, N_S = \frac{T_0^2 h^2 E_G}{k(T_f - T_0)^2}, \\ \Omega = \frac{T_f - T_0}{T_0}, v = \frac{\mu}{\rho}, H^2 = \frac{\sigma B_0^2 h^2}{\mu}, Gr = \frac{g\zeta\rho h^2(T_h - T_0)}{\mu v} \end{aligned} \tag{3.73}$$

Substituting equation (3.73) into equations (3.69)-(3.72), the following dimensionless equations are obtained

$$s\frac{du}{dy} = G + \frac{d^2u}{dy^2} - \frac{1}{a}\frac{d^4u}{dy^4} - H^2u - \beta^2 u - \alpha^2 u^2 + Gr\theta \tag{3.74}$$

$$\frac{d^2\theta}{dy^2} = sPr\frac{d\theta}{dy} - Br\left\{\left(\frac{du}{dy}\right)^2 + \frac{1}{a^2}\left(\frac{d^2u}{dy^2}\right)^2 + H^2u^2 + \beta^2u^2 + \alpha^2u^3\right\}, \tag{3.75}$$

$$Ns = \left(\frac{d\theta}{dy}\right)^2 + \frac{Br}{\Omega}\left\{\left(\frac{du}{dy}\right) + \frac{1}{a^2}\left(\frac{d^2u}{dy^2}\right)^2 + H^2u^2 + \beta^2u^2 + \alpha^2u^3\right\} \tag{3.76}$$

with the boundary conditions

$$\begin{aligned} u(0) = 0 = \frac{d^2u(0)}{dy^2}, \frac{d\theta(0)}{dy} = Bi_1(0)(\theta - 1); \\ u(1) = 0 = \frac{d^2u(1)}{dy^2}, \frac{d\theta(1)}{dy} = -Bi_2(\theta(1)) \end{aligned} \tag{3.77}$$

3.3.13 Solution by Adomian Decomposition Method

The integral form of equations (3.74) and (3.75) are in the form

$$u(y) = a_1y + \frac{a_2}{3!}y^3 + a^2\int_0^y\int_0^y\int_0^y\int_0^y\left\{G + \frac{d^2u}{dY^2} - s\frac{du}{dY} - H^2u - \beta^2u - \alpha^2u^2 + Gr\theta\right\}dYdYdYdY \tag{3.78}$$

and

$$\theta(y) = a_3 + a_4(y) + \int_0^y\int_0^y\left\{sPr\frac{d\theta}{dY} - Br\left\{\left(\frac{du}{dY}\right)^2 + \frac{1}{a^2}\left(\frac{d^2u}{dY^2}\right)^2 + H^2u^2 + \beta^2u^2 + \alpha^2u^3\right\}\right\}dYdY \tag{3.79}$$

where a_1 ,a_2 ,a_3 , a_4 are the parameters to be determined later.

The ADM infinite series solutions are of the form

$$u(y) = \sum_{n=0}^{\infty}u_n(y), \theta(y) = \sum_{n=0}^{\infty}\theta_n(y) \tag{3.80}$$

Now using equation (3.80) in equations (3.78)-(3.79), gives

$$\sum_{n=0}^{\infty}u_n(y) = a_1y + \frac{a_2}{3!}y^3 + a^2\int_0^y\int_0^y\int_0^y\int_0^y\left\{G + \sum_{n=0}^{\infty}\frac{d^2u_n}{dY^2} - s\sum_{n=0}^{\infty}\frac{du_n}{dY} - H^2\sum_{n=0}^{\infty}u_n - \beta^2\sum_{n=0}^{\infty}u_n - \alpha^2\sum_{n=0}^{\infty}u_n^2 + Gr\sum_{n=0}^{\infty}\theta_n\right\}dYdYdYdY \tag{3.81}$$

and

$$\sum_{n=0}^{\infty}\theta_n(y) = a_3 + a_4 y + \int_0^y\int_0^y \Bigg\{ sPr\sum_{n=0}^{\infty}\frac{d\theta_n}{dY} - Br\Bigg\{\Bigg(\sum_{n=0}^{\infty}\frac{du_n}{dY}\Bigg)^2 + \frac{1}{a^2}\Big(\sum_{n=0}^{\infty}\frac{d^2u_n}{dY^2}\Big)^2 + H^2\sum_{n=0}^{\infty}u_n^2 + \beta^2\sum_{n=0}^{\infty}u_n^2 + \alpha^2\sum_{n=0}^{\infty}u_n^3\Bigg\}\Bigg\}dYdY \tag{3.82}$$

From equations (3.81)-(3.82), the zeroth order terms can be written as

$$\sum_{n=0}^{\infty}u_0(y)a_1 y + \frac{a_2}{3!}y^3 + a^2\int_0^y\int_0^y\int_0^y\int_0^y \Big\{G\Big\}dYdYdYdY \tag{3.83}$$

$$\sum_{n=0}^{\infty}\theta_0(y) = a_3 + a_4 y \tag{3.84}$$

and the recurrence relations below are used to determine other terms.

$$\sum_{n=0}^{\infty}u_{n+1}(y) = a^2\int_0^y\int_0^y\int_0^y\int_0^y \Bigg\{\sum_{n=0}^{\infty}\frac{d^2u_n}{dY^2} - s\sum_{n=0}^{\infty}\frac{du_n}{dY} - H^2\sum_{n=0}^{\infty}u_n - \beta^2\sum_{n=0}^{\infty}u_n - \alpha^2\sum_{n=0}^{\infty}u_n^2 + Gr\sum_{n=0}^{\infty}\theta_n\Bigg\}dYdYdYdY \tag{3.85}$$

and

$$\sum_{n=0}^{\infty}\theta_{n+1}(y) = \int_0^y\int_0^y \Bigg\{ sPr\sum_{n=0}^{\infty}\frac{d\theta_n}{dY} - Br\Bigg\{\Bigg(\sum_{n=0}^{\infty}\frac{du_n}{dY}\Bigg)^2 + \frac{1}{a^2}\Big(\sum_{n=0}^{\infty}\frac{d^2u_n}{dY^2}\Big)^2 + H^2\sum_{n=0}^{\infty}u_n^2 + \beta^2\sum_{n=0}^{\infty}u_n^2 + \alpha^2\sum_{n=0}^{\infty}u_n^3\Bigg\}\Bigg\}dYdY \tag{3.86}$$

Substituting (3.61) for the the nonlinear terms in equation (3.86) gives

$$\sum_{n=0}^{\infty}\theta_{n+1}(y) = \int_0^y\int_0^y \Bigg\{ sPr\sum_{n=0}^{\infty}\frac{d\theta_n}{dY} - Br\Bigg\{\Bigg(\sum_{n=0}^{\infty}\frac{du_n}{dY}\Bigg)^2 + \frac{1}{a^2}\Big(\sum_{n=0}^{\infty}\frac{d^2u_n}{dY^2}\Big)^2 + H^2\sum_{n=0}^{\infty}B_n + \beta^2\sum_{n=0}^{\infty}B_n + \alpha^2\sum_{n=0}^{\infty}C_n\Bigg\}\Bigg\}dYdY \tag{3.87}$$

Adomian polynomials for (3.87) are represented as given in equation (3.62).

Solution to equations (3.83) - (3.85) and (3.87) can be obtained by solving at $n = 0, 1, 2, 3, \ldots$

3.3.14 Entropy Generation

The expression for entropy generation according to Bejan (1996) in equation (3.71) given below suggests five sources of entropy production. The first term is irreversibility due to heat transfer, the second term is irreversibility due to fluid friction while the last three terms are entropy generation due to couple stresses, magnetic field and porosity respectively.

$$E_G = \frac{k}{T_0^2}\left(\frac{dT'}{dy'}\right)^2 + \frac{\mu}{T_0}\left(\frac{du'^2}{dy'}\right)^2 + \frac{\eta}{T_0}\left(\frac{d^2u'}{dy'^2}\right)^2 + \frac{\sigma B_0^2 u^2}{T_0} + \frac{\mu u'^2}{T_0 K} + \frac{bu'^3}{T_0\sqrt{K}}$$

The dimensionless form of the entropy generation expression in equation (3.76) is also written as:

$$Ns = \left(\frac{d\theta}{dy}\right)^2 + \frac{Br}{\Omega}\left\{\left(\frac{du}{dy}\right)^2 + \frac{1}{a^2}\left(\frac{d^2u}{dy^2}\right)^2 + H^2u^2 + \beta^2u^2 + \alpha^2u^3\right\}$$

entropy generation rate is investigated by setting

$$N_1 = \left(\frac{d\theta}{dy}\right)^2, N_2 = \frac{Br}{\Omega}\left\{\left(\frac{du}{dy}\right)^2 + \frac{1}{a^2}\left(\frac{d^2u}{dy^2}\right)^2 + H^2u^2 + \beta^2u^2 + \alpha^2u^3\right\} \tag{3.88}$$

where N_1 is irreversibility due to heat transfer and N_2 represents fluid friction irreversibility with couple stresses, magnetic field and porosity. To describe the contribution of heat transfer irreversibility to the overall entropy generation, the Bejan number Be is employed. It gave the ratio of heat transfer and viscous dissipation with magnetic field within the channel as shown in (3.42)

3.3.15 Model 4: Combined Effects of Velocity Slip, Temperature Jump and Thermal Radiation on Entropy Generation of a Reactive Hydromagnetic Couple Stress Fluid Through Vertical Porous Medium

Optimal energy utilization has been the concern of engineers and scientists over the years. It is in the light of this that various investigations have been conducted to reduce all forms of wastage. Available research works in literature reveal that not much has been done on the effect of velocity slip and temperature jump on entropy generation. Most of the works on entropy generation did not address the impact of slip and temperature jump on entropy generation (Adesanya, 2014; Adesanya and Falade, 2015; Adesanya and Makinde, 2015c; Adesanya *et al.*, 2015; Ajibade *et al.*, 2011). Motivated by studies Adesanya and Makinde (2015b), Adesanya *et al.* (2015) and Rashidi and Freidoonimehr (2012), the aim of this section is to investigate the effects of velocity slip, temperature jump and thermal radiation on the entropy generation of hydromagnetic reactive couple stress fluid through vertical porous medium.

3.3.16 Formulation of Model 4

Consider the steady and thermally developed flow of an incompressible reactive couple stress fluid in the presence of velocity slip and temperature jump placed between two parallel impermeable plates with isothermal boundary conditions. A constant magnetic field of strength B_0 is applied. It is assumed that the fluid motion is induced by applied axial pressure gradient. It is further assumed that the radiative heat flux in the energy equation follows Roseland approximation. Neglecting the consumption of the reactant, then the governing equations for Navier-Stokes, heat balance equation and entropy generation expression are written as Adesanya *et al.* (2015); Adesanya, (2015); Rashidi and Freidoonimehr, (2012) (see Figure 3.4).

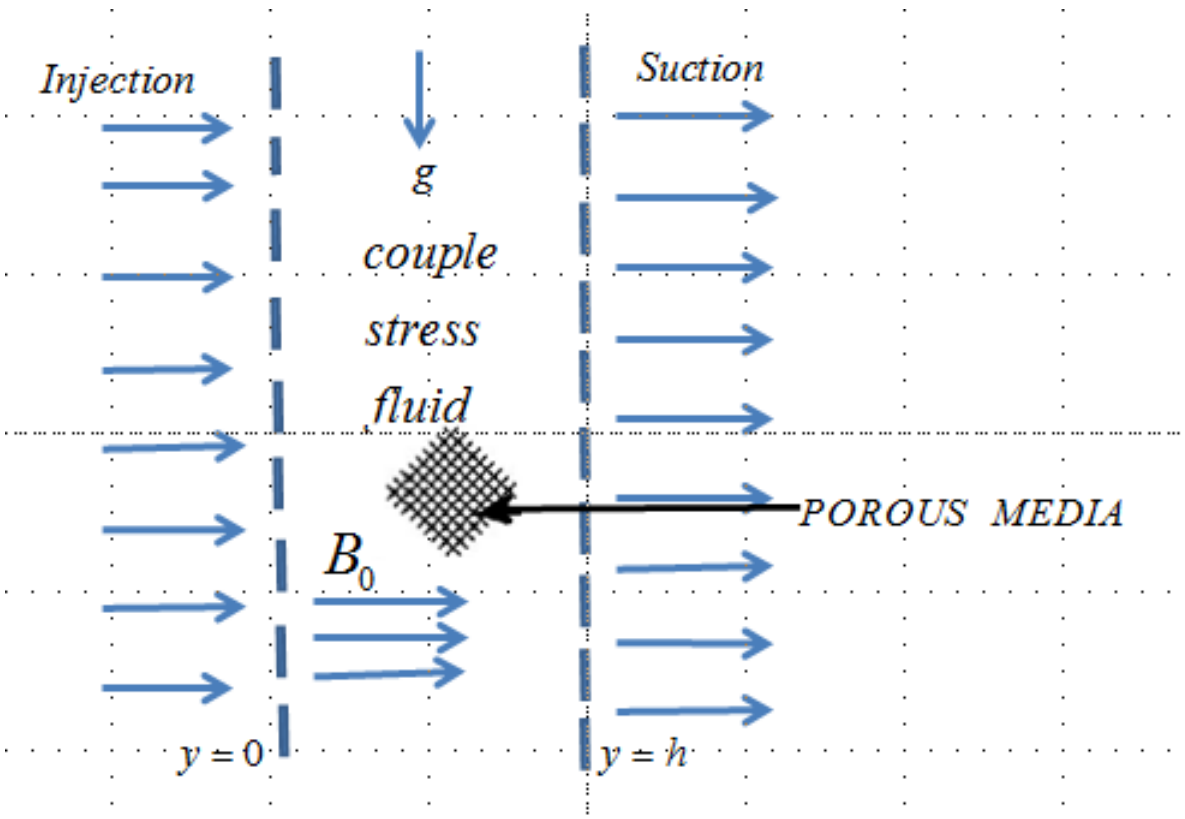

Figure 3.4: Schematic diagram for Model 4

$$0 = -\frac{dp}{dx'} + \mu\frac{d^2u'}{dy'^2} - \eta\frac{d^4u'}{dy'^4} - \sigma B_0^2 u' - \frac{\mu u'}{K} - \frac{bu'^2}{\sqrt{K}} + g\zeta(T - T_0) \tag{3.89}$$

$$0 = \frac{d^2T'}{dy'^2} + \frac{QC_0A}{k}e^{-\frac{E}{RT}} + \mu\Big(\frac{du'}{dy'}\Big)^2 + \eta\frac{d^2u'}{dy'^2} + \frac{\mu u'^2}{K} + \frac{bu'^3}{\sqrt{K}} + \sigma B_0^2 u'^2 - \frac{dq_r}{dy'} \tag{3.90}$$

$$E_G = \frac{k}{T_0^2}\Big(\frac{dT'}{dy'}\Big)^2 + \frac{16\sigma^c T_0^3}{3k^*}\Big(\frac{dT'}{dy'}\Big)^2 + \frac{\mu}{T_0}\Big(\frac{du'}{dy'}\Big)^2 + \frac{\eta}{T_0}(\frac{d^2u'}{dy'^2})^2 + \frac{\mu u'^2}{T_0 K} + \frac{bu'^3}{T_0\sqrt{K}} + \frac{\sigma B_0^2 u'^2}{T_0} \tag{3.91}$$

and the associated boundary conditions are

$$u(0) = 0, u'(0) = u_w + \frac{2-\xi}{\xi}\Psi\frac{du'}{dy'}; u(h) = u'(h) = 0 \tag{3.92}$$

and

$$T'(0) = T_w + \frac{2-\sigma_T}{\sigma_T}\frac{2\phi}{\phi+1}\frac{\Psi}{Pr}\frac{dT'}{dy'}; T'(h) = 0 \tag{3.93}$$

Invoking the Roseland approximation (Raptis *et al.*, 2004) for radiation to obtain

$$q_r = \frac{4\sigma}{3k^*}\frac{dT'^4}{dy'} \tag{3.94}$$

Equation (3.94) can be expressed as a linear function of temperature by expanding T'^4 in a Taylor series about T_0

$$T'^4 = T_0'^4 + 4T_0'^4(T' - T_0') + 6T_0'^2(T' - T_0')^2 + 4T_0'(T' - T_0')^3 + (T' - T_0')^4 \tag{3.95}$$

and neglecting second and higher order terms to have

$$T'^4 \equiv 4T_0^3 T - 3T_0^3 \tag{3.96}$$

Substituting equations (3.95) and (3.96) in equation (3.90) gives

$$0 = \frac{d^2T^{'}}{dy^{'2}} + \frac{QC_0A}{k}e^{-\frac{E}{RT}} + \mu\Big(\frac{du^{'}}{dy^{'}}\Big) + \eta\frac{d^2u^{'}}{dy^{'2}} + \frac{\mu u^{'2}}{K} + \frac{bu^{'3}}{\sqrt{K}} + \sigma B_0^2 u^{'2} + \frac{16\sigma T_0^3}{3k^*}\frac{d^2T}{dy^{'2}} \tag{3.97}$$

the following are the dimensionless variables

$$y = \frac{y^{'}}{h}, u = \frac{u^{'}}{UM}, \theta = \frac{E(T-T_0)}{RT_0^2}, \lambda = \frac{QEAC0h^2e^{-\frac{E}{RT}}}{RT_0^2k},$$
$$M = -\frac{h^2}{\mu U}\frac{dP}{dx}, \epsilon = \frac{RT_0}{E}, \delta = \frac{U^2\mu M^2 e^{\frac{E}{RT}}}{QAC_0h^2}, a = \frac{h}{l}, l = \sqrt{\frac{\eta}{\mu}},$$
$$\beta = \sqrt{\frac{1}{Da}}, Da = \frac{k}{h^2}, N_s = \frac{h^2E^2E_G}{kR^2T_0^2}, H^2 = \frac{\sigma B_0^2h^2}{\rho},$$
$$Gr = \frac{g\zeta\rho h^2(T_h-T_0)}{\mu v}, k_n = \frac{\Psi}{h}(\frac{2-\sigma_T}{\sigma_T})\frac{2\phi}{\phi+1},$$
$$\gamma = \frac{(2-\xi)\Psi}{\xi h}, N = \frac{4\sigma^c T_0^{'3}}{kk^*} \tag{3.98}$$

Using equation (3.98) in equations (3.89), (3.91)-(3.93) and (3.97) yields the boundary value problems and the dimensionless entropy generation expression

$$0 = 1 + \frac{d^2u}{dy^2} - \frac{1}{a^2}\frac{d^4u}{dy^4} - H^2u - \beta^2u - \alpha^2u^2 + Gr\theta \tag{3.99}$$

$$0 = \left(1+\frac{4N}{3}\right)\frac{d^2\theta}{dy^2} + \lambda\left\{e^{\frac{\theta}{1+\epsilon\theta}} + \delta\Big(\frac{du}{dy}\Big) + \frac{\delta}{a^2}\Big(\frac{d^2u}{dy^2}\Big)^2 + \delta\beta^2u^2 + \delta\alpha^2u^3 + \delta H^2u^2\right\} \tag{3.100}$$

$$Ns = \left(1+\frac{4N}{3}\right)\Big(\frac{d\theta}{dy}\Big)^2 + \frac{\delta\lambda}{\epsilon}\left\{\Big(\frac{du}{dy}\Big)^2 + \frac{1}{a^2}\Big(\frac{d^2u}{dy^2}\Big)^2 + \beta^2u^2 + \alpha^2u^3 + H^2u^2\right\} \tag{3.101}$$

as well as the boundary conditions

$$u(-1) = 0, u^{'}(-1) = 1 + \gamma u^{''}(-1); u(1) = u^{'}(1) = 0,$$
$$\theta(-1) = 1 + \frac{k_n}{Pr}\theta^{'}(0); \theta(1) = 0 \tag{3.102}$$

3.3.17 Solution by Adomian Decomposition

Expressing equations (3.99) and (3.100) in the integral form to obtain

$$u(y) = c_1 y + \frac{c_2}{3!}y^3 + a^2 \int_0^y \int_0^y \int_0^y \int_0^y \Big\{ 1 + \frac{d^2u}{dY^2} - H^2 u - \beta^2 u - \\ -\alpha^2 u^2 + Gr\theta \Big\} dY dY dY dY \tag{3.103}$$

and

$$\theta(y) = c_3 + c_4(y) - \left(\frac{3}{3+4N}\right) \int_0^y \int_0^y \lambda \Big\{ e^{\frac{\theta}{1+\epsilon\theta}} + \delta \Big(\frac{du}{dY}\Big)^2 + \\ \frac{\delta}{a}\Big(\frac{d^2u}{dY^2}\Big)^2 + \delta H^2 u^2 + \delta\beta^2 u^2 + \delta\alpha^2 u^3 \Big\} dY dY \tag{3.104}$$

where c_1 ,c_2 ,c_3 , c_4 are the parameters which will be determined later.

The infinite series solutions by ADM are written as:

$$u(y) = \sum_{n=0}^{\infty} u_n(y), \theta(y) = \sum_{n=0}^{\infty} \theta_n(y) \tag{3.105}$$

Now using equation (3.105) in equations (3.103)-(3.104), gives

$$\sum_{n=0}^{\infty} u_n(y) = c_1 y + \frac{c_2}{3!}y^3 + a^2 \int_0^y \int_0^y \int_0^y \int_0^y \Big\{ 1 + \sum_{n=0}^{\infty} \frac{d^2u_n}{dY^2} - \\ \beta^2 \sum_{n=0}^{\infty} u_n^2 - H^2 \sum_{n=0}^{\infty} u_n - \alpha^2 \sum_{n=0}^{\infty} u_n^2 + Gr \sum_{n=0}^{\infty} \theta_n \Big\} dY dY dY dY \tag{3.106}$$

and

$$\sum_{n=0}^{\infty} \theta_n(y) = c_3 + c_4 - \frac{3}{3+4N} \int_0^y \int_0^y \lambda \Big\{ e^{\frac{\sum_{n=0}^{\infty} \theta_n(y)}{1+\epsilon \sum_{n=0}^{\infty} \theta_n(y)}} + \delta \Big(\sum_{n=0}^{\infty} \frac{du}{dY} \Big)^2 + \frac{\delta}{a} \Big(\sum_{n=0}^{\infty} \frac{d^2u}{dY^2} \Big)^2 + \\ \delta\beta^2 \sum_{n=0}^{\infty} u^2 + \delta H^2 \sum_{n=0}^{\infty} u^2 + \delta\alpha^2 \sum_{n=0}^{\infty} u_n^3 \Big\} dY dY \tag{3.107}$$

From equations (3.106) and (3.107), the zeroth order terms can be written as

$$\sum_{n=0}^{\infty} u_0(y) = c_1 y + \frac{c_2}{3!}y^3 + a^2 \int_0^y \int_0^y \int_0^y \int_0^y \Big\{ 1 \Big\} dY dY dY dY \tag{3.108}$$

$$\sum_{n=0}^{\infty}\theta_0(y) = c_3 + c_4 y \tag{3.109}$$

while other terms can be determined using the recurrence relations

$$\sum_{n=0}^{\infty}u_{n+1}(y) = a^2\int_0^y\int_0^y\int_0^y\int_0^y\left\{\sum_{n=0}^{\infty}\frac{d^2u_n}{dY^2} - \beta^2\sum_{n=0}^{\infty}u_n^2 - H^2\sum_{n=0}^{\infty}u_n - \alpha^2\sum_{n=0}^{\infty}u_n^2 + Gr\sum_{n=0}^{\infty}\theta_n\right\}dY\,dY\,dY\,dY \tag{3.110}$$

and

$$\sum_{n=0}^{\infty}\theta_{n+1}(y) = -\frac{3}{3+4N}\int_0^y\int_0^y\lambda\left\{e^{\frac{\sum_{n=0}^{\infty}\theta_n(y)}{1+\epsilon\sum_{n=0}^{\infty}\theta_n(y)}} + \delta\left(\sum_{n=0}^{\infty}\frac{du}{dY}\right)^2 + \frac{\delta}{a}\left(\sum_{n=0}^{\infty}\frac{d^2u}{dY^2}\right)^2 + \delta\beta^2\sum_{n=0}^{\infty}u^2 + \delta H^2\sum_{n=0}^{\infty}u^2 + \delta\alpha^2\sum_{n=0}^{\infty}u_n^3\right\}dY\,dY \tag{3.111}$$

The non-linear term in equation (3.111) can be written as

$$B_n = u^2; C_n = u^3; A_n = e^{\frac{\theta_n(y)}{1+\epsilon\theta_n(y)}} \tag{3.112}$$

The Adomian polynomials are computed as

$$B_0 = u_0^2,\ B_1 = 2u_0u_1,\ B_2 = 2u_0u_2 + u_1^2, \ldots;\ C_0 = u_0^3,\ C_1 = 3u_0^2u_1,$$
$$C_2 = 3u_0^2u_2 + 3u_0u_1^2, \ldots; A_0 = e^{\frac{\theta_0(y)}{1+\epsilon\theta_0(y)}}, A_1 = \frac{e^{\frac{\theta_0(y)}{1+\epsilon\theta_0(y)}}\theta_1(y)}{[1+\epsilon\theta_0(y)]^2},$$
$$A_2 = \frac{e^{\frac{\theta_0(y)}{1+\epsilon\theta_0(y)}}[(1-2\epsilon-2\epsilon^2\theta_0(y))\theta_1(y)^2 + 2(1+\epsilon\theta_0(y)^2\theta_2(y))]}{2[1+\epsilon\theta_0(y)]^2} \tag{3.113}$$

Substituting (3.112) in equation (3.111) yields

$$\sum_{n=0}^{\infty}\theta_{n+1}(y) = -\frac{3}{3+4N}\int_0^y\int_0^y\lambda\left\{A_n + \delta\left(\sum_{n=0}^{\infty}\frac{du}{dY}\right)^2 + \frac{\delta}{a}\left(\sum_{n=0}^{\infty}\frac{d^2u}{dY^2}\right)^2 + \delta\beta^2\sum_{n=0}^{\infty}u^2 + \delta H^2\sum_{n=0}^{\infty}u^2 + \delta\alpha^2\sum_{n=0}^{\infty}u_n^3\right\}dY\,dY \tag{3.114}$$

3.3.18 Entropy Generation

The local entropy generation rate according to Bejan (1996), given in equation (3.91) is written below:

$$E_G = \frac{k}{T_0^2}\left(\frac{dT^{'}}{dy^{'}}\right)^2 + \frac{16\sigma^c T_0^3}{3k^*}\left(\frac{dT^{'}}{dy^{'}}\right)^2 + \frac{\mu}{T_0}\left(\frac{du^{'}}{dy}\right)^2 + \frac{\eta}{T_0}\left(\frac{d^2u^{'}}{dy^{'2}}\right)^2 + \frac{\sigma B_0^2 u^{'2}}{T_0} + \frac{bu^{'3}}{T_0\sqrt{K}} + \frac{\mu u^{'2}}{T_0 k}$$

The first term in the above equation is the entropy generation due to heat transfer, the second, third, fourth, fifth, sixth and seventy terms are the entropy generation due to radiation, fluid friction, couple stresses and magnetic field and porosity respectively . The dimensionless form in equation (3.101) is given as

$$Ns = \left(1 + \frac{4N}{3}\right)\left(\frac{d\theta}{dy}\right)^2 + \frac{\delta\lambda}{\epsilon}\left\{\left(\frac{du}{dy}\right)^2 + \frac{1}{a}\left(\frac{d^2u}{dy^2}\right)^2 + \beta^2u^2 + \alpha^2u^3 + H^2u^2\right\}$$

Investigating entropy generation within the flow by letting

$$N_1 = \left(1 + \frac{4N}{3}\right)\left(\frac{d\theta}{dy}\right)^2, N_2 = \frac{\delta\lambda}{\epsilon}\left\{\left(\frac{du}{dy}\right)^2 + \frac{1}{a}\left(\frac{d^2u}{dy^2}\right)^2 + \beta^2u^2 + \alpha^2u^3 + H^2u^2 + \delta\alpha^2u^3\right\} \tag{3.115}$$

The Bejan number is given in (3.42)

CHAPTER FOUR

RESULTS AND DISCUSSION

4.1 Introduction

This chapter presents the results of this work, the plots are shown for models 1-4. To be realistic, we have chosen physically meaningful values for Prandtl number between 0.004 and 2 to accommodate fluids such as mercury (0.008-0.041), oxygen (0.729-0.759), air (0.703-0.784) and water vapour (0.882-0.994) (Lienhard IV and Lienhard V, 2006).

4.2 Model 1

Influence of hydromagnetic couple stress fluid with entropy generation through porous channel is analyzed in this model. Semi-analytical solutions by Adomian decomposition method for the velocity and temperature profiles are obtained and validated by DTM solution. The results are used to compute the entropy generation rate and Bejan number. The results are presented in Figures 4.1 - 4.12

4.2.1 Effects of Parameter Variation on Velocity and Temperature Profiles

The effect of parameters variation on velocity and temperature are shown in Figures 4.1-4.6. Figure 4.1 shows the effect of magnetic field parameter on fluid velocity. It is observed that an increase in the magnetic field parameter leads to a decrease in the velocity of the fluid. This is as a result of the presence of Lorentz force that opposes the fluid flow; the force is caused by the applied magnetic field which clusters the fluid particles and thus impedes the free flow of the fluid. In Figure 4.2, variation in suction/injection parameter on fluid velocity is presented. It is observed that as injection of hot fluid into the channel increases there is shift in flow symmetry due

to decrease in fluid kinematic viscosity. Figure 4.3 illustrates the effect of the inverse of couple stress parameter on fluid velocity. Increase in the inverse of couple stresses increases fluid velocity which indicates that couple stress parameter will decrease fluid velocity. The result is physically true because increase in couple stresses enhances fluid viscosity as fluid particles size increases. This is in perfect agreement with result reported in (Adesanya and Makinde, 2015b).

Furthermore, Figure 4.4 depicts the effect of magnetic field on fluid temperature. As seen from the plot, there is an increase in fluid temperature as magnetic field parameter (H^2) increases. The increase can be attributed to the increase in viscous heating which increases the rate of heat transfer from the fluid to the walls. Figure 4.5 shows the plot of suction/injection on temperature profile. Expectedly, we observed an increase in temperature as injection of hot fluid into the channel increases. Figure 4.6 presents the effect of couple stress inverse on temperature. It shows that fluid temperature decreases as couple stress parameter increases. The reason is that fluid viscosity rises with increase in couple stresses.

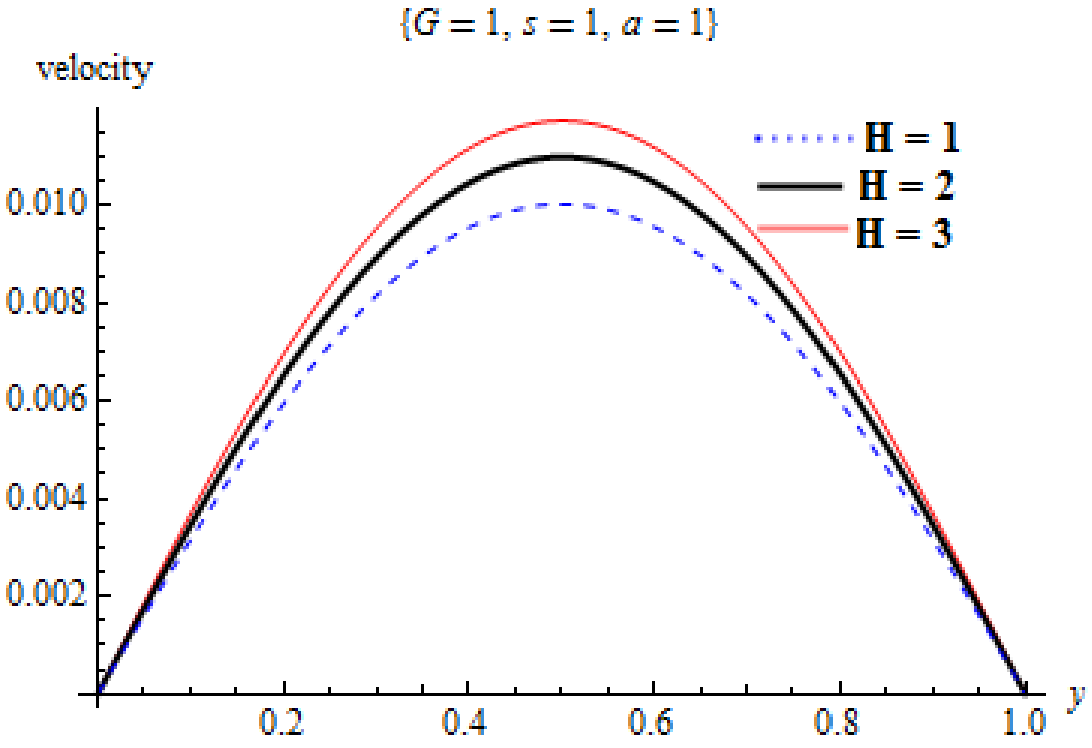

Figure 4.1: Effect of magnetic field parameter (H^2) on velocity profile

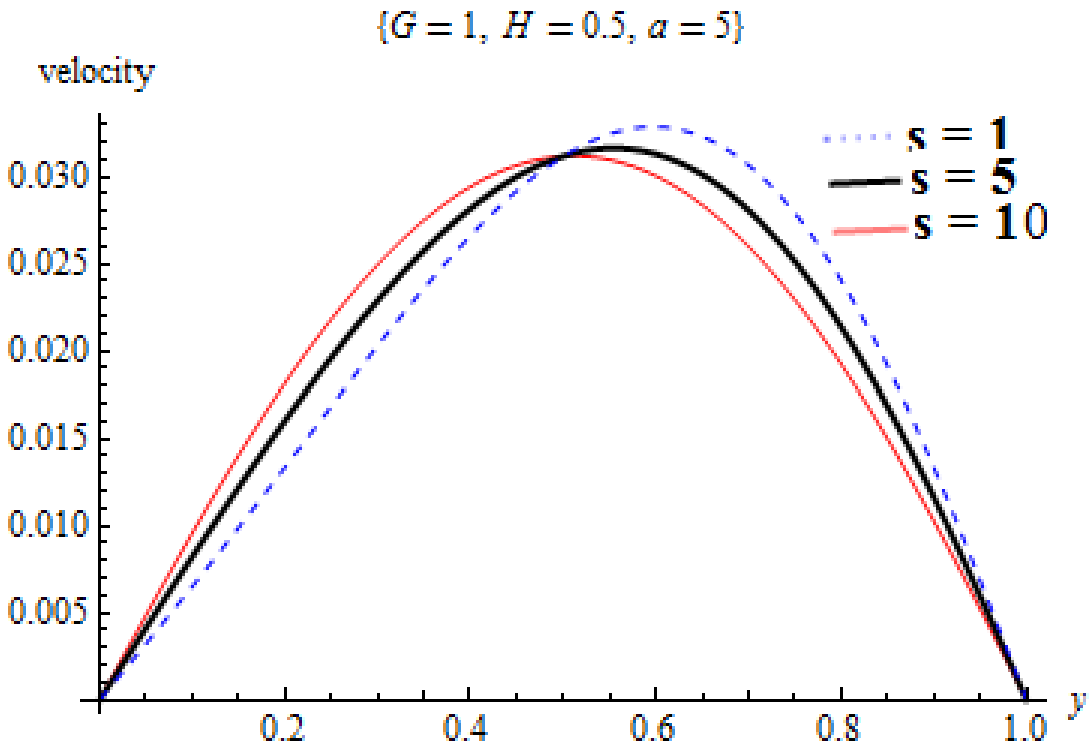

Figure 4.2: Effect of suction/injection (s) on velocity profile

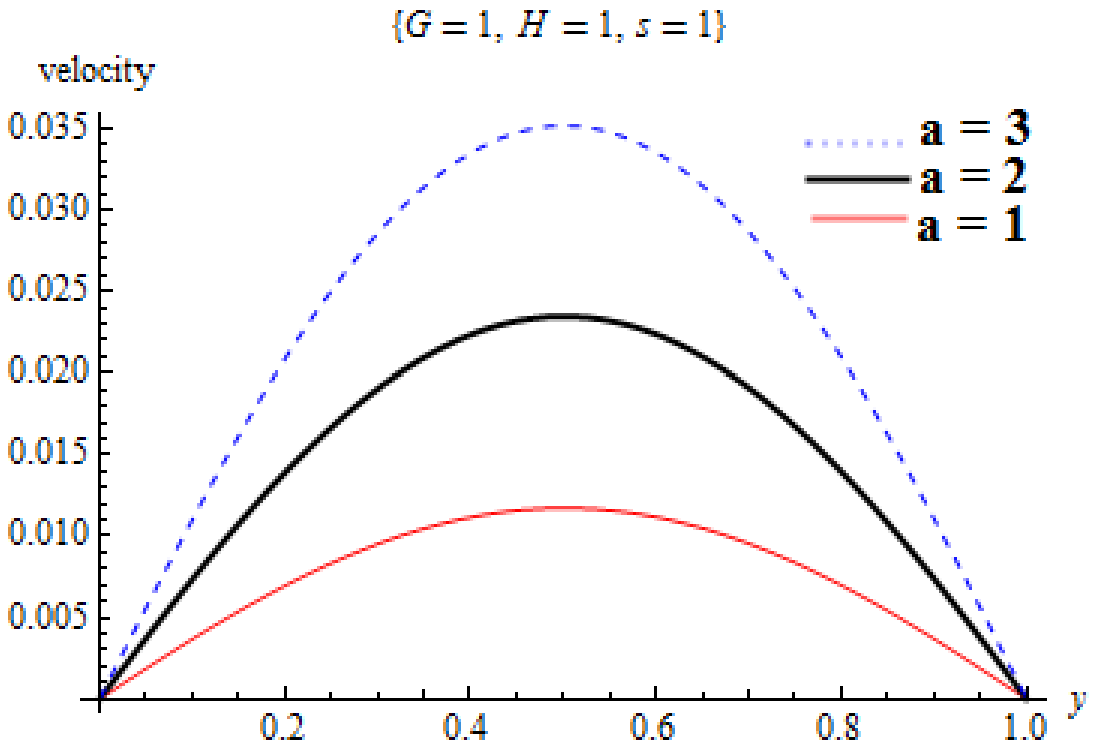

Figure 4.3: Effect of couple stress inverse parameter (a) on velocity profile

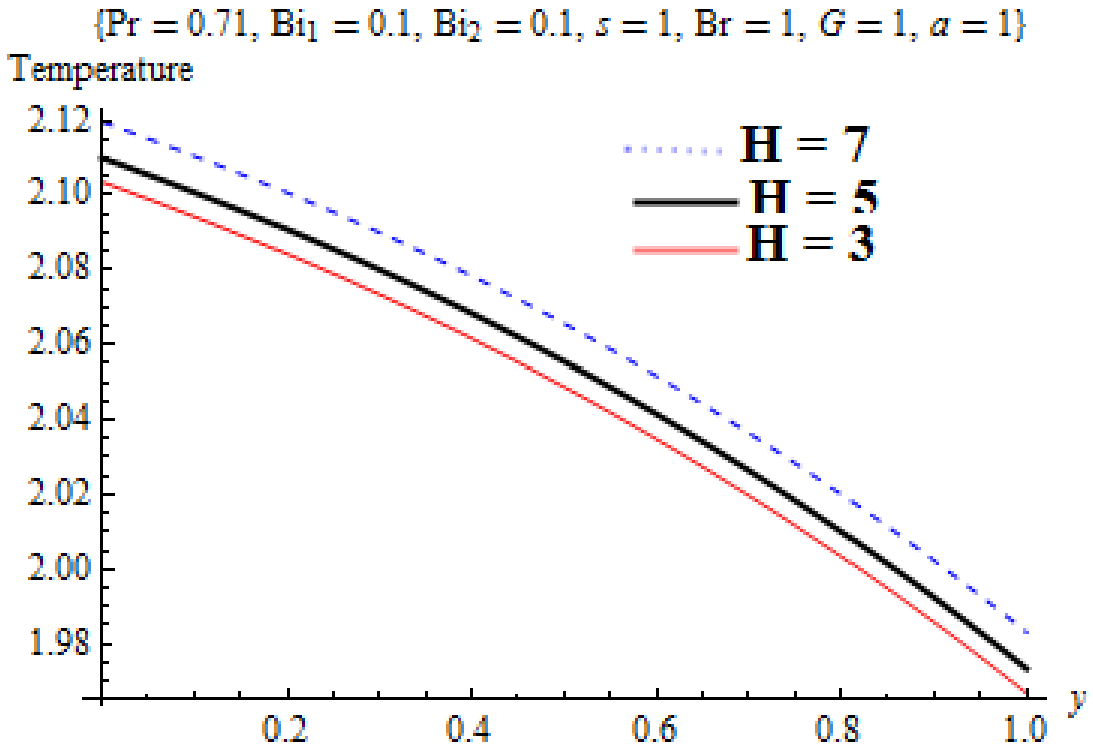

Figure 4.4: Effect of magnetic field parameter (H^2) on temperature profile

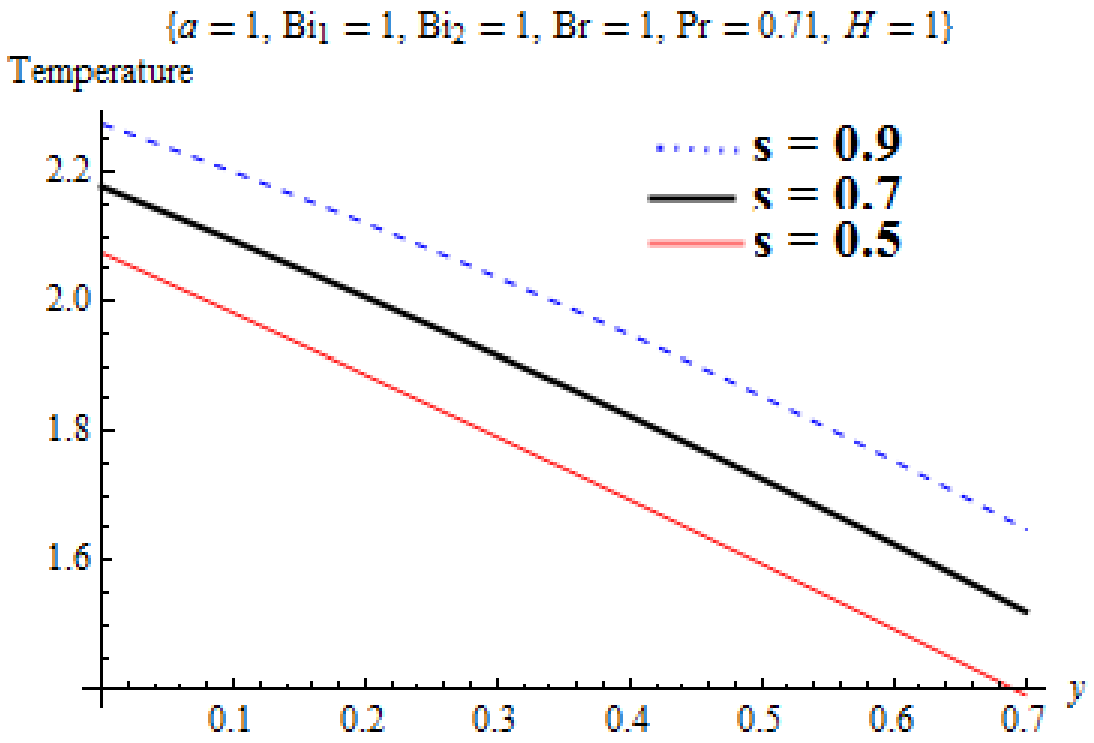

Figure 4.5: Effect of suction/injection (s) on temperature profile

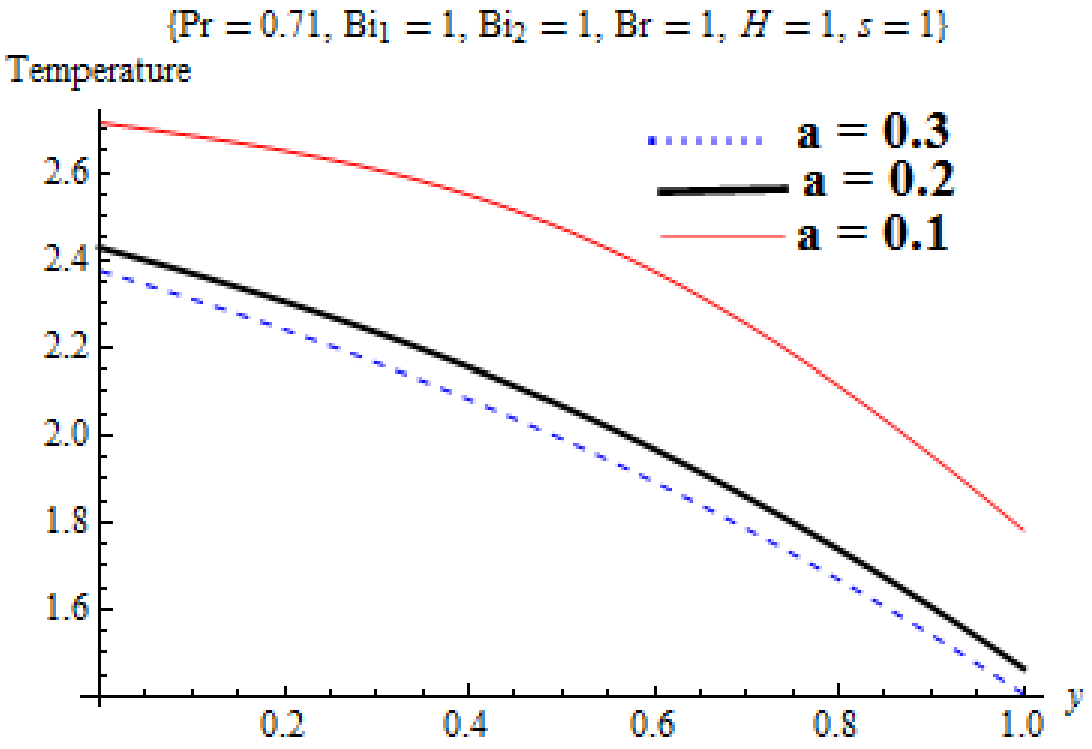

Figure 4.6: Effect of couple stress inverse parameter (a) on temperature profile

4.2.2 Effects of Parameter Variation on Entropy Generation Rate

In Figures 4.7-4.9, the effects of variation of some governing parameters on entropy generation rate are presented. Figure 4.7 depicts the plot of variation in magnetic field parameter on entropy generation. As shown in Figure 4.1, rise in Hartman number decreases the flow velocity while increasing the fluid temperature as reported in Figure 4.4. The net effect on entropy generation rate is presented in Figure 4.7. As observed, increased Hartman number enhances entropy generation. This is true since Hartman number decreases velocity thereby clustering the fluid particle. This clustering enhances viscous dissipation within the layers. Moreover, Hartman number increases fluid temperature implies that the rate of heat transfer from the fluid to the walls must increase. The totality of these is shown to increase entropy generation significantly as confirmed in the plot.

In Figure 4.8, it is shown that entropy generation decreases at the lower wall with injection and in the middle of the channel while it increases at the upper wall with suction. This can be traced to Figure 4.2 where it was submitted that increase in suction/injection parameter leads to a break in flow symmetry within the channel. Figure 4.9, depicts the effect of couple stresses on the entropy generation rate, it is observed that entropy generation increases with increase in couple stress inverse. This implies that increase in couple stresses decreases entropy generation rate. The reason is shown in Figure 4.3 where the plot indicates that fluid velocity reduces with increase in couple stresses due to increase in fluid viscosity as fluid particle size increases. The effect of this on the flow system is to lower the random movement of the fluid particles and consequently the drop in entropy production rate in the core region of the channel than the channel walls.

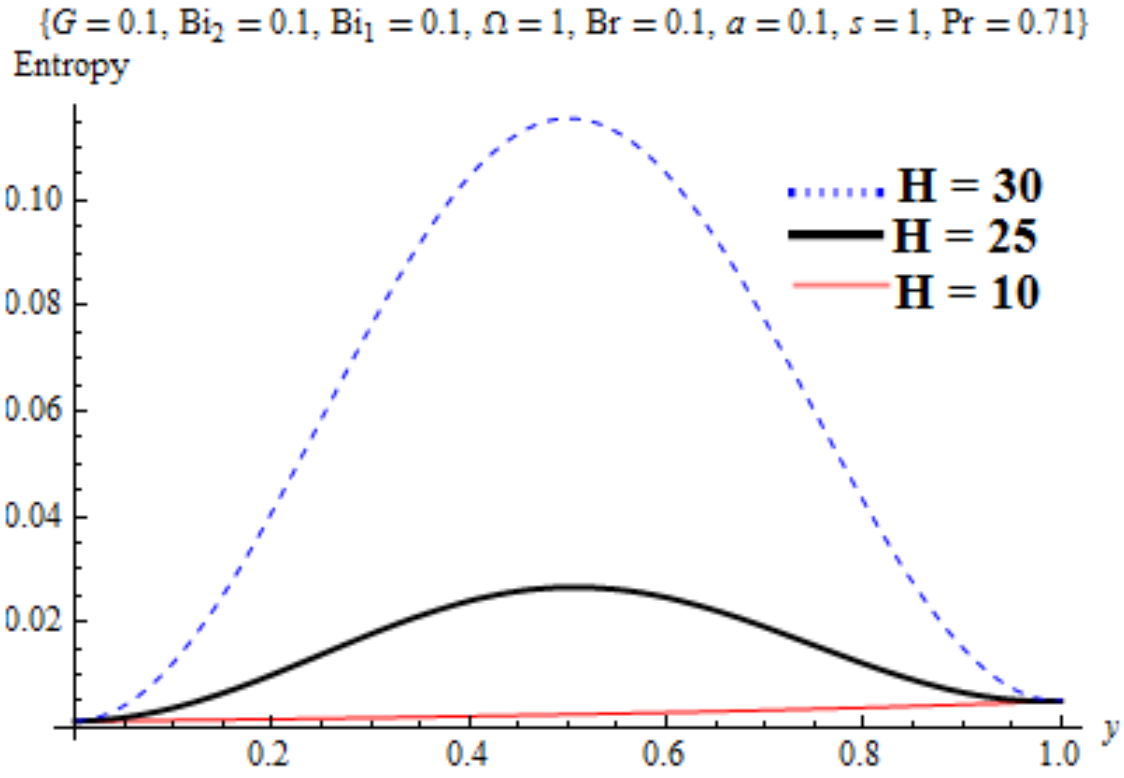

Figure 4.7: Effect of magnetic field parameter (H^2) on entropy generation rate

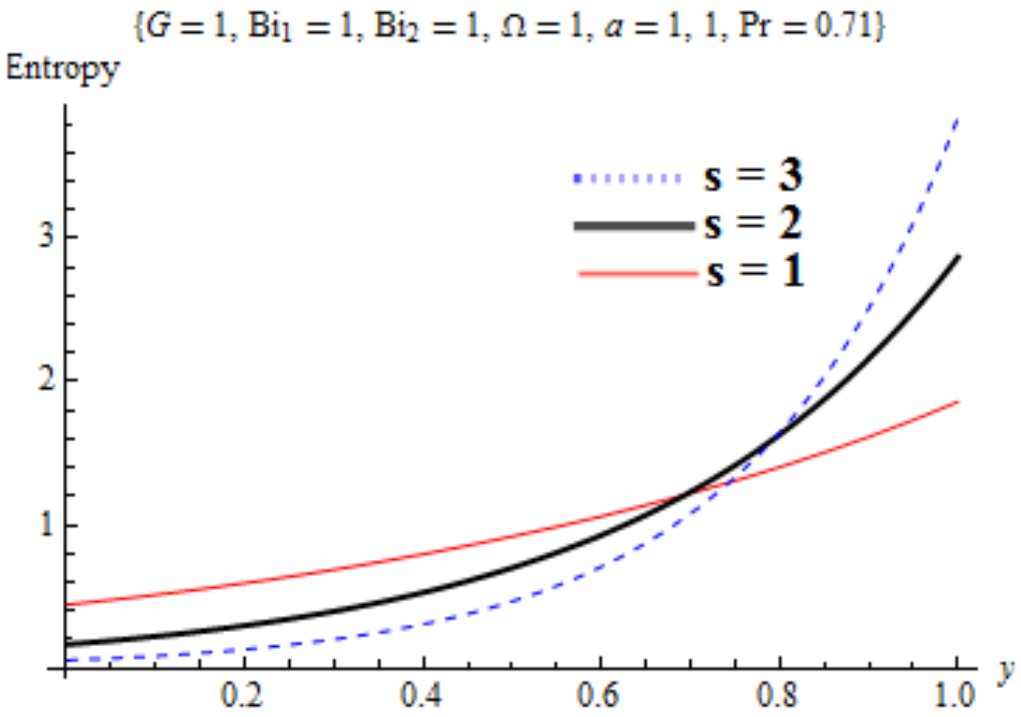

Figure 4.8: Effect of suction/injection (s) on entropy generation rate

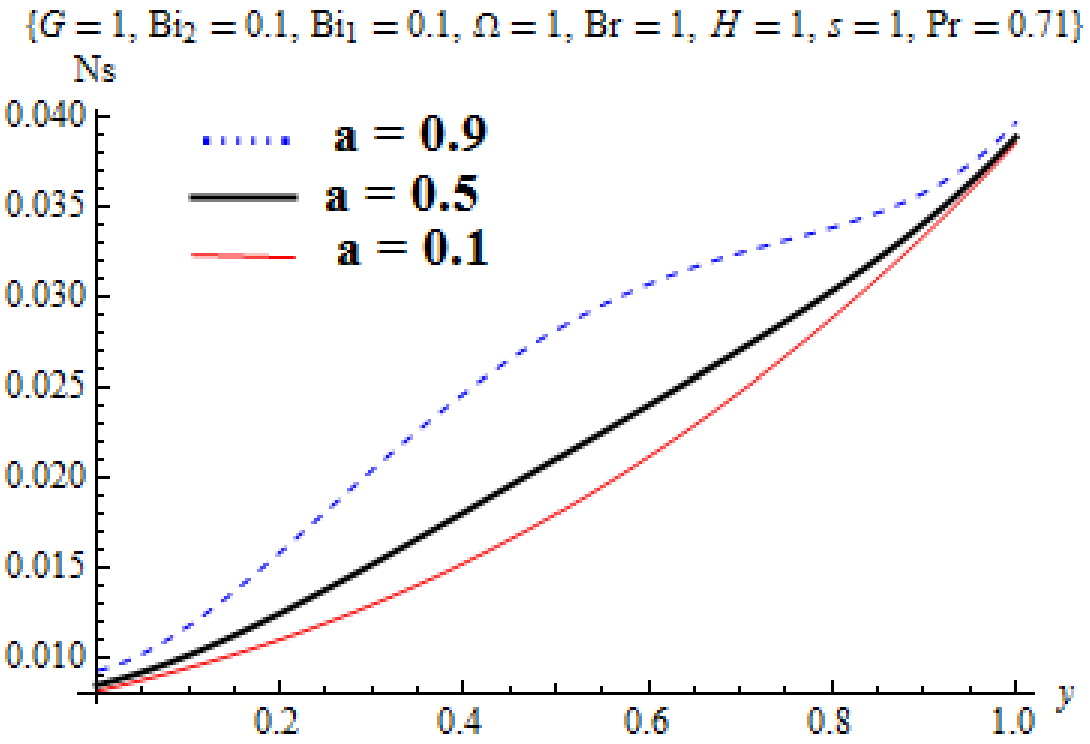

Figure 4.9: Effect of couple stress inverse parameter (a) on entropy generation

4.2.3 Effects of Parameter Variation on Bejan Number

The influence of parameters variation on Bejan number are presented in Figures 4.10-4.12. Figure 4.10 depicts the graph of magnetic field parameter on Bejan number. It is observed that Bejan number increases across the channel as magnetic field parameter increases. This is an indication that heat transfer is the major contributor to irreversibility across the channel. Figure 4.11 represents the effect of suction/injection on Bejan number. The plot indicates that increase in suction/injection decreases Bejan number at the lower wall and at the center of the channel with a slight increase at the upper wall. This shows that irreversibility due to viscous dissipation dominates the flow at the upper wall. Finally the effect of couple stress inverse on entropy generation in Figure 4.12 is presented; it is found that couple stress inverse decreases Bejan number, which indicates that couple stresses retard Bejan number. This suggests the dominance of irreversibility by viscous dissipation over heat transfer.

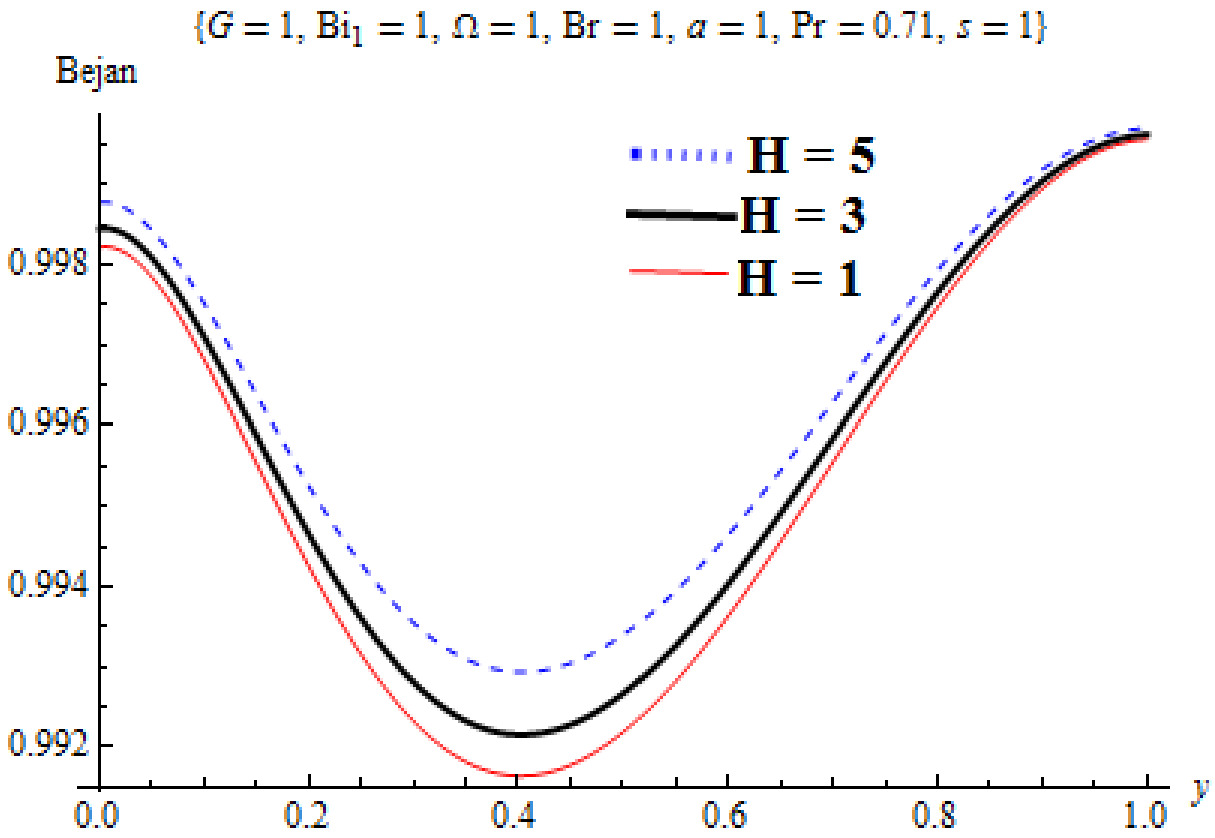

Figure 4.10: Effect of magnetic field parameter (H^2) on Bejan number

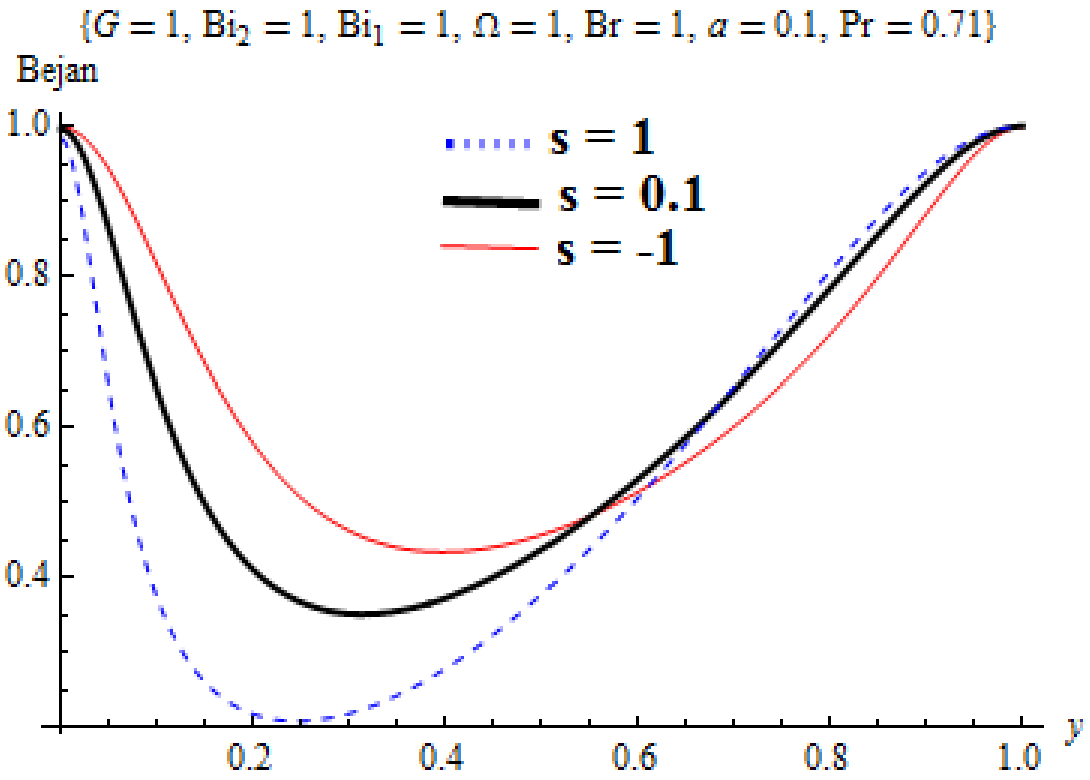

Figure 4.11: Effect of suction/injection (s) on Bejan number

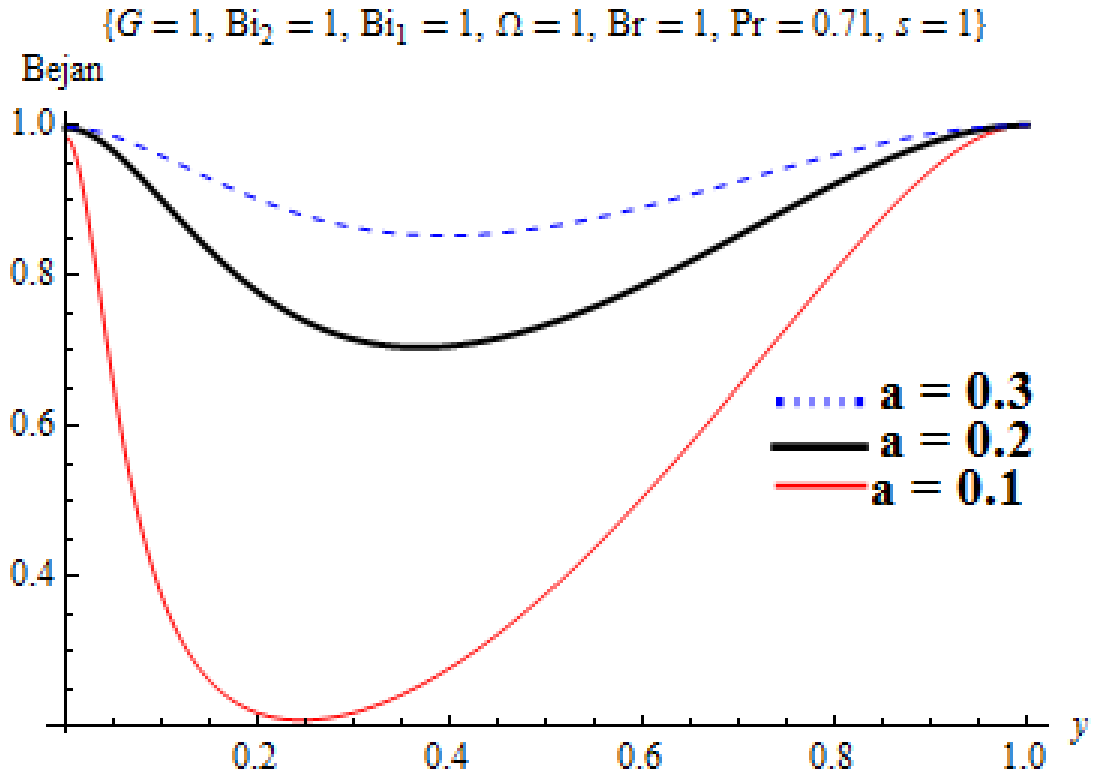

Figure 4.12: Effect of couple stress inverse (a) on Bejan number

4.2.4 Effects of Parameter Variation on Skin Friction

Tables 4.2-4.4 present the effect of parameters variation on skin friction coefficient. Tables 4.2 and 4.3 indicate that skin friction decreases as the value of magnetic field parameter and suction/injection increase while in Table 4.4 skin friction increases with increase in pressure gradient parameter.

Table 4.1: Effect of Magnetic field variation on Skin friction

G	H	s	a	Cf
1	1	1	1	0.03535583
1	2	1	1	0.0344646
1	3	1	1	0.0331398

Table 4.2: Effect of suction/injection on variation on Skin friction

G	H	s	a	Cf
1	1	1	1	0.03535583
1	1	2	1	0.0352547
1	1	3	1	0.0351476

Table 4.3: Effect of Pressure gradient variation on Skin friction

G	H	s	a	Cf
1	1	1	1	0.0353583
2	1	1	1	0.0707166
3	1	1	1	0.106075

4.2.5 Effects of Parameter Variation on Nusselt Number

Tables 4.5-4.7 present the effect of parameters variation on Nusselt number. Table 4.5 presents the effect of variation in magnetic field parameter on Nusselt number. It is noticed that increase in magnetic field parameter leads to a decrease in Nusselt number. Table 4.6 illustrates suction/injection variation on Nusselt number. Increase in suction/injection decreases Nusselt number. Table 4.7 displays the effect of couple stresses on Nusselt number. The table shows that increase in couple stresses increases the Nusselt number.

Table 4.4: Effect of Magnetic field variation on Nusselt number

G	H	s	Pr	Br	a	Nu
1	1	1	0.71	1	1	0.0605638
1	2	1	0.71	1	1	0.0605517
1	3	1	0.71	1	1	0.605316

Table 4.5: Effect of suction/injection variation on Nusselt number

G	H	s	Pr	Br	a	Nu
1	1	1	0.71	1	1	0.605638
1	1	2	0.71	1	1	0.312725
1	1	3	0.71	1	1	0.144648

Table 4.6: Effect of couple stress variation on Nusselt number

G	H	s	Pr	Br	a	Nu
1	1	1	0.71	1	1	0.605638
1	1	1	0.71	1	2	0.608578
1	1	1	0.71	1	3	0.609122

4.3 Model 2

Second law analysis of hydromagnetic couple stress fluid through non-Darcian porous medium has been considered in this model. The graphical results in Figures 4.13-4.27 are presented to explain the influence of pertinent parameters on velocity, temperature, entropy generation and Bejan number.

4.3.1 Effects of Parameters Variation on Velocity and Temperature Profiles

Effect of parameters variation on velocity and temperature are shown in Figures 4.13-4.19. Figure 4.13 depicts the plot of magnetic field parameter on velocity profile; the figure shows that increase in the magnetic field parameter reduces fluid velocity. This can be attributed to the force exerted by the applied magnetic field on fluid particles which clumps the fluid particles together leading to an increase in viscosity and consequently, the drop in fluid velocity. In Figures 4.14 and 4.15, the effects of porous media parameters (β, α) are presented; the graphs reveal that fluid velocity reduces as porous media parameters increase. This can be attributed to the reduction in the porous media permeability (K) of the fluid which reduces the free flow of fluid particles. Figure 4.16 shows the plot of couple stress inverse on velocity profile. As observed from the plot, increase in couple stress inverse parameter increases the velocity profile. It means that couple stress parameter will eventually reduce fluid velocity due to increased viscosity of the fluid.

Figure 4.17 displays the graph of magnetic field parameter variation on fluid temperature. It is observed that fluid temperature increases with increase in magnetic field parameter. This is due to an increase in heat source from the Ohmic heating present in the flow; which enhances transfer of heat to the boundaries. Furthermore, Figure 4.18 indicates that as porous media shape factor parameter rises in value fluid temperature is enhanced. The study shows that reduction in the porous media per-

meability of the fluid is responsible for the rise in temperature. The influence of the inverse of couple stress parameter on temperature is shown in Figure 4.19. It is noticed from the graph that as couple stress inverse parameter increases the temperature of the fluid drops. The implication of this is that, increase in couple stresses enhances fluid thickness that is, the dynamic viscosity increases which increases the temperature.

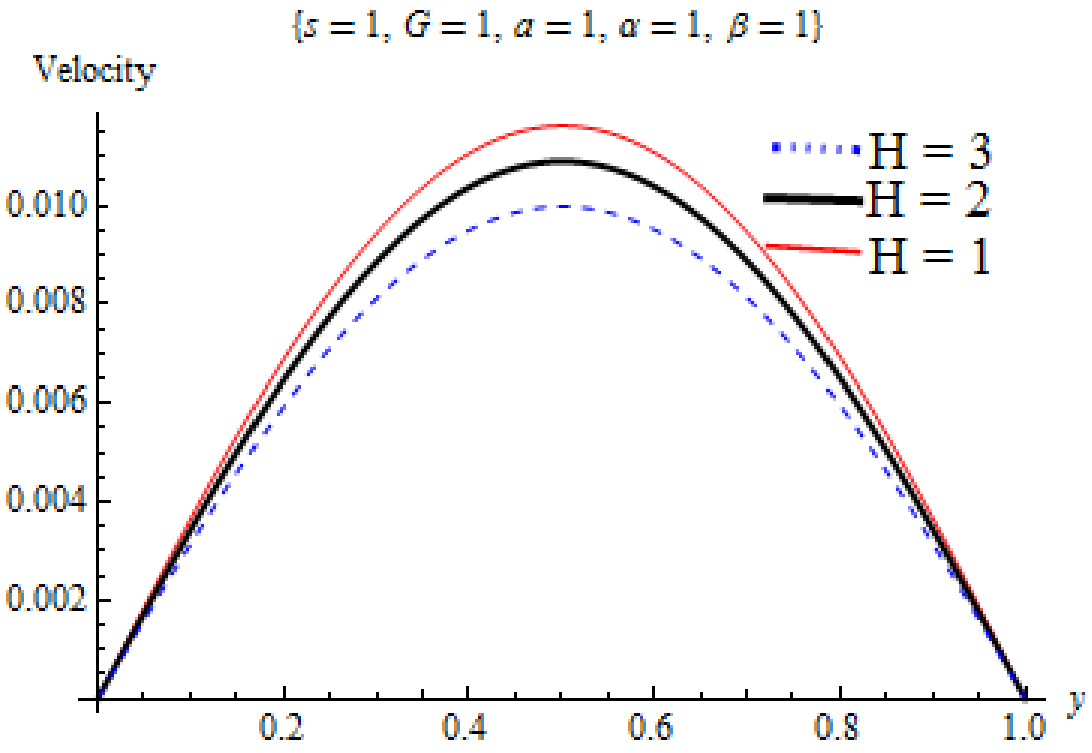

Figure 4.13: Effect of magnetic field parameter (H^2) on velocity profile

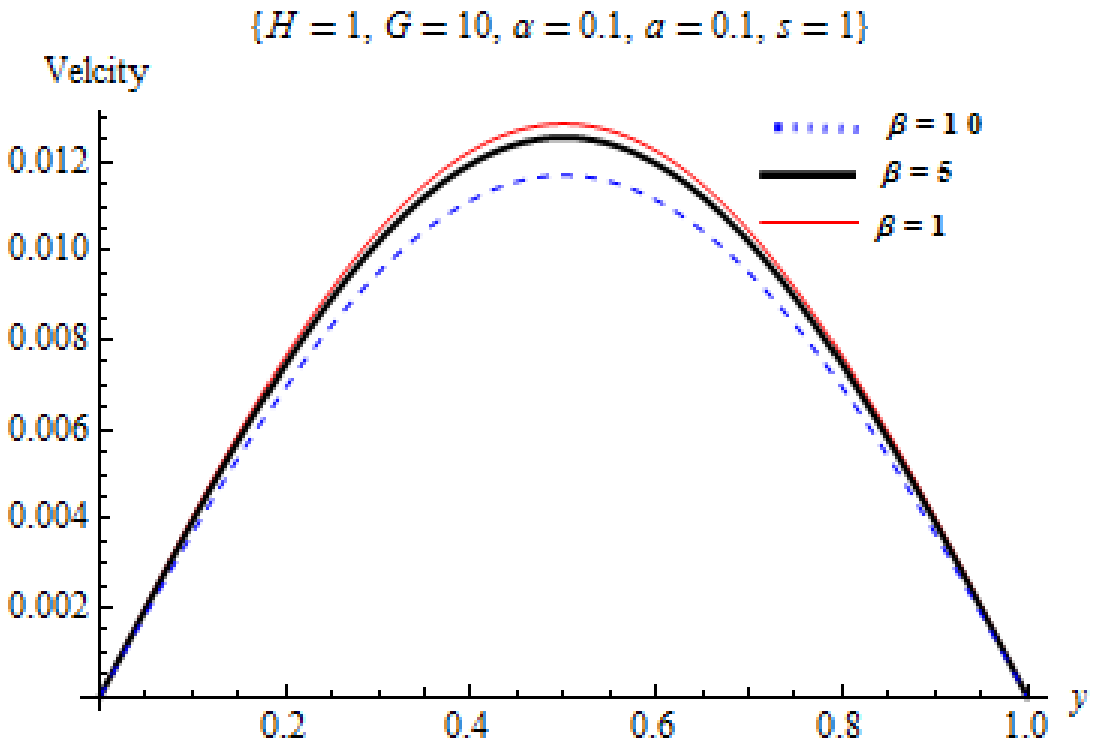

Figure 4.14: Effect of porous media shape factor parameter (β) on velocity profile

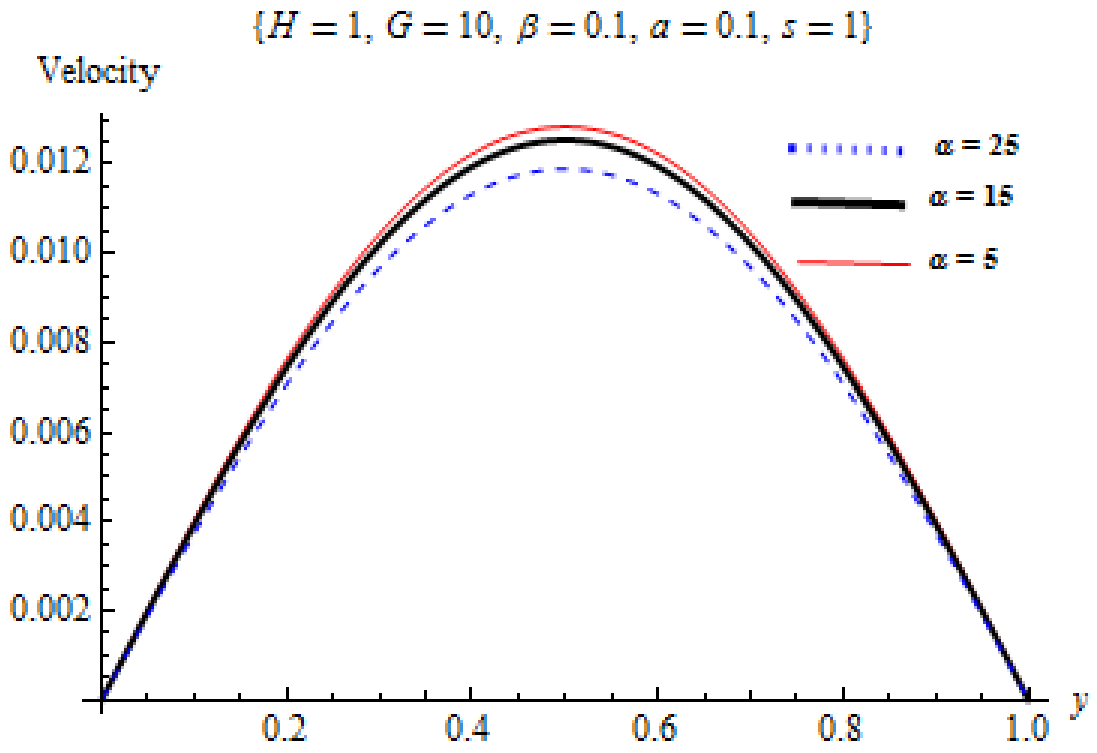

Figure 4.15: Effect of second order porous media resistance parameter (α) on velocity profile

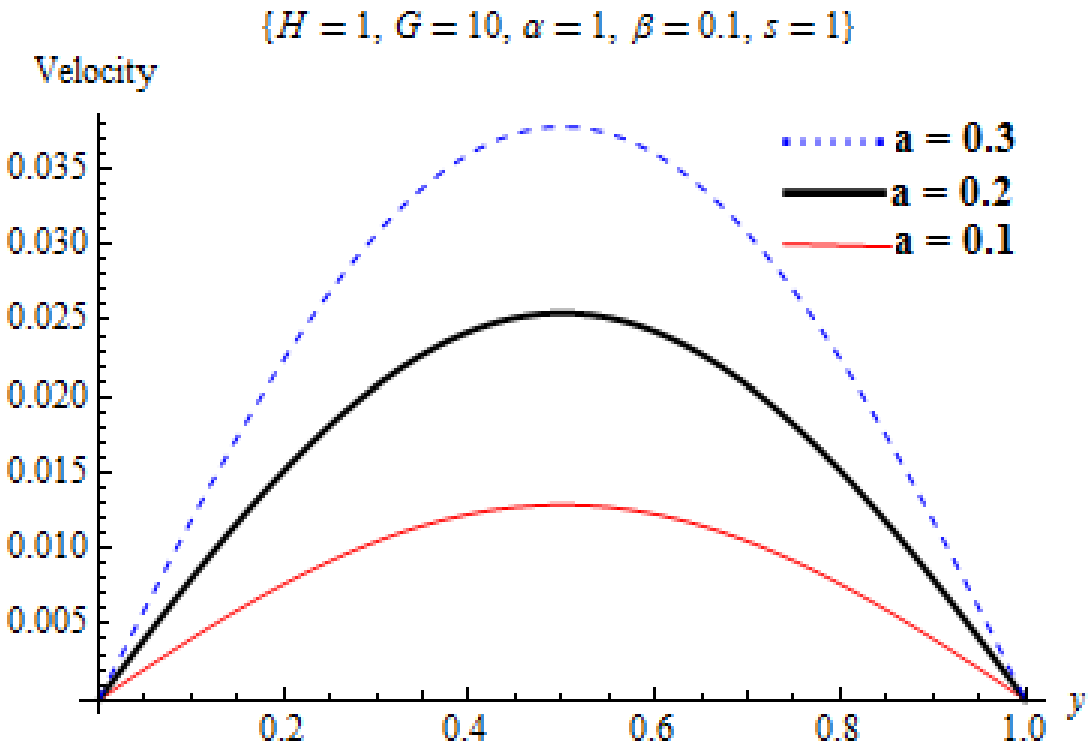

Figure 4.16: Effect of couple stress inverse parameter (a) on velocity profile

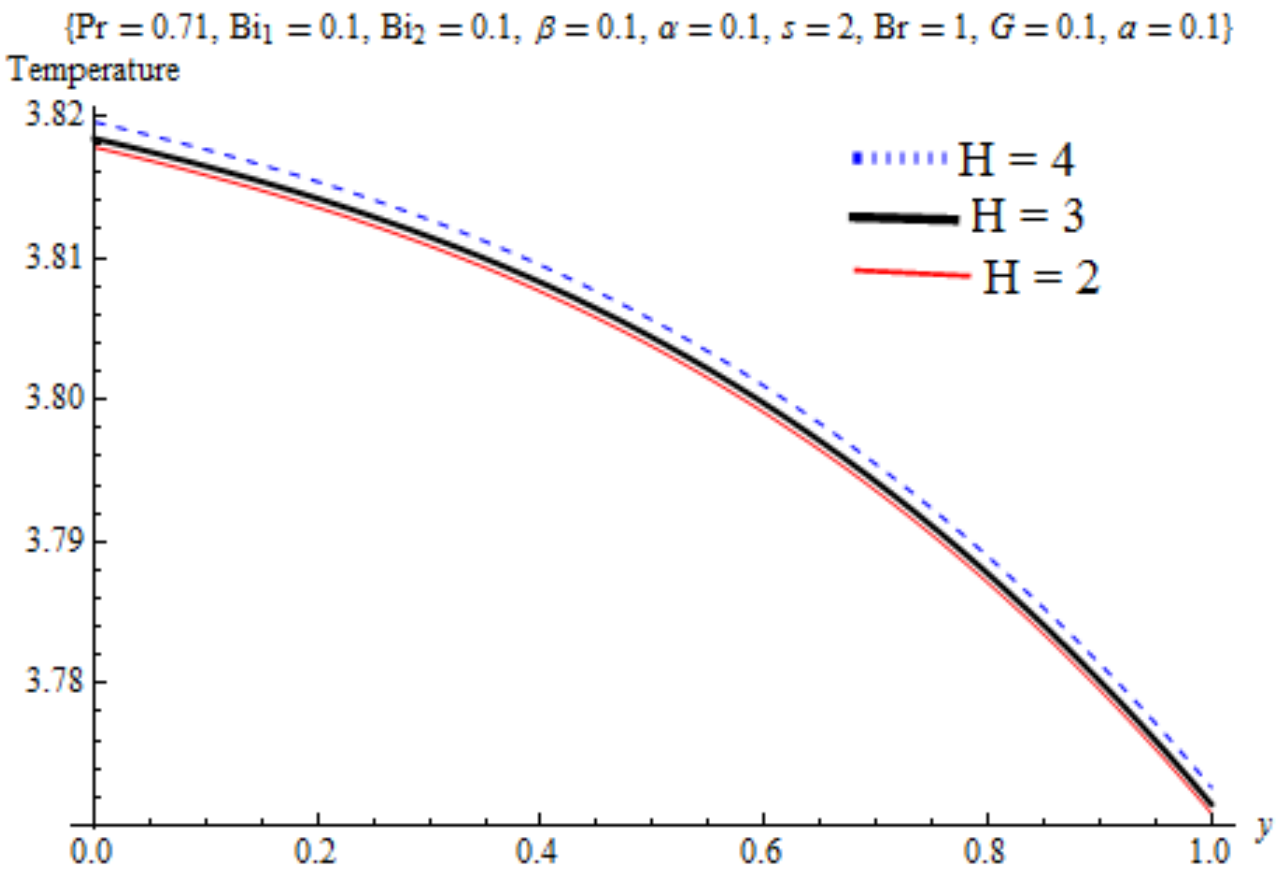

Figure 4.17: Effect of magnetic field parameter (H^2) on temperature profile

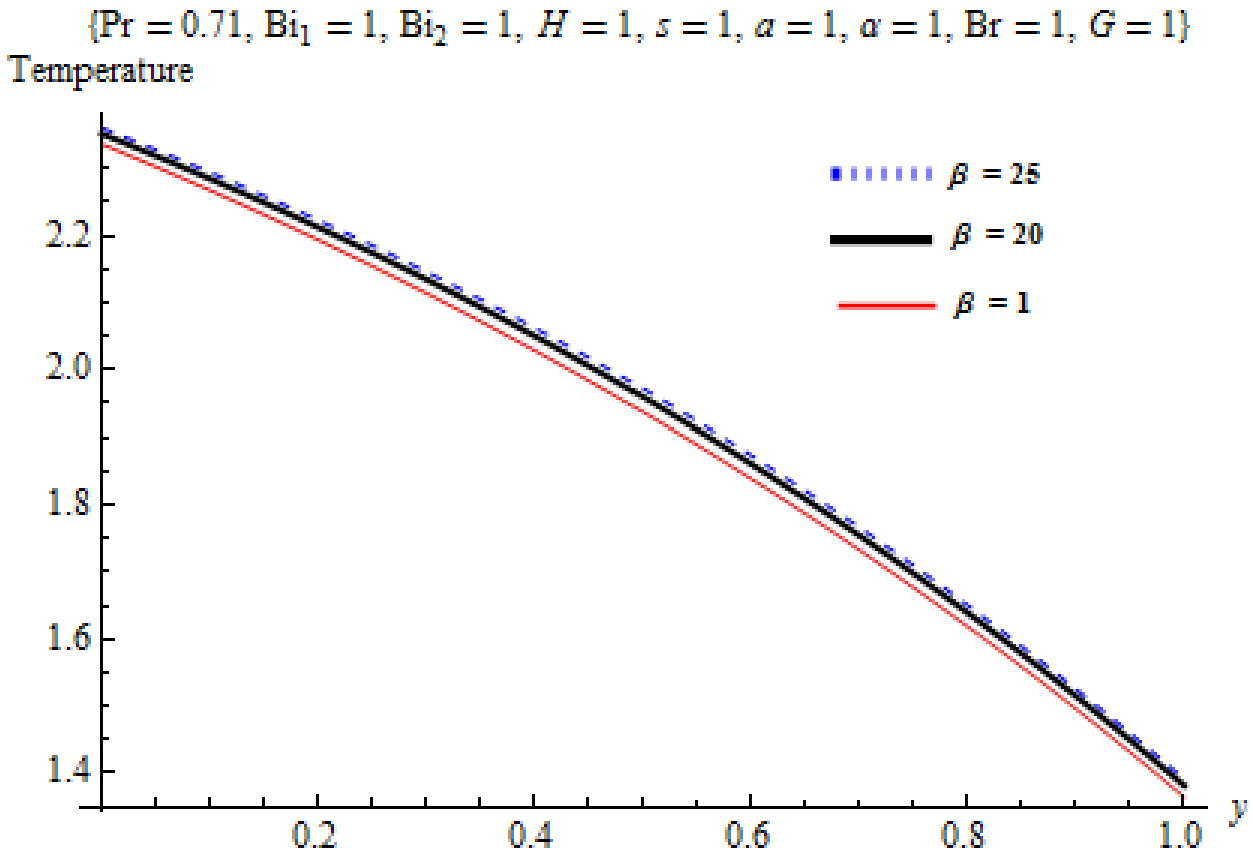

Figure 4.18: Effect of porous media shape factor parameter (β) on temperature profile

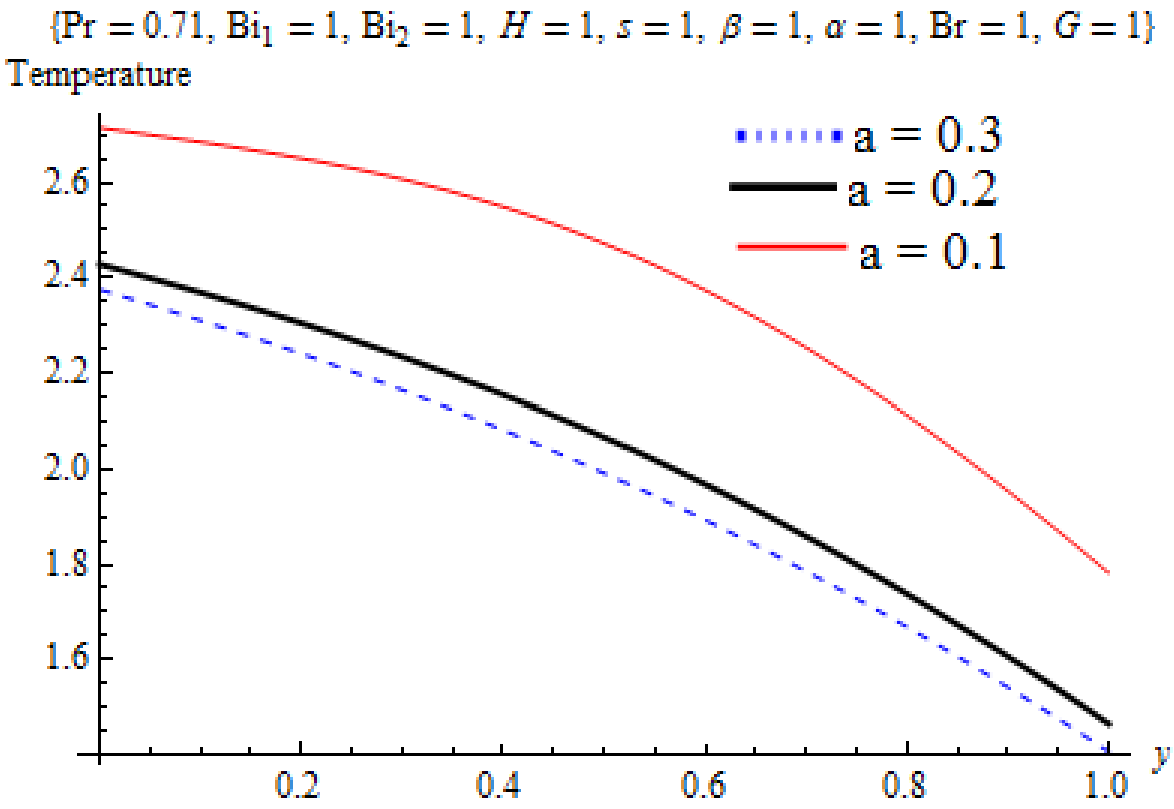

Figure 4.19: Effect of couple stresses (a)on temperature profile

4.3.2 Effects of Parameter Variation on Entropy Generation

The effect of parameters variation on entropy generation rate in Figures 4.20-4.23 are presented. In Figure 4.20, the influence of magnetic field parameter on entropy generation is depicted. It is indicated in the graph that entropy generation is enhanced with increase in magnetic field parameter. This can be traced to Figure 4.13 which shows that fluid velocity decreases with increased Hartman number caused by clumping of fluid particle. Furthermore, it is shown in Figure 4.17 that fluid temperature rises as Hartman number is increased due to increased heat transfer to the boundaries from Ohmic heating. The effect of these is the significant rise in entropy generation displayed in Figure 4.20. In Figures 4.21 and 4.22, the effects of porous shape parameters on entropy generation are displayed. The plots indicate that increase in the porous shape parameters reduces entropy generation. This is clearly shown in Figures 4.14 and 4.15 that fluid velocity reduces with increase in porous media parameters; the drop in fluid velocity reduces the random movement of fluid particles and consequently the reduction in entropy generation rate.

Moreover in Figure 4.23 the graph displays the influence of couple stress inverse parameter on the entropy generation rate. It is revealed that entropy generation rises with increase in couple stress inverse parameter (a). This implies that couple stresses reduce entropy generation due to the reduction in random movement of fluid particles. The drop in the randomness of fluid particles is clearly revealed in Figure 4.16 which shows that fluid velocity decreases with increase in couple stresses.

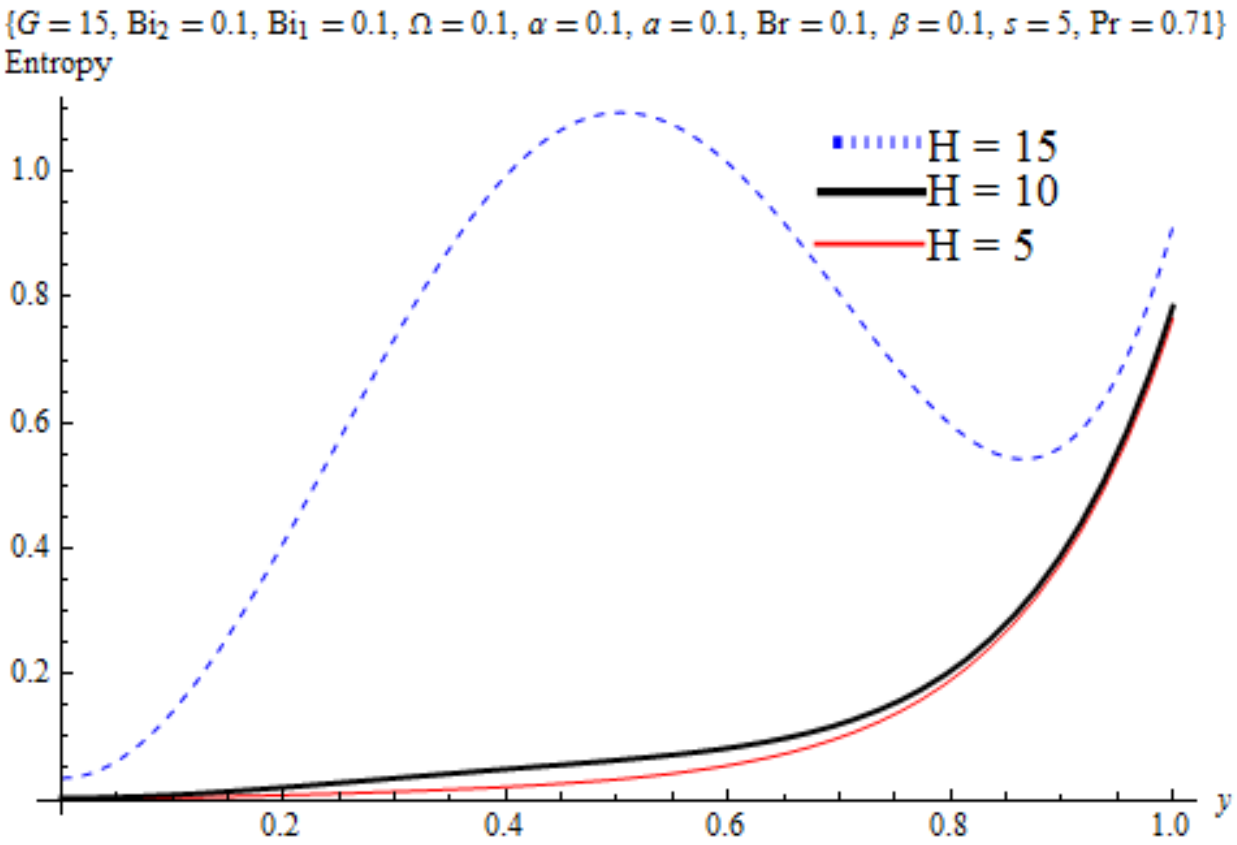

Figure 4.20: Effect of magnetic field parameter (H^2) on entropy generation rate

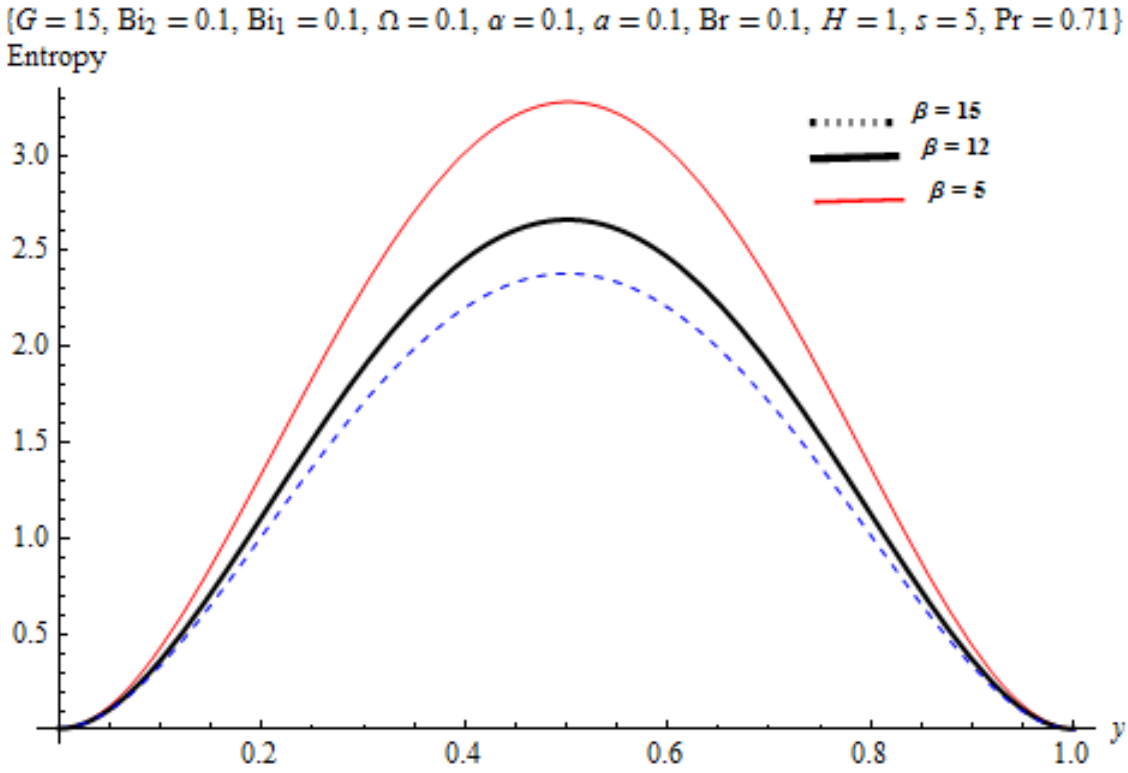

Figure 4.21: Effect of porous media shape factor parameter (β) on entropy generation rate

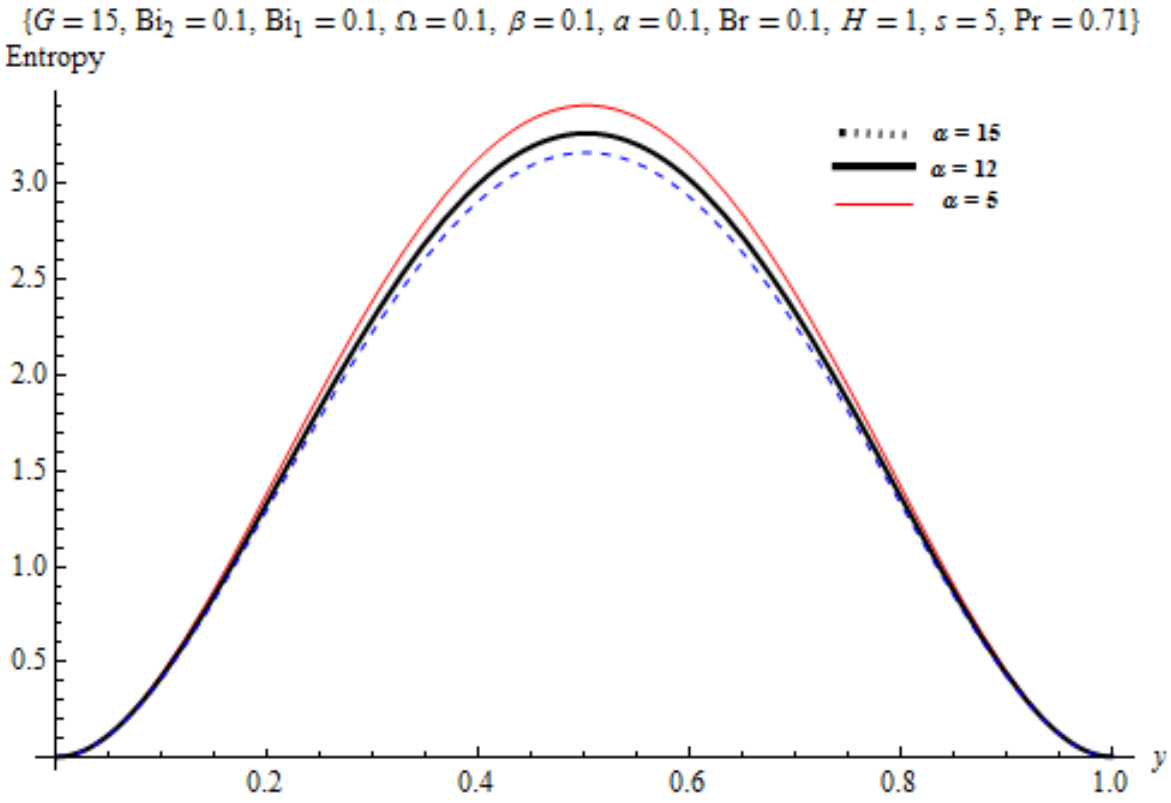

Figure 4.22: Effect of second order porous media resistance parameter (α) on entropy generation rate

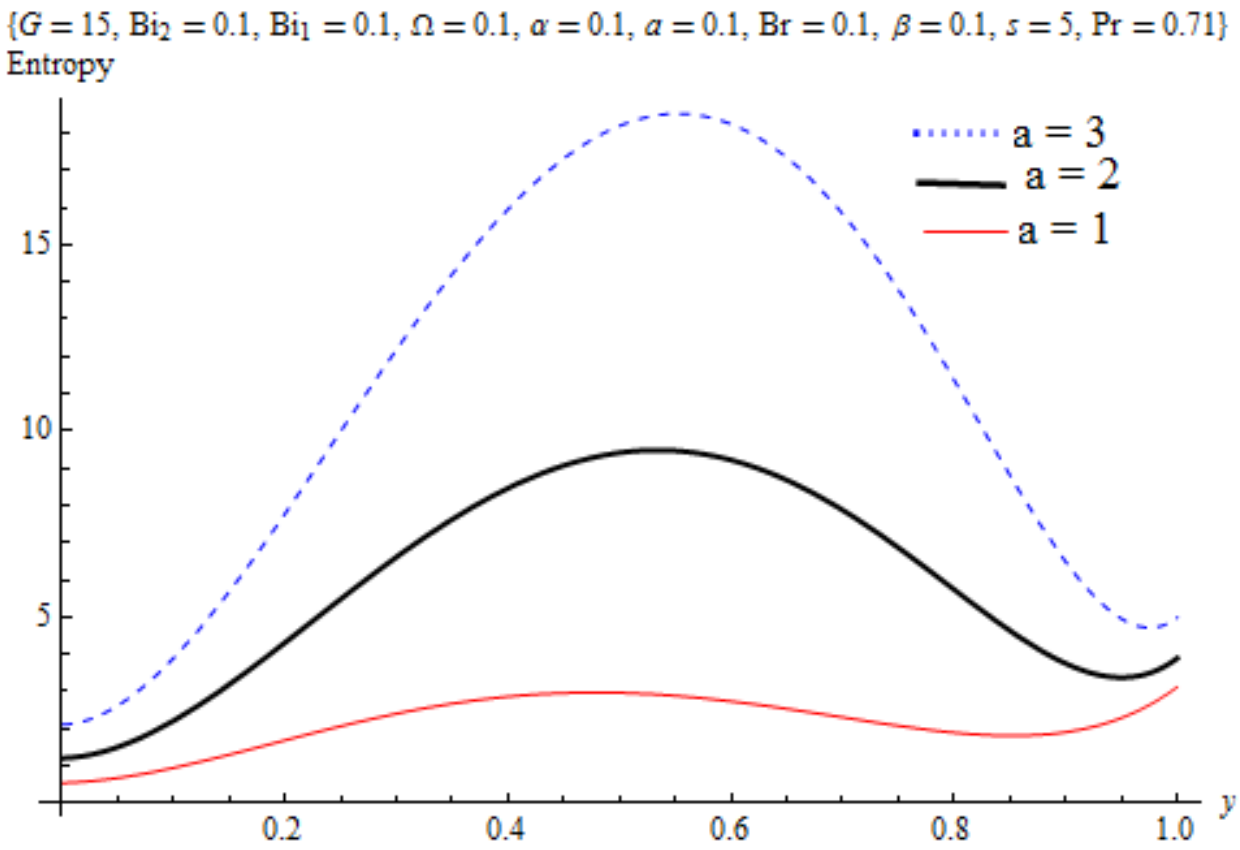

Figure 4.23: Effect of couple stresses (a) on entropy generation rate

4.3.3 Effects of Parameter Variation on Bejan Number

Influence of parameters variation on Bejan number are presented in Figures 4.24-4.27. Figures 4.24-4.26 display the plots of variation in magnetic field parameter, porous media shape factor parameter and Brinkman number respectively on Bejan number. The plots indicate that increase in the parameters increases Bejan number. Furthermore, Figure 4.27 presents the influence of Prandtl number on Bejan number. It is shown from the plot that Bejan number decreases slightly at the lower wall while there is a significant increase in the middle and upper walls of the channel as Prandtl number increases. The results indicate the dominance of irreversibility due to heat transfer in the middle and upper walls of the channel.

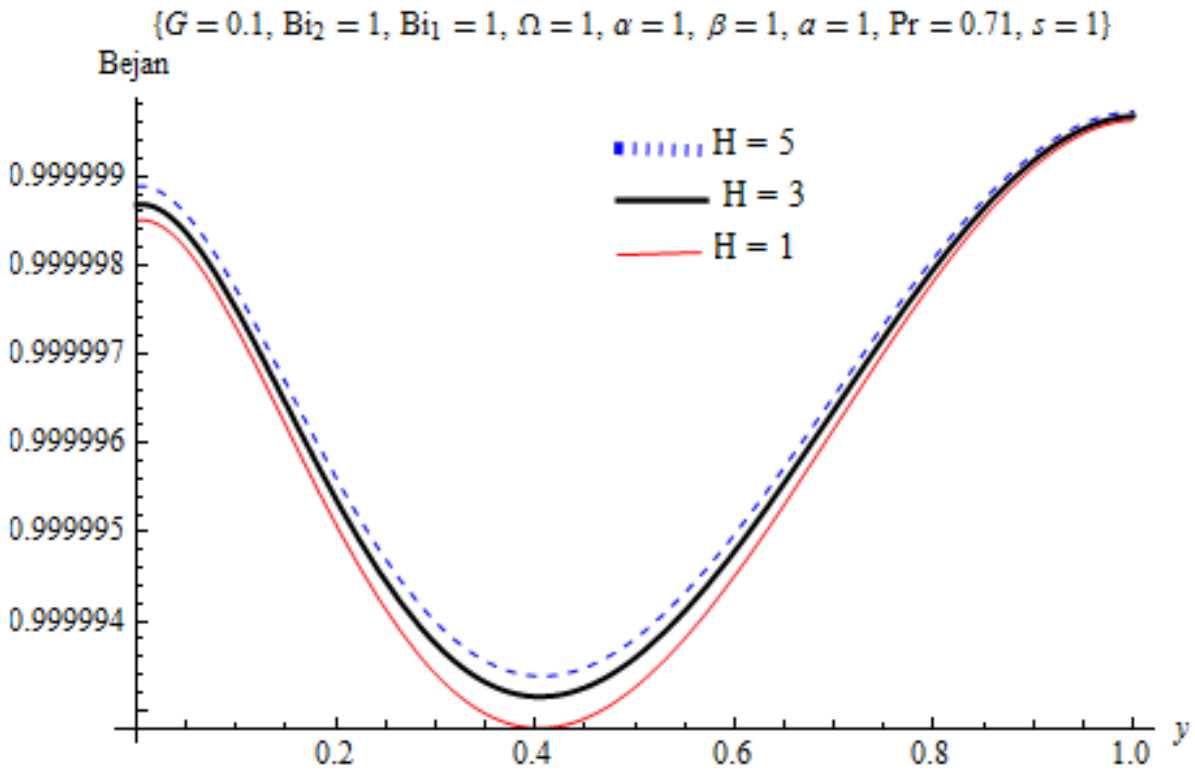

Figure 4.24: Effect of magnetic field parameter (H^2) on Bejan number

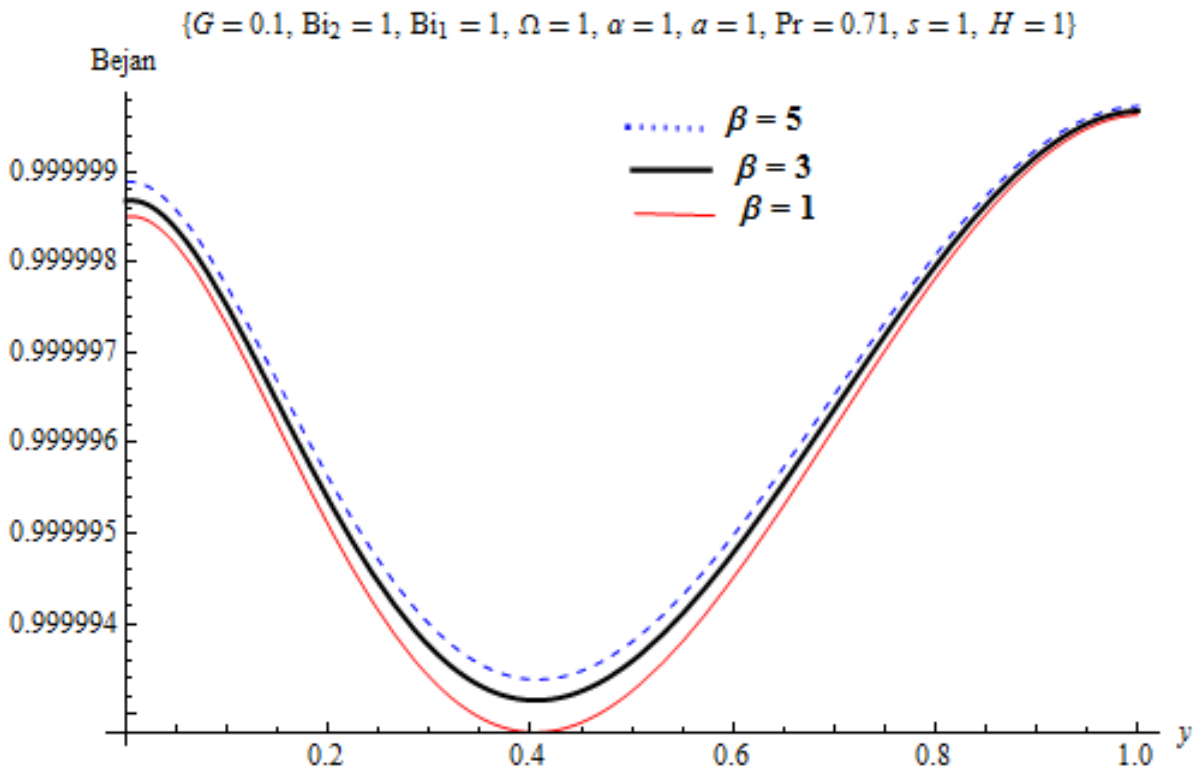

Figure 4.25: Effect of porous media shape factor parameter (β) on Bejan number

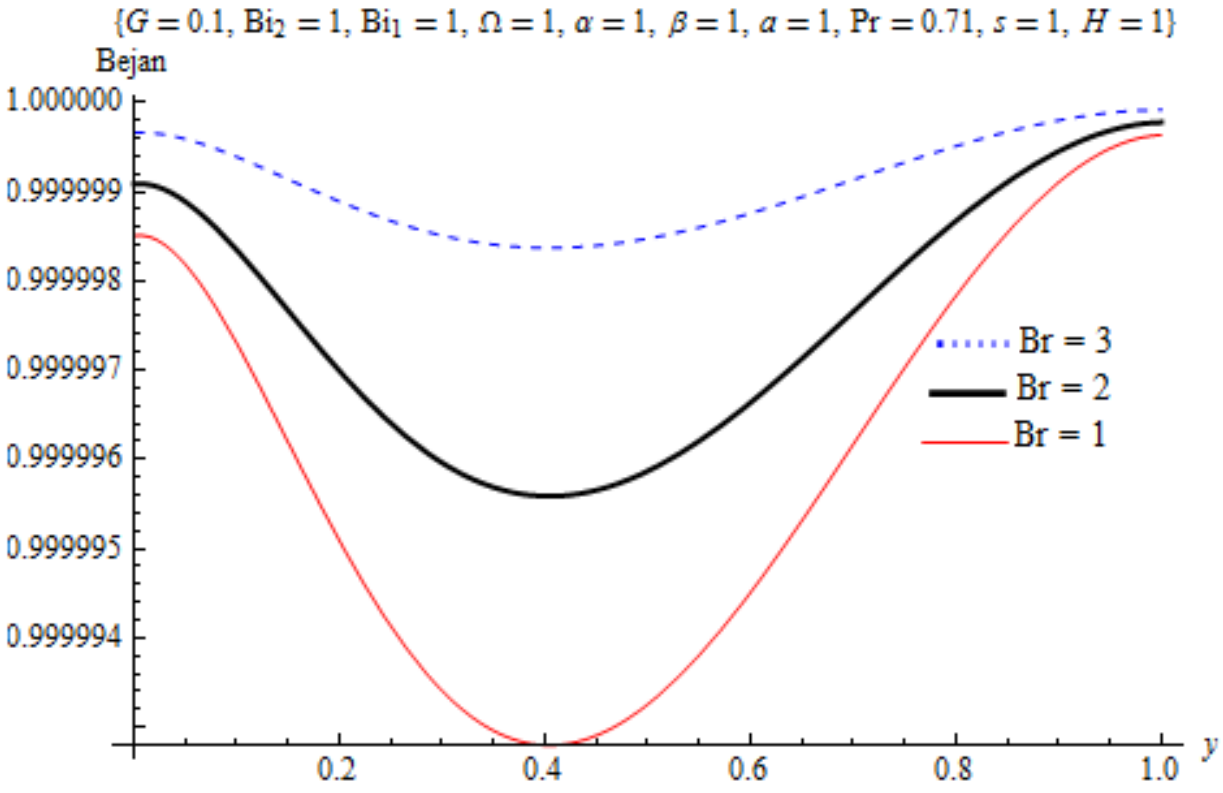

Figure 4.26: Effect of Brinkman number (Br) on Bejan number

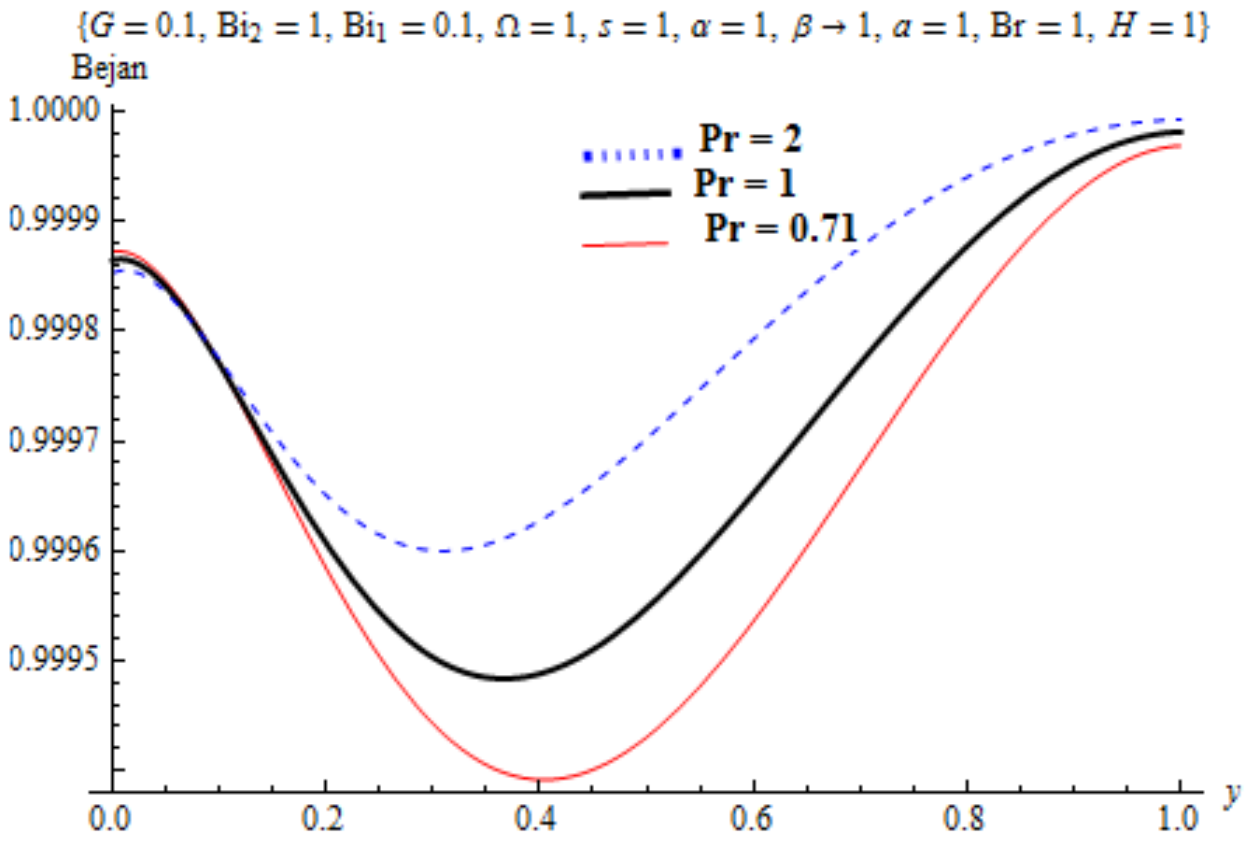

Figure 4.27: Effect of Prandtl number (Pr) on Bejan number

4.4 Model 3

In this model, irreversibility analysis of MHD couple stress fluid flow through vertical porous medium has been investigated using the rapidly convergent Adomian decomposition method. The velocity and temperature profiles are obtained and used to compute the entropy generation rate. The effects of various parameters are considered on velocity, temperature, entropy generation and Bejan number to provide insight to the problems, and the results are graphically displayed in Figs. 4.28-4.46

4.4.1 Effects of Parameters Variation on Velocity Profile

Figures 4.28-4.31 present the variations of velocity for different flow parameters. Figure 4.28 represents the effect of variation in Grashof number parameter on velocity profile. There is a rise in the velocity of the fluid as Grashof number parameter increases. It is observed that buoyancy force speeds up fluid velocity. Figure 4.29 presents the effect of suction/injection on fluid velocity. The plot shows a rise in fluid velocity as suction/injection parameter increases; the rise in fluid velocity is due to the reduction in fluid kinematic viscosity as more hot fluid is injected into the channel while in Figure 4.30 the influence of Prandtl number on the velocity of the fluid is displayed. The Figure reveals that fluid velocity accelerates as the value of Prandtl number rises from water vapour to water. Furthermore, Figure 4.31 portrays the effect of the inverse of couple stresses on fluid velocity. It is clearly shown that fluid velocity increases as the inverse of couple stresses increases. The fluid velocity will eventually reduce as couple stresses increases due to increase in fluid thickness which reduces fluid motion.

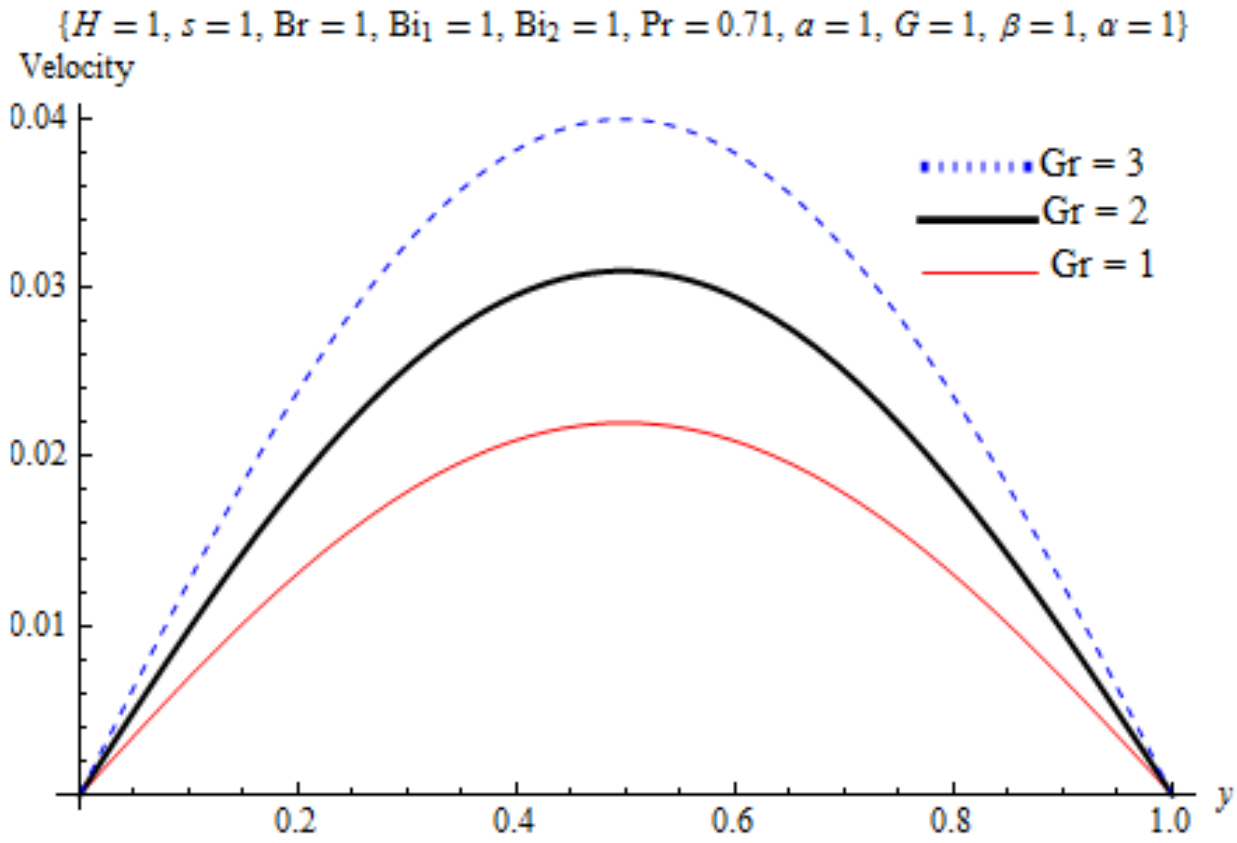

Figure 4.28: Effect of Grashof number (Gr) on velocity profile

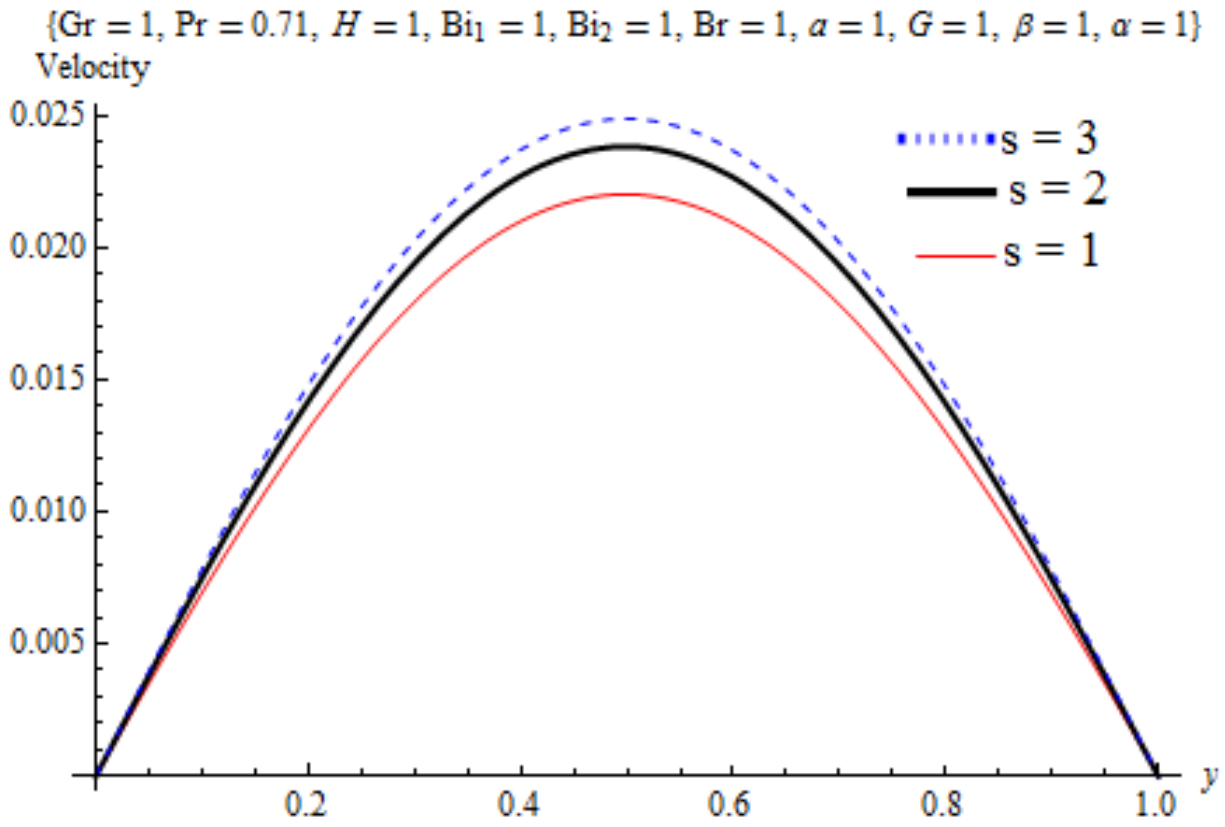

Figure 4.29: Effect of suction/injection (s) on velocity profile

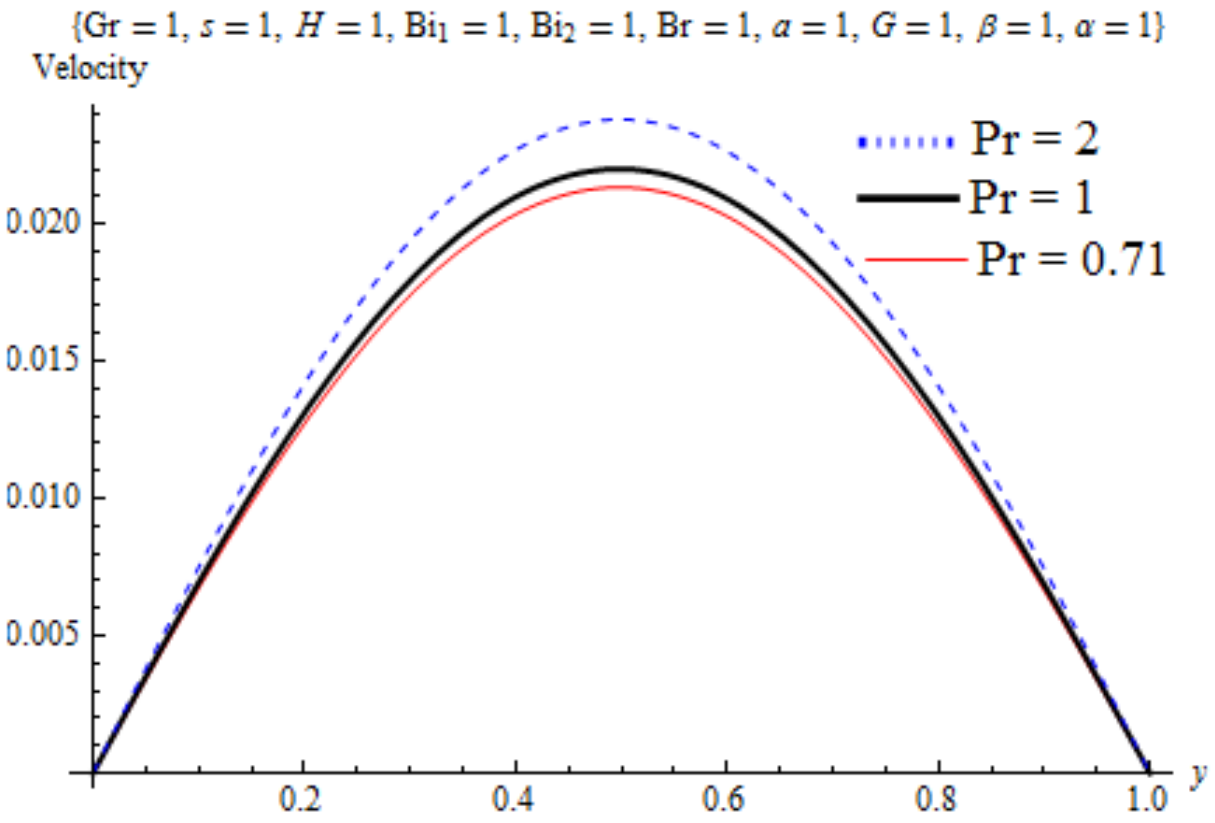

Figure 4.30: Effect of Prandtl number (Pr) on velocity profile

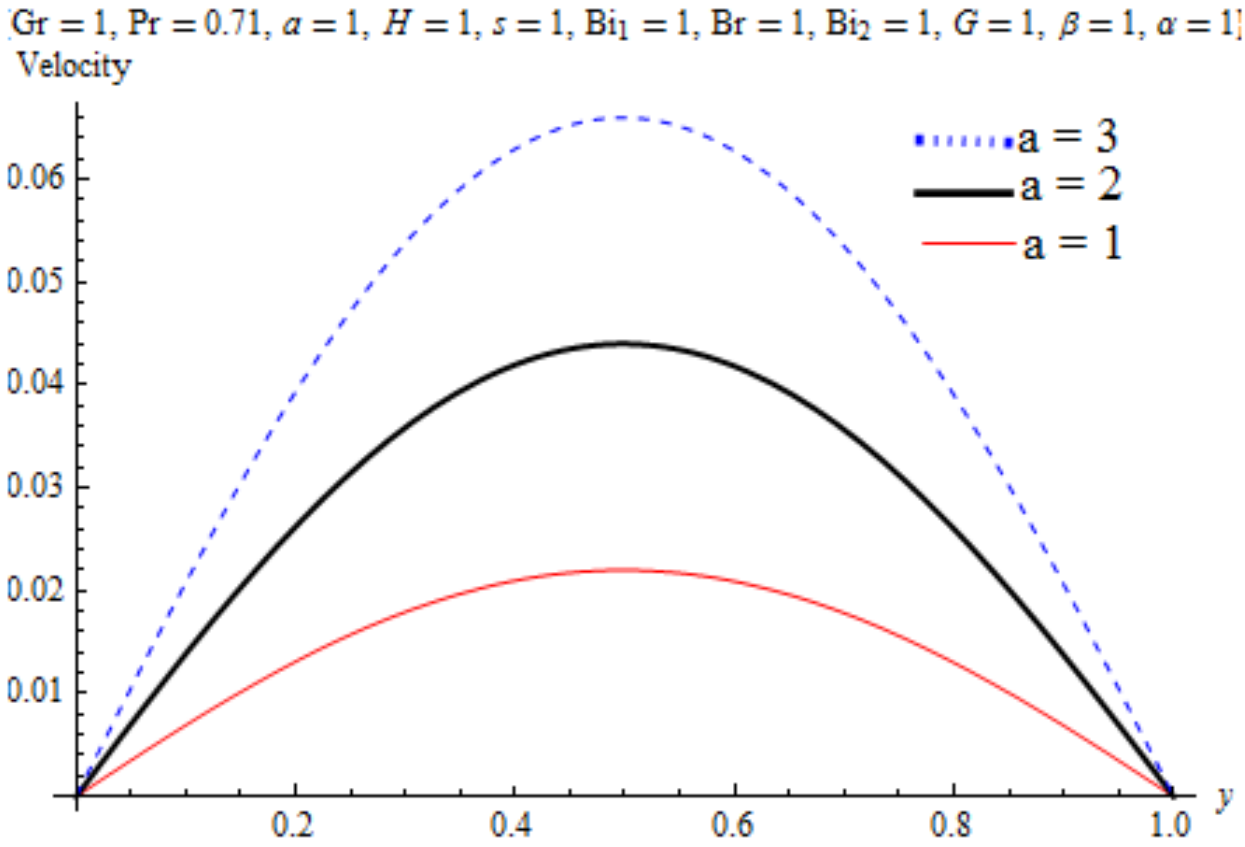

Figure 4.31: Effect of couple stress inverse (a) on velocity profile

4.4.2 Effect of Parameters Variation on Temperature Profile

The influences of different governing parameters on temperature are presented in Figures 4.32-4.36 Figure 4.32 portrays the effect of Grashof number on fluid temperature. Fluid temperature is enhanced across the channel as the value of Grashof number increases due to increase in fluid volumetric expansion. The effect of magnetic field parameter on fluid temperature is shown in Figure 4.33. It is clear from the plot that fluid temperature increases as magnetic field parameter increases. The Lorentz heating effect is attributed to the rise in temperature. Figure 4.34 displays the effect of suction/injection parameter on fluid temperature; the figure reveals that temperature increases as suction/injection parameter increases. This is true as injection of hot fluid into the channel will definitely increase fluid temperature. Figure 4.35 displays the effect of lower Biot number (Bi_1) on fluid temperature. As seen from the graph, the temperature increases as convective heating from the lower wall increases, while the trend is reversed in Figure 4.36 with upper Biot number (Bi_2) due to the cooling effect.

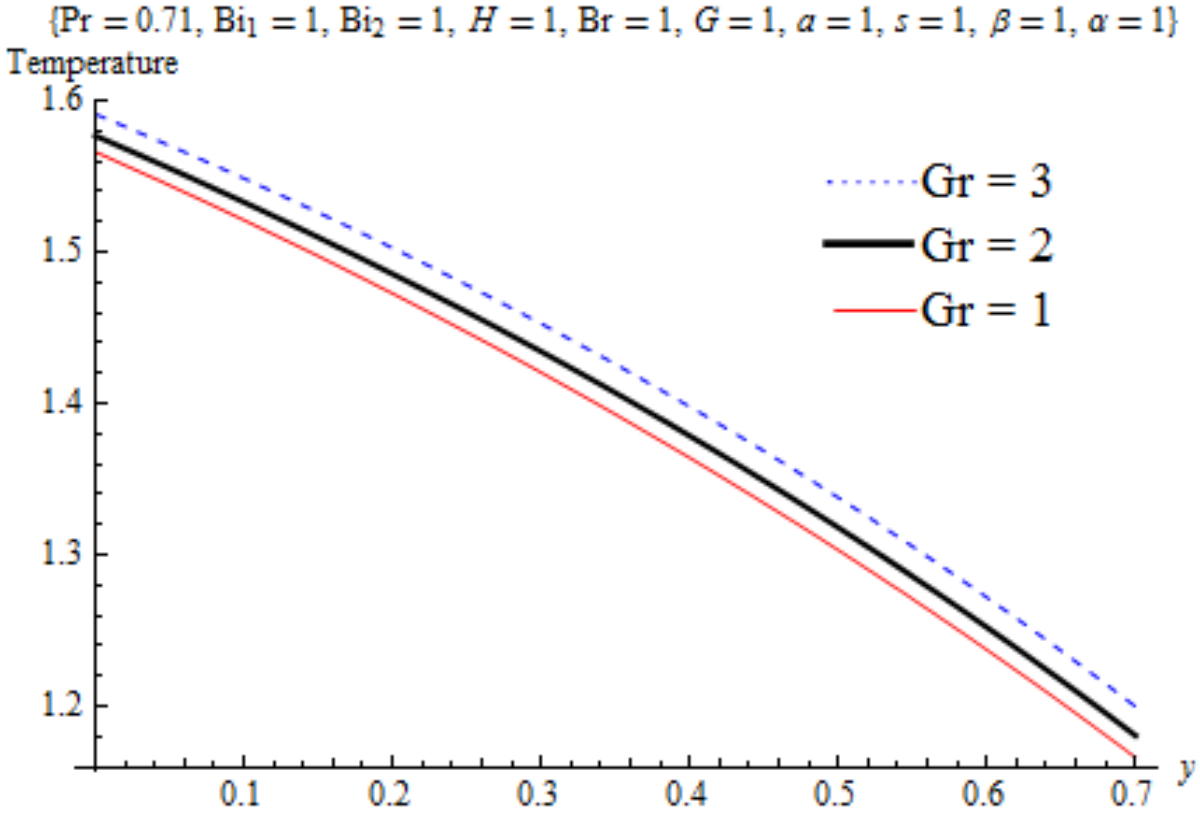

Figure 4.32: Effect of Grashof number (Gr) on temperature profile

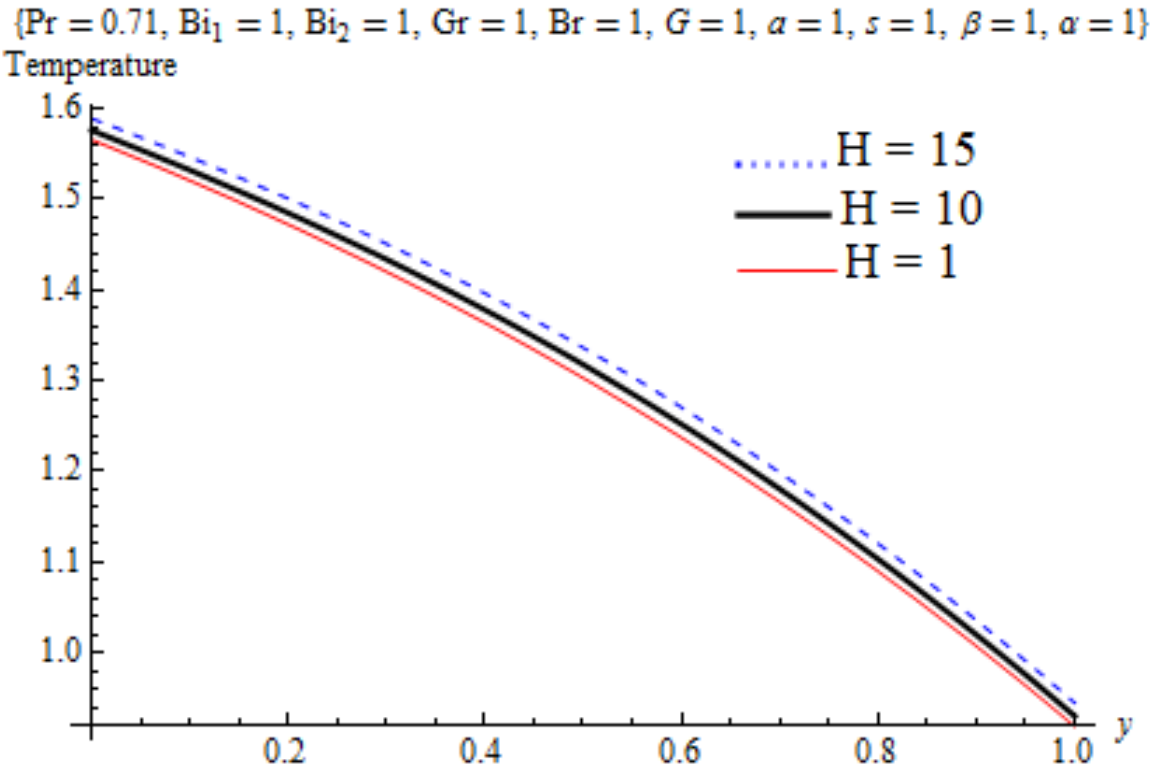

Figure 4.33: Effect of magnetic field parameter (H^2) on temperature profile

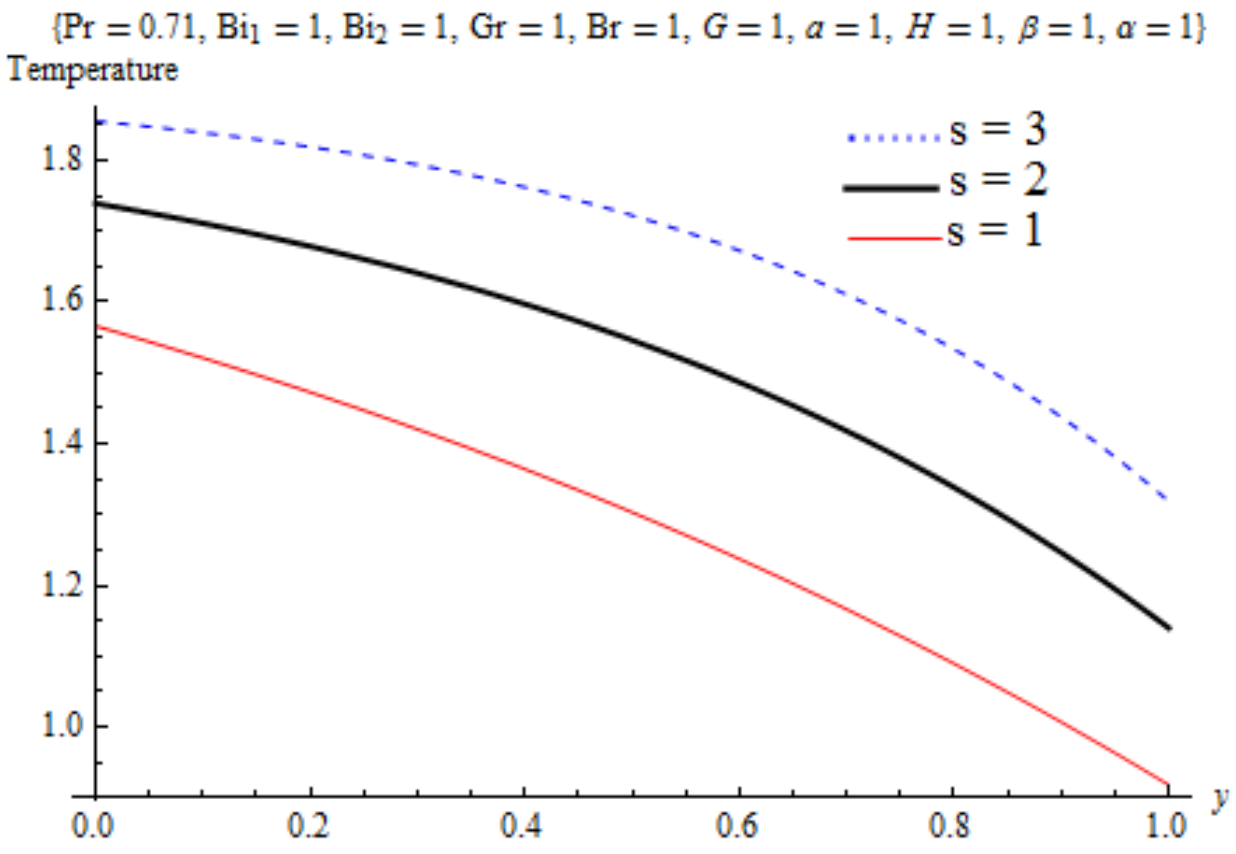

Figure 4.34: Effect of suction/injection (s) on temperature profile

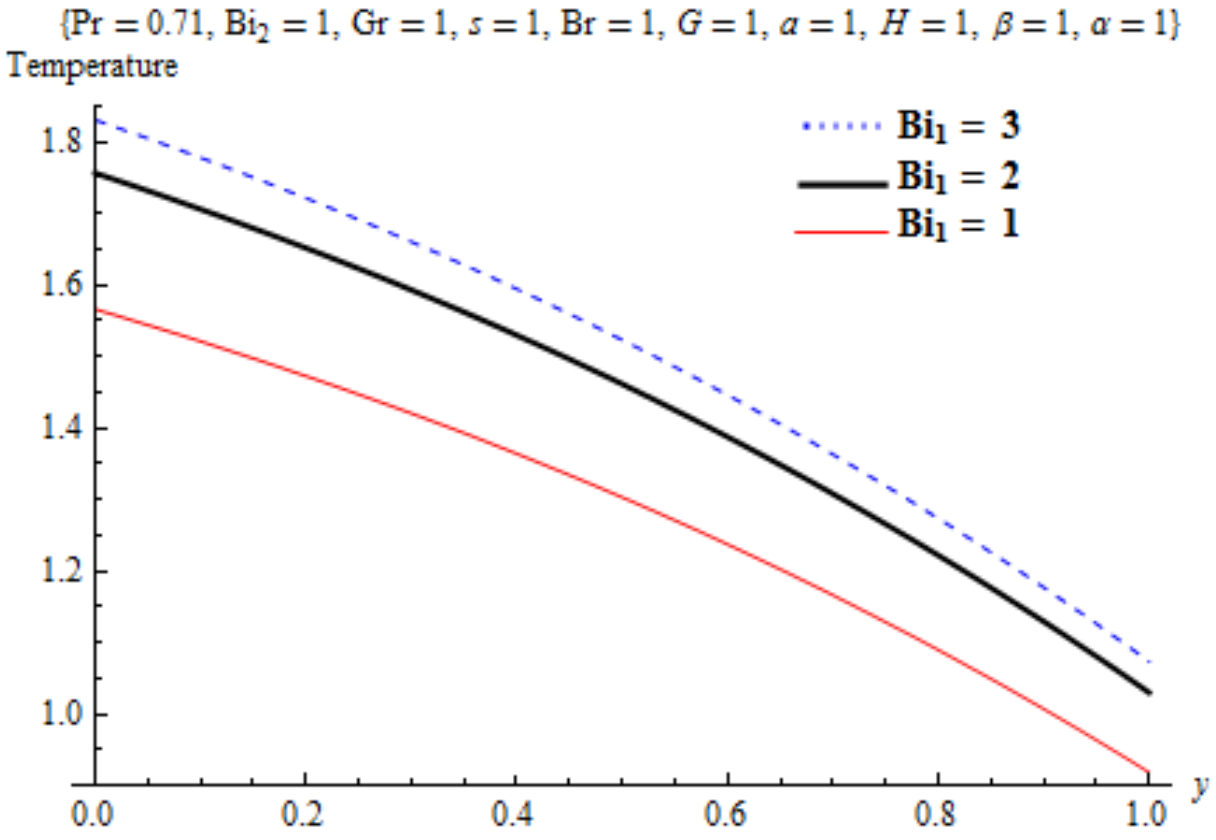

Figure 4.35: Effect of lower Biot number (Bi_1) on temperature profile

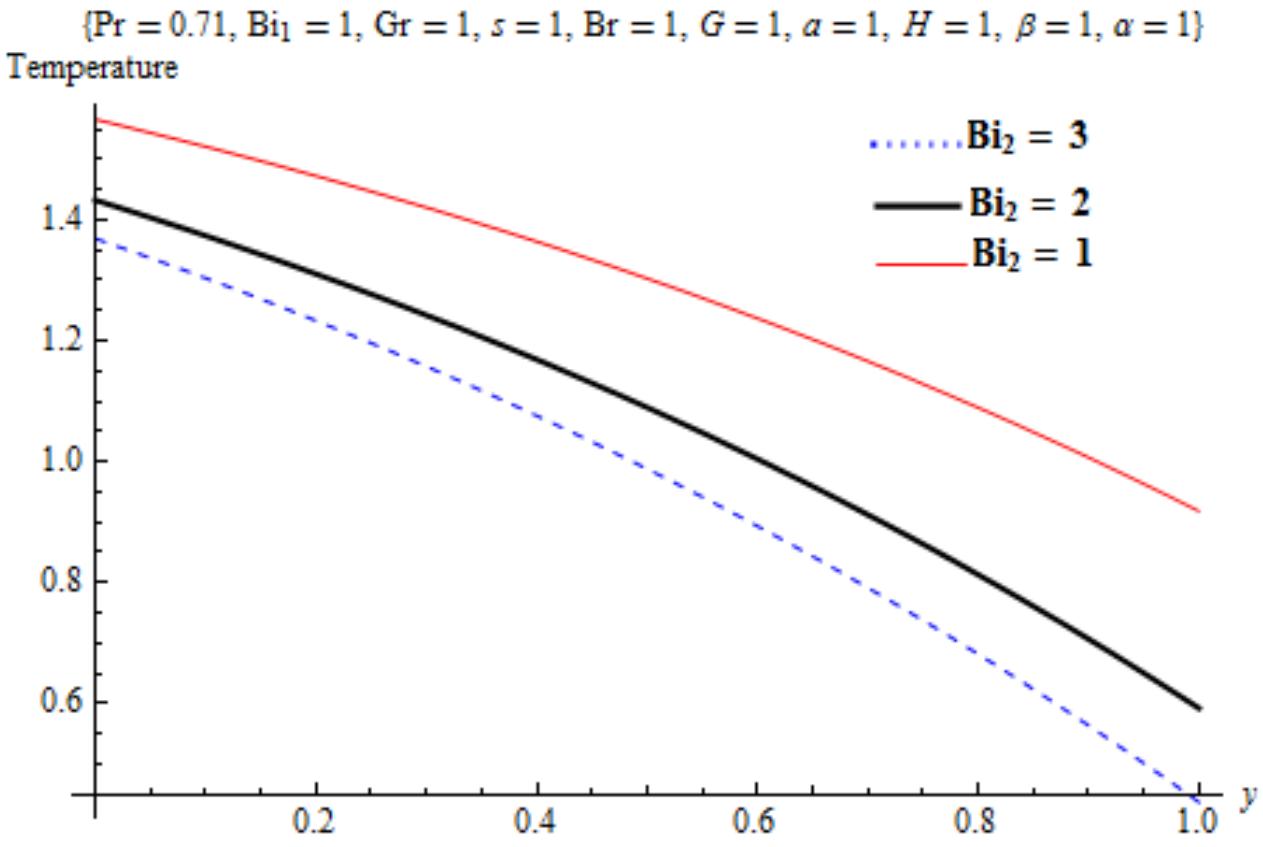

Figure 4.36: Effect of upper Biot number (Bi_2) on temperature profile

4.4.3 Effect of Parameters Variation on Entropy Generation Rate

The influences of various parameters on entropy generation rate are presented in Figures 4.37-4.41. Figure 4.37 describes the effect of Grashof number on entropy generation rate. The plot depicts that entropy generation registers an increase as Grashof number rises in values. In Figures 4.28 and 4.32, it is presented that fluid velocity and temperature increased as Grashof number increases due to the impact of buoyancy force as well as rise in fluid volumetric expansion respectively. The net effect is the increased randomness of fluid particles which leads to increase in entropy production. Figure 4.38 displays the effect of magnetic field parameter on entropy generation. Entropy production becomes higher at the upper wall as magnetic field value rises. This is explained in Figure 4.33 that increase in Hartman number has a corresponding increase in fluid temperature because the applied magnetic field clustered fluid particles together thereby enhancing viscous dissipation. Consequently, fluid velocity is reduced and the temperature rises leading to loss of available energy as entropy production rises.

Furthermore, Figure 4.39 depicts the influence of suction/injection on entropy generation rate. From the plot, we observed that entropy generation increases considerably as suction/injection parameter varies. This is because of the injection of hot fluid into the channel which resulted into increased velocity and temperature as revealed in Figures 4.29 and 4.34. Finally, Figures 4.40 and 4.41 show similar result, the plots depict the effect of Biot numbers on entropy generation. As observed from the figures, entropy generation increases considerably across the channel as both lower and upper Biot numbers increase in values.

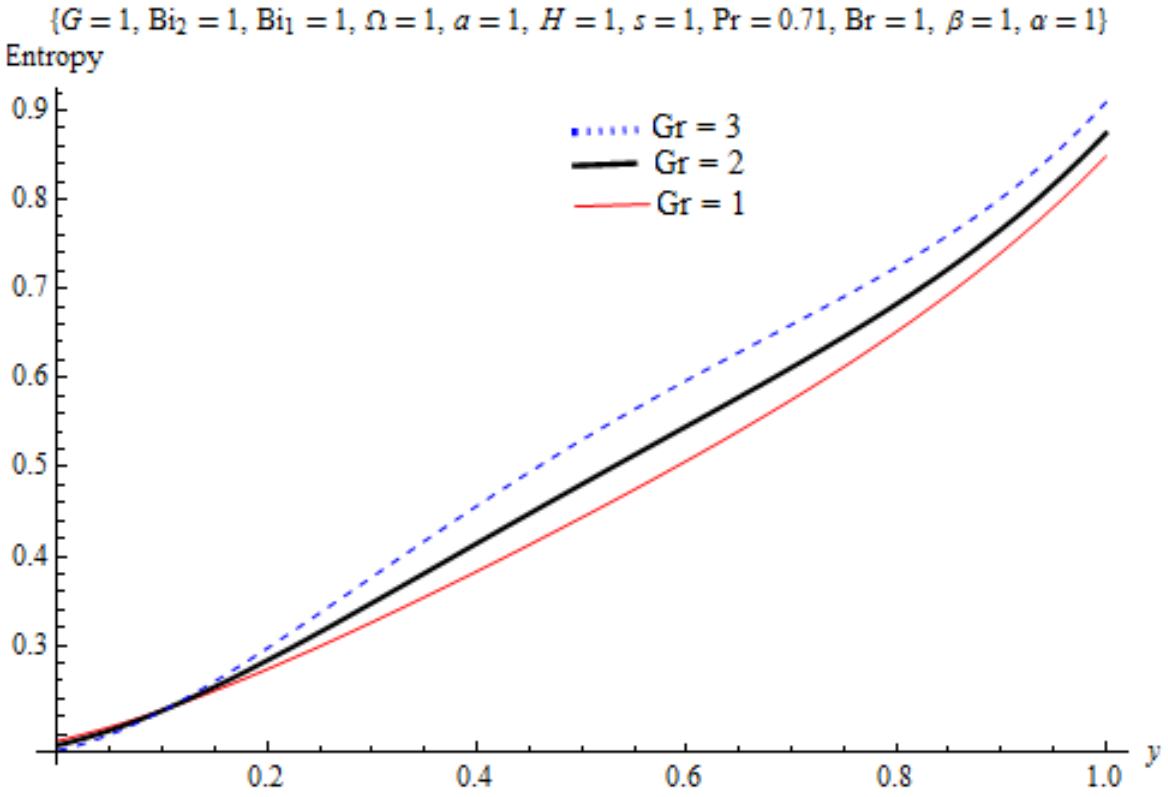

Figure 4.37: Effect of Grashof number (Gr) on entropy generation rate

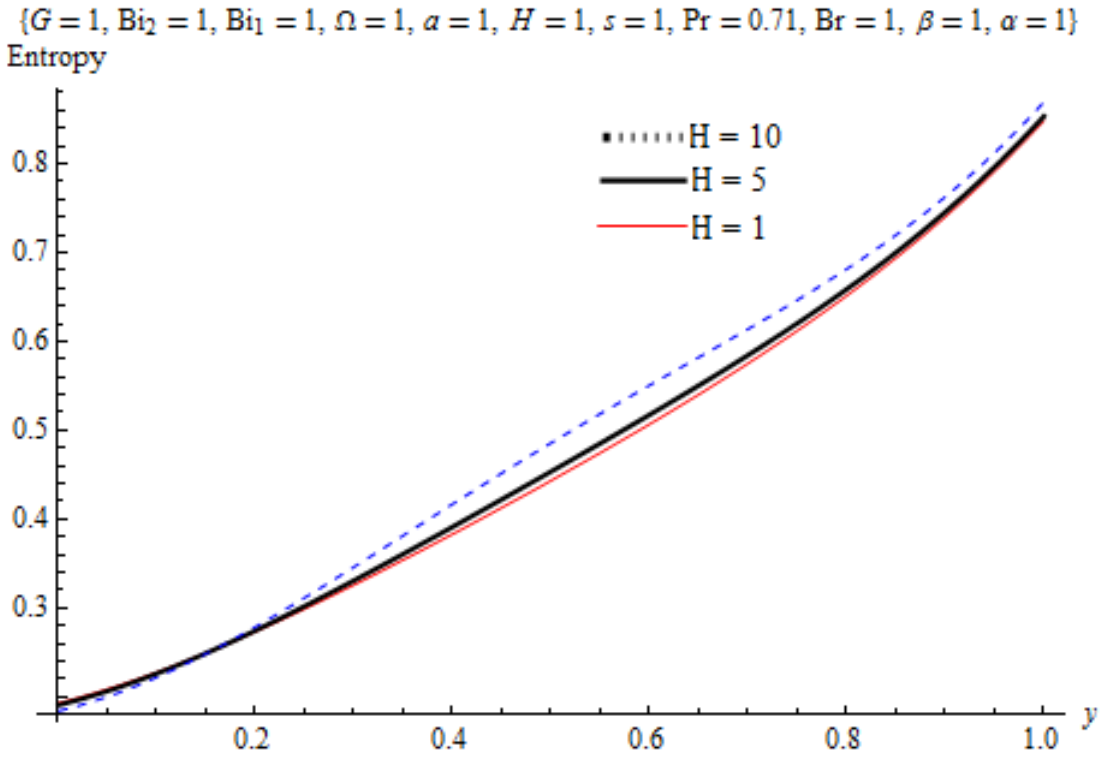

Figure 4.38: Effect of magnetic field parameter (H^2) on entropy generation rate

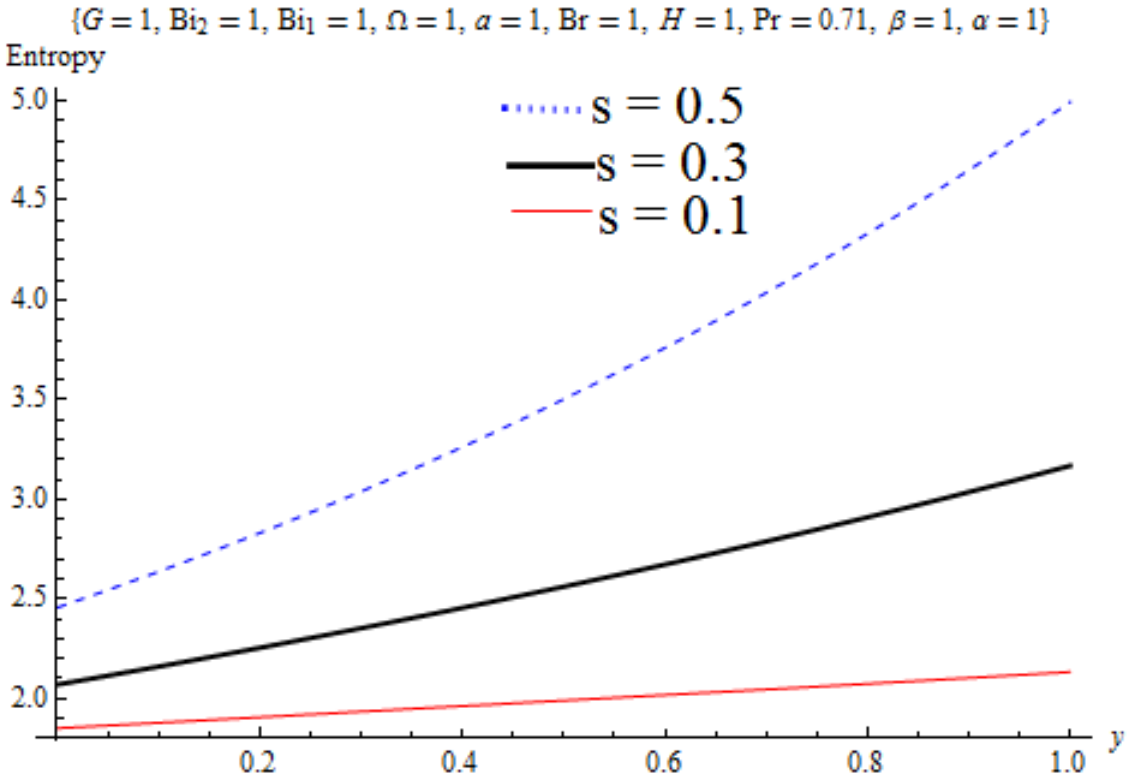

Figure 4.39: Effect of suction/injection (s) on entropy generation rate

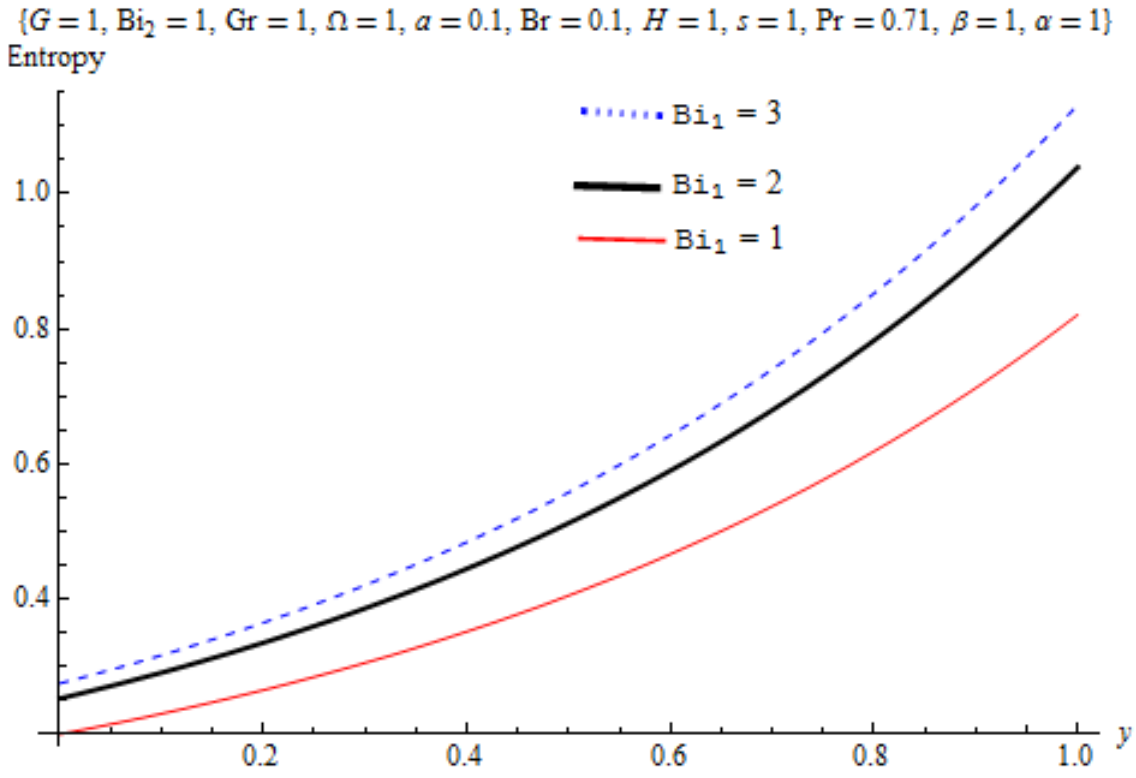

Figure 4.40: Effect of lower Biot number (Bi_1) on entropy generation rate

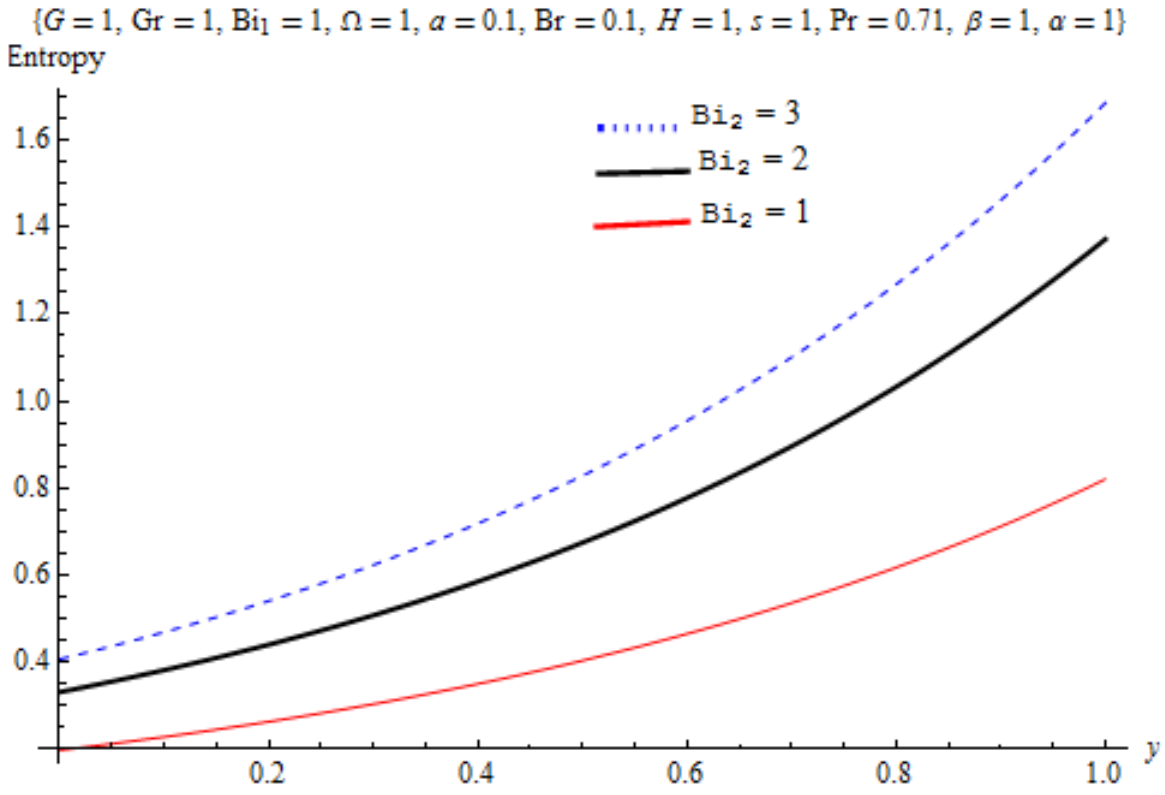

Figure 4.41: Effect of upper Biot number (Bi_2) on entropy generation rate

4.4.4 Effect of Parameters Variation on Bejan Number

This section presents the effect of variation of parameters on Bejan number in Figures 4.42-4.46. Figures 4.42 depicts the effect of Grashof number on Bejan number the plots indicate that Bejan number decreases as the values of Grashof number increases. Therefore entropy generation due to viscous dissipation dominates over heat transfer, while Figures 4.43-4.46 display the plots of Hartman number, suction/injection parameter, lower and upper Biot numbers respectively on Bejan number, the plots show that Bejan number increases as the values of the parameters increase. This is an indication that heat transfer dominates entropy generation for Hartman number, suction/injection, lower and upper Biot numbers.

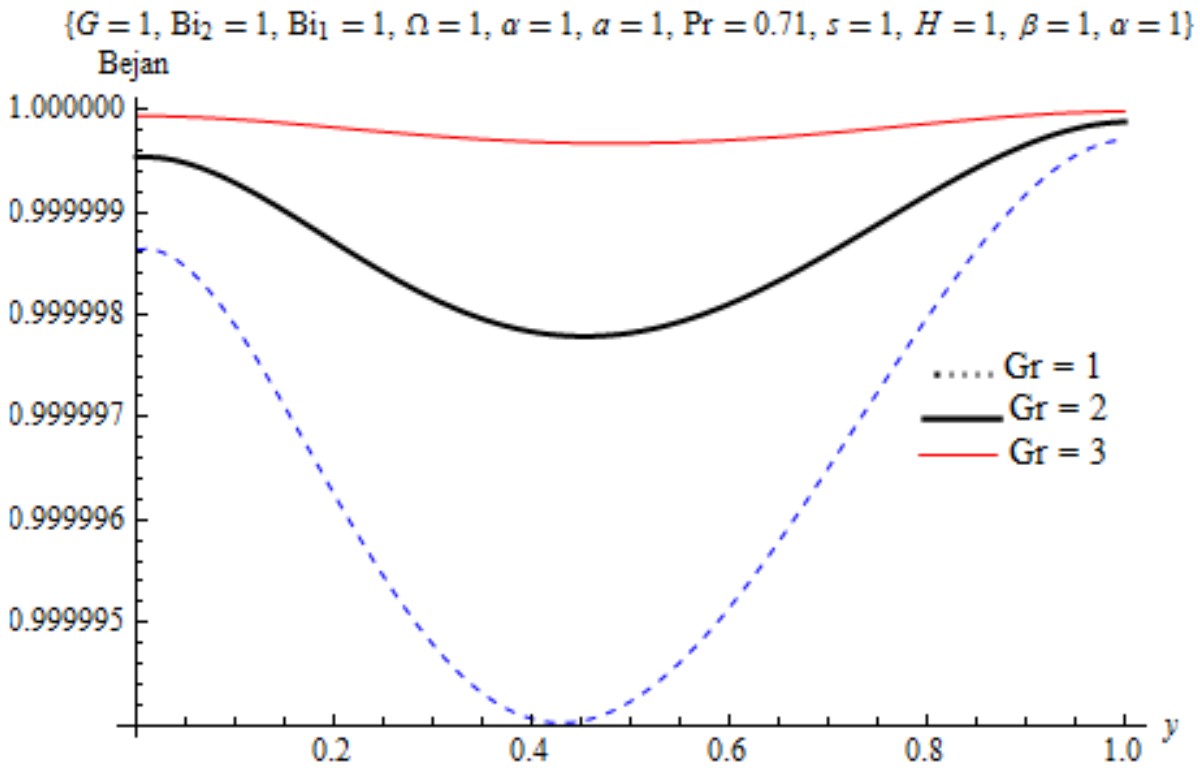

Figure 4.42: Effect of Grashof number (Gr) on Bejan number

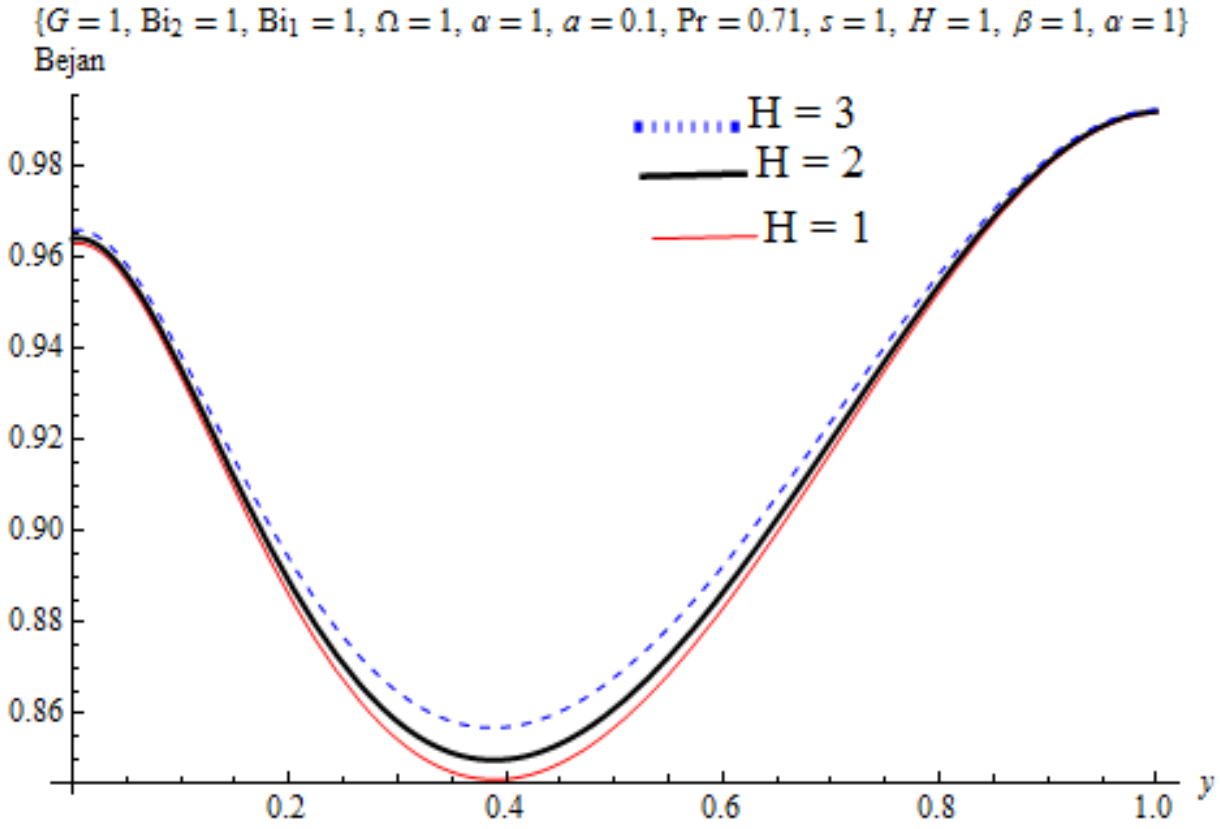

Figure 4.43: Effect of magnetic field parameter (H^2) on Bejan number

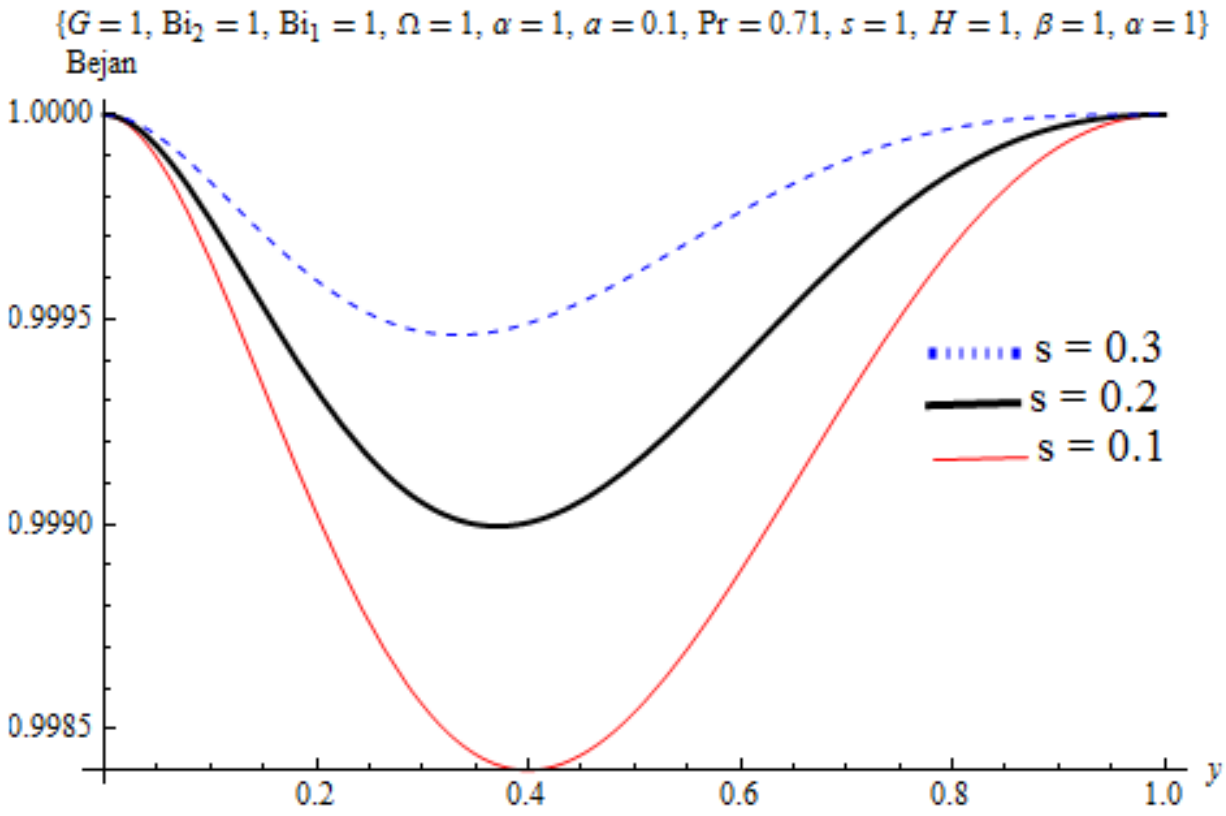

Figure 4.44: Effect of suction/injection (s) on Bejan number

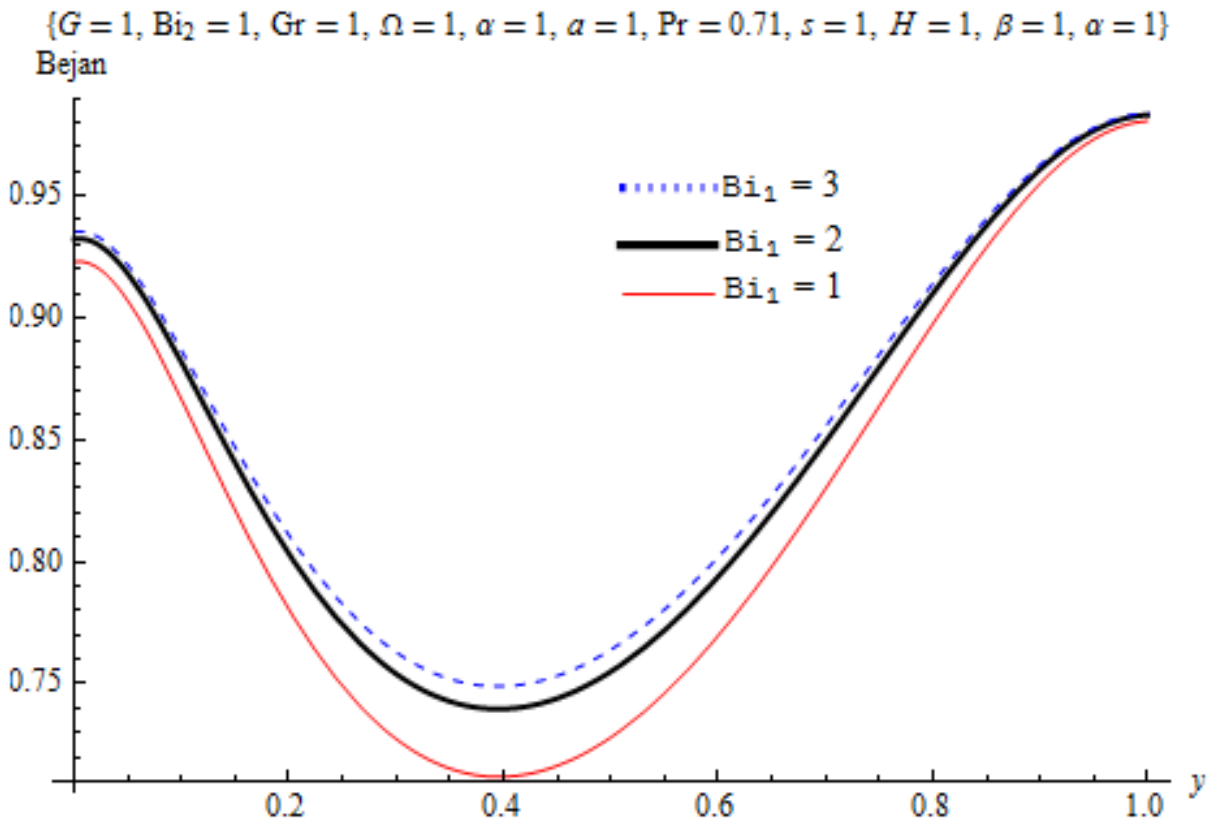

Figure 4.45: Effect of lower Biot number (Bi_1) on Bejan number

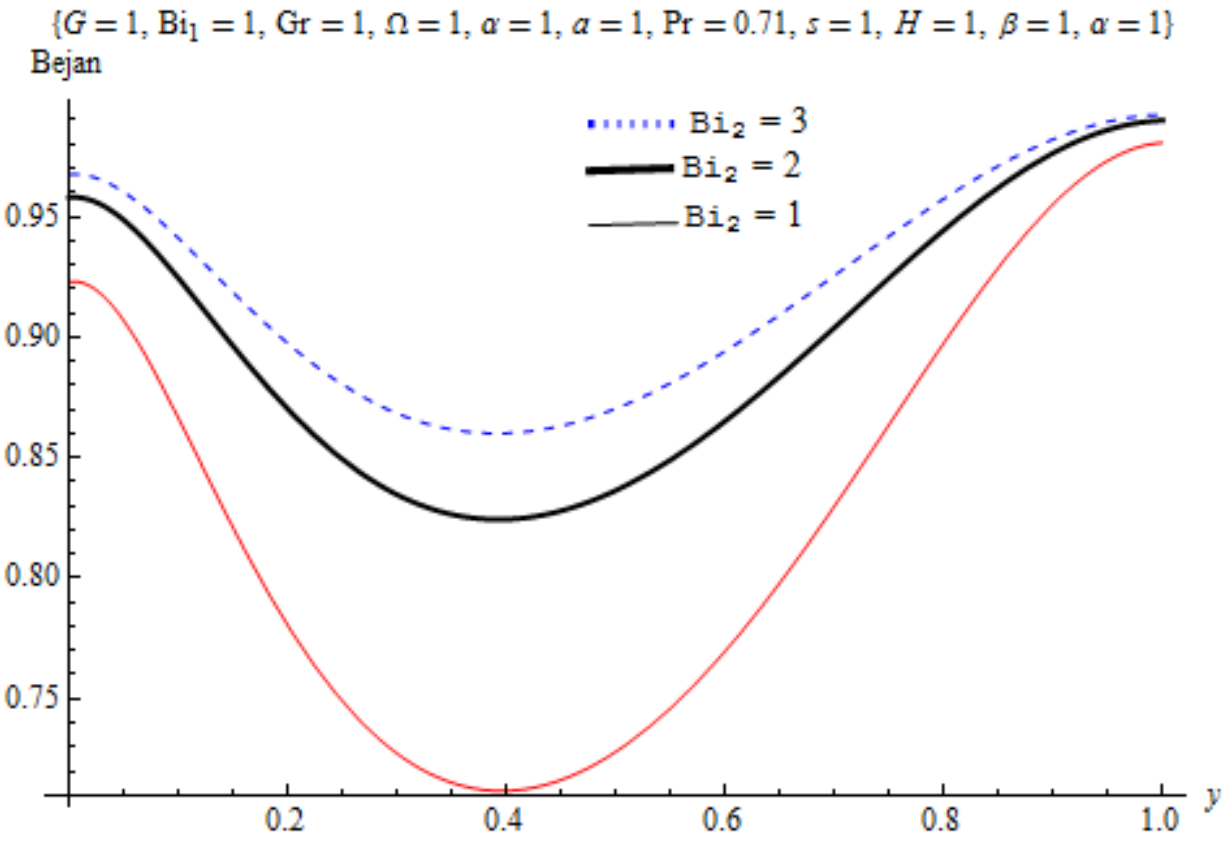

Figure 4.46: Effect of upper Biot number (Bi_2) on Bejan number

4.5 Model 4

This model considers the effect of velocity slip, temperature jump and thermal radiation on the entropy generation rate of hydromagnetic reactive couple stress fluid through vertical porous medium. The boundary value problems are solved by the rapidly convergent Adomian decomposition method. The results showing the effects of some pertinent parameters on the velocity, temperature, entropy generation and Bejan number are discussed with the aid of graphs as in Figs. 4.47-4.62

4.5.1 Effect of Parameter Variation on Velocity Profile

The effects of parameters variation on the velocity profile are displayed in Figures 4.47-4.50. Figure 4.47 depicts the effect of increasing velocity slip parameter on the flow velocity. It is clear from the plot that an increase in velocity slip parameter increases fluid velocity. The reason is that increase in velocity slip corresponds to an increase in the molecular mean free path of each fluid particle and reduction in the frictional forces which increases fluid velocity. In Figure 4.48, the velocity profile is shown for an increasing values of temperature jump parameter. It is observed that fluid velocity reduces as temperature jump parameter increases due to increased molecular distance of each fluid particle. In Figure 4.49 effect of variation in Grashof number on velocity profile is displayed. As observed from the plot, buoyancy force speeds up the motion of fluid particles. Figure 4.50 represents the effect of radiation parameter on the fluid velocity. From the plot, one observes that as the radiation parameter increases, there is an increase in fluid velocity. It is shown that the increase in radiation parameter corresponds to an enhancement in the intensity of heat generated through thermal radiation and the bond holding the components of the fluid particles is easily broken therefore the fluid velocity rises.

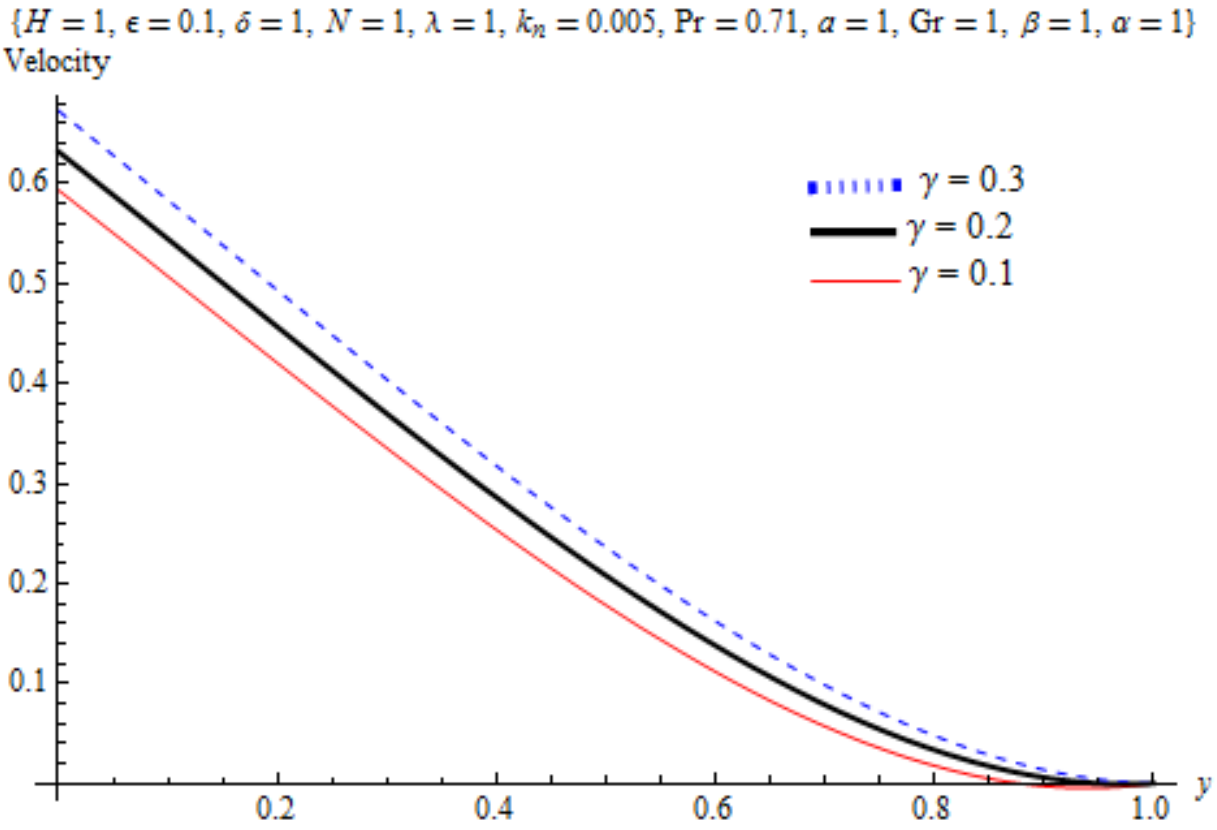

Figure 4.47: Effect of velocity slip parameter (γ) on velocity profile

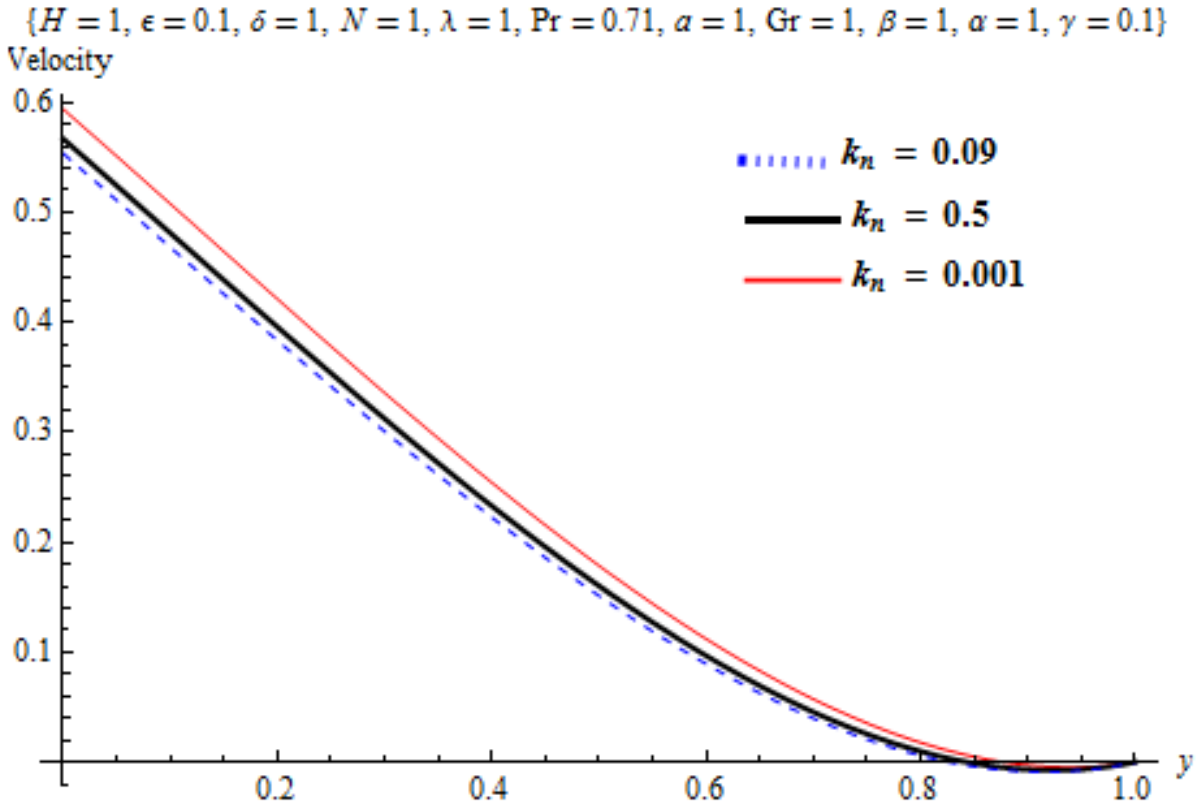

Figure 4.48: Effect of temperature jump parameter (k_n) on velocity profile

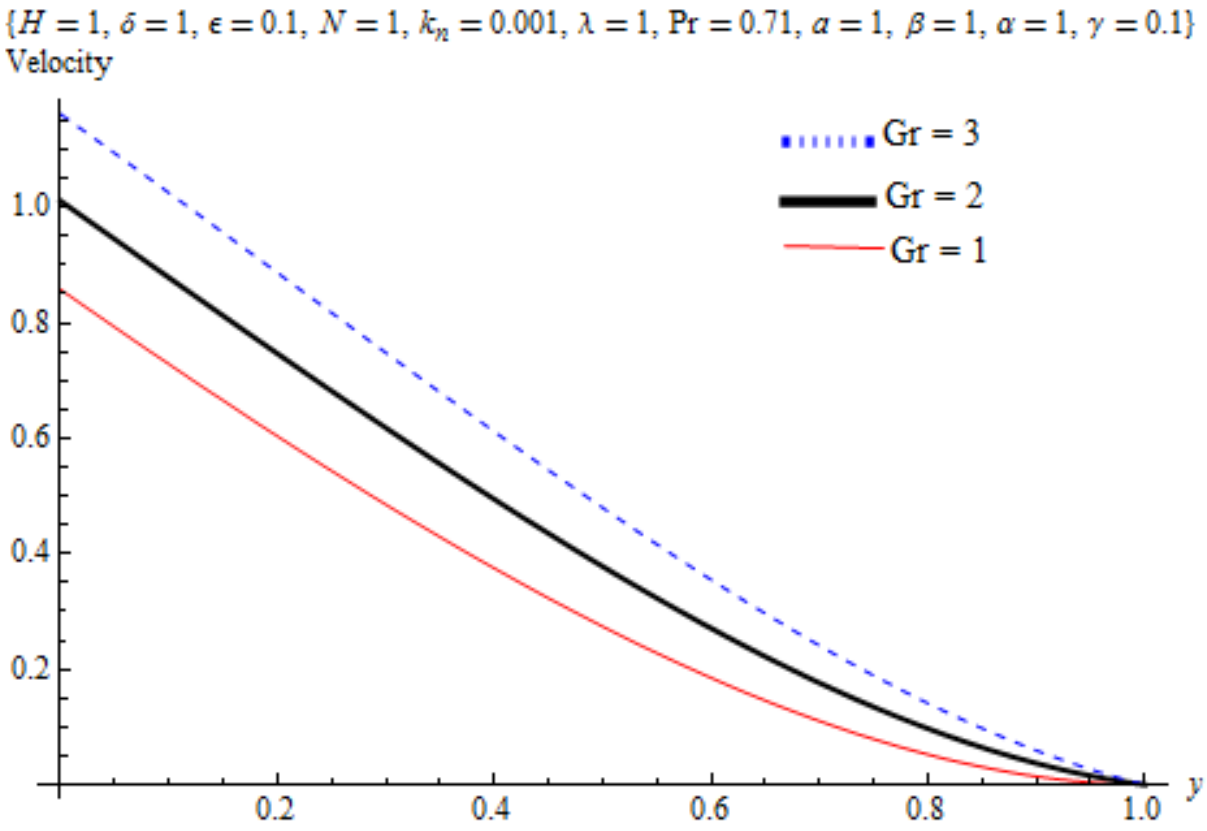

Figure 4.49: Effect of Grashof number (Gr) on velocity profile

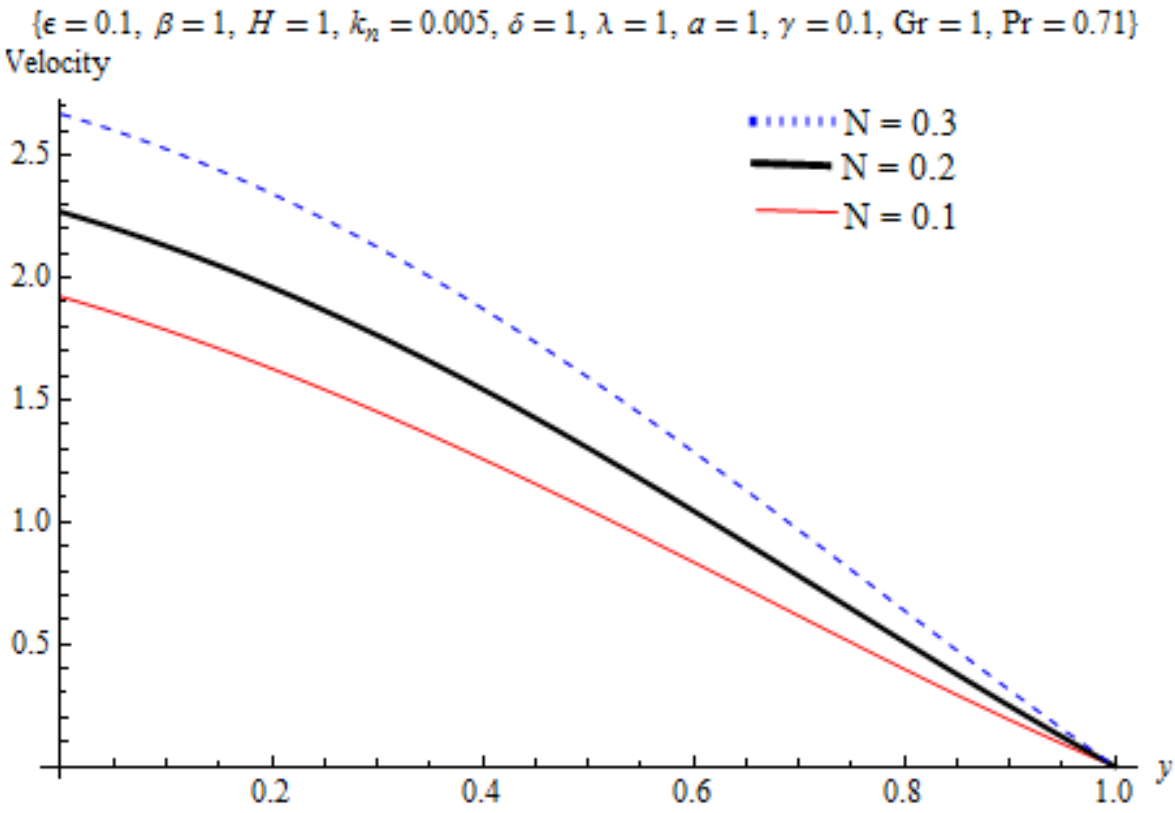

Figure 4.50: Effect of thermal radiation parameter (N) on velocity profile

4.5.2 Effect of Parameters Variation on Temperature Profile

In Figures 4.51-4.54, effect of parameters variations on temperature profiles are shown in the plots. In Figure 4.51 it is observed that as velocity slip parameter increases it reduces the fluid temperature which can be attributed to the gain in momentum of fluid. Figure 4.52 demonstrates the effect of temperature jump parameter on fluid temperature. From the plot it shows that there is a rise in fluid temperature as temperature jump parameter increases. The rise is caused by an increase in the molecular mean free path of the fluid. Moreover, Figure 4.53 depicts the influence of thermal radiation on the temperature. Clearly it is seen that increase in thermal radiation parameter implies a drop in fluid temperature due to increase in the absorptivity rate which lowers the radiated heat and hence the drop in temperature. Furthermore, in Figure 4.54 the representative profile of Grashof number for fluid temperature is displayed. The plot reflects that as Grashof number increases fluid temperature increases due to the significant rise in the volumetric expansion of the fluid.

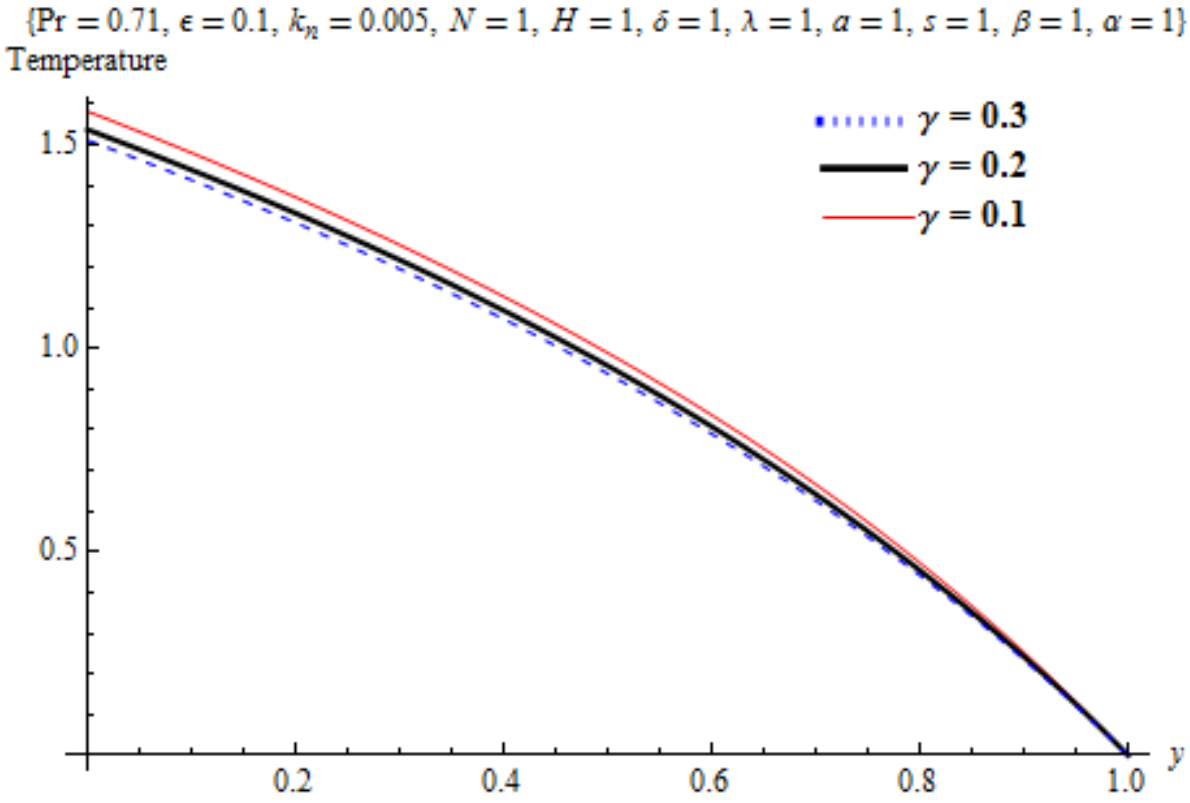

Figure 4.51: Effect of velocity slip parameter (γ) on temperature profile

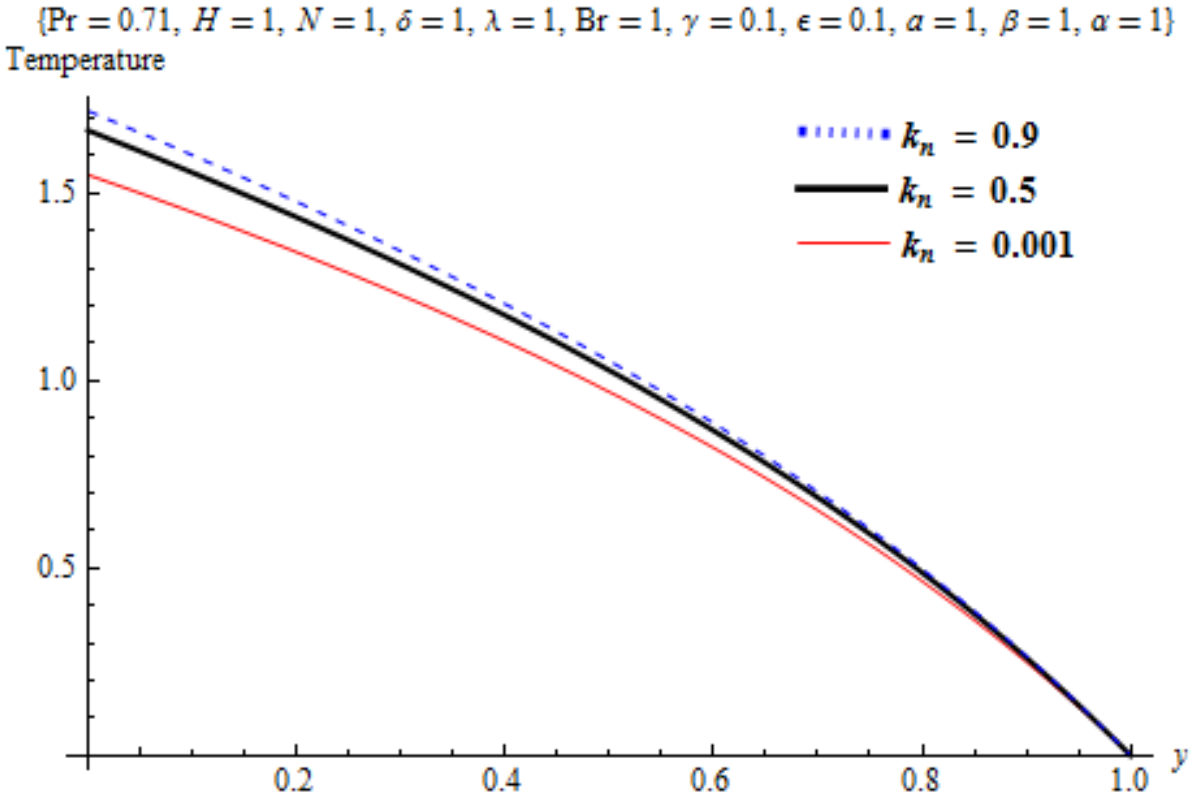

Figure 4.52: Effect of temperature jump parameter (k_n) on temperature profile

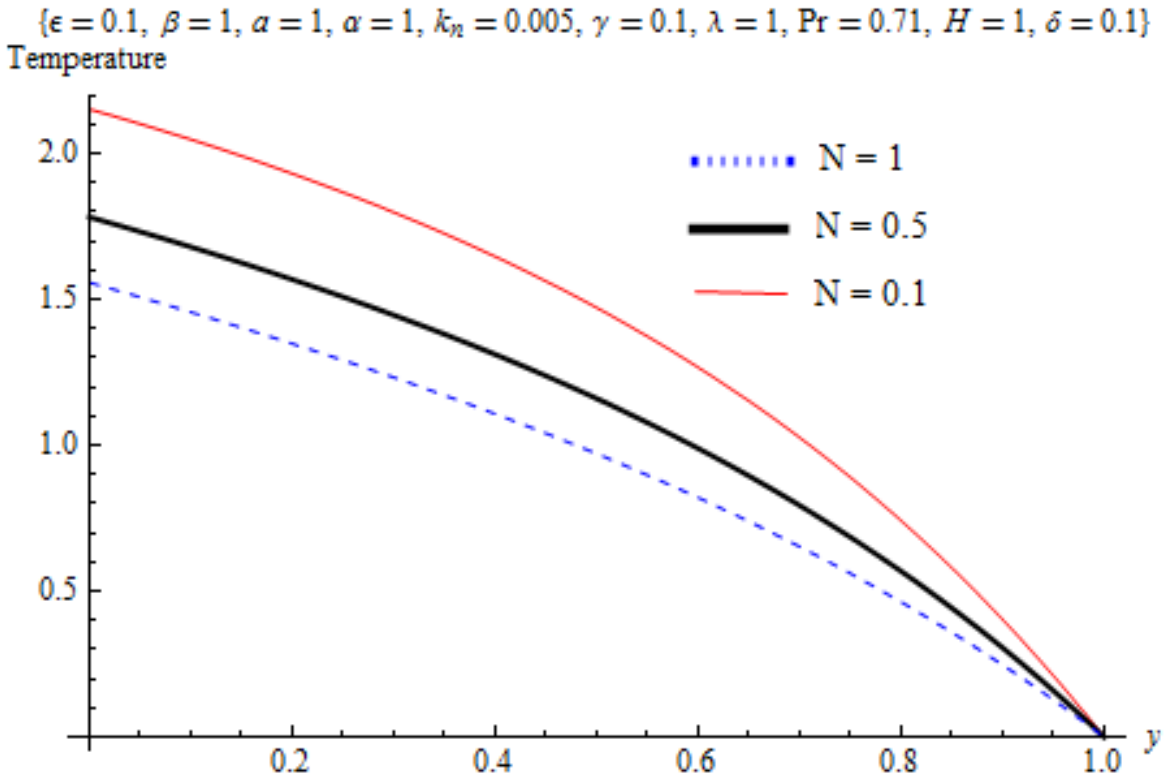

Figure 4.53: Effect of thermal radiation parameter (N) on temperature profile

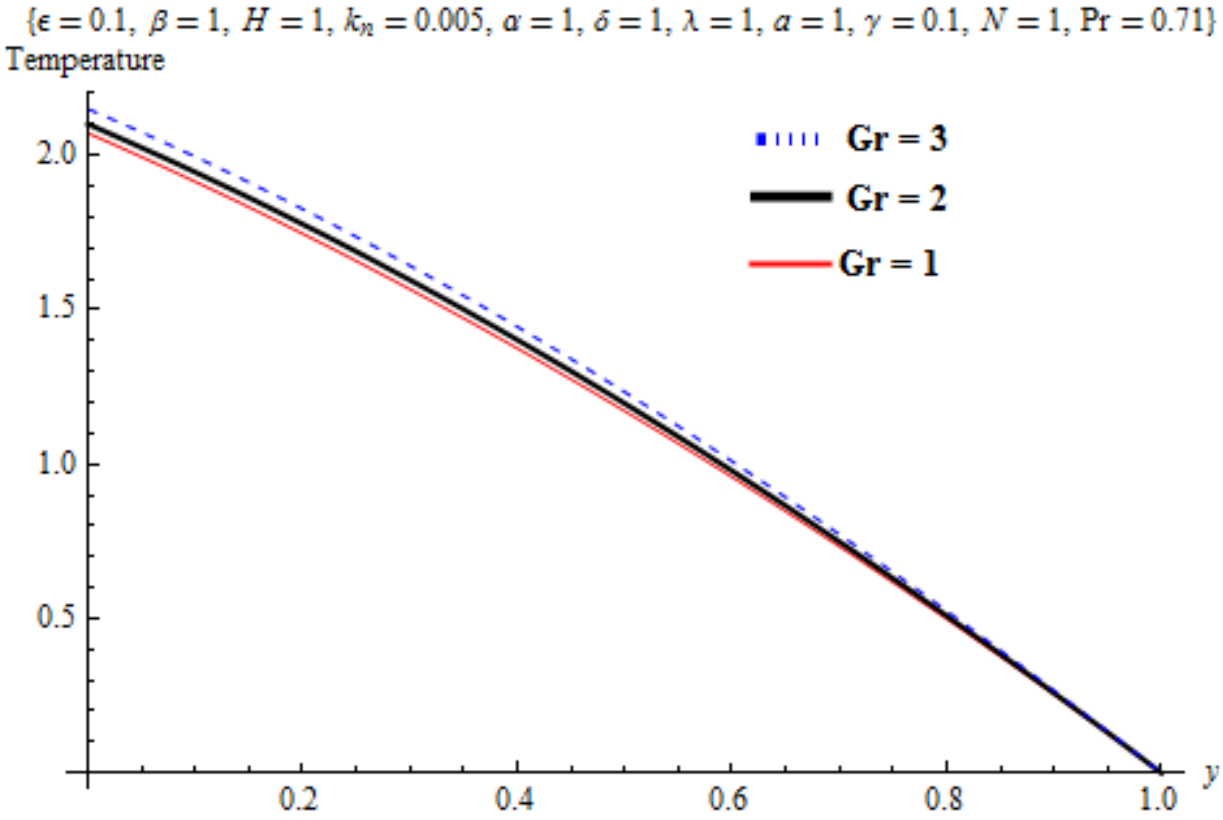

Figure 4.54: Effect of Grashof number (Gr) on temperature profile

4.5.3 Effect of Parameters Variation on Entropy Generation

The effects of variations in slip velocity, temperature jump, thermal radiation and Grashof number on entropy generation are displayed in Figures 4.55-4.58. Figure 4.55 shows that the rate of entropy generation reduces with increase in velocity slip parameter as a result of the reduction in the heat generated as shown in Figure 4.51. Moreover, Figures 4.56-4.58 show similar results on the influence of temperature jump, thermal radiation parameters and Grashof number on entropy generation. It is observed that increase in temperature jump parameter, thermal radiation parameter and Grashof number increases entropy generation significantly. Specifically in Figure 4.56 the rise in the entropy generation is due to the high temperature of fluid particles which is caused by rise in temperature jump parameter as confirmed in Figure 4.52. Also, thermal radiation in Figure 4.57 increases entropy generation due to increase in the emission rate of radiation, while Grashof number in Figure 4.58 increases entropy generation as a result of increased randomness due to the increased rate of change of momentum in the fluid as the parameter Gr increases.

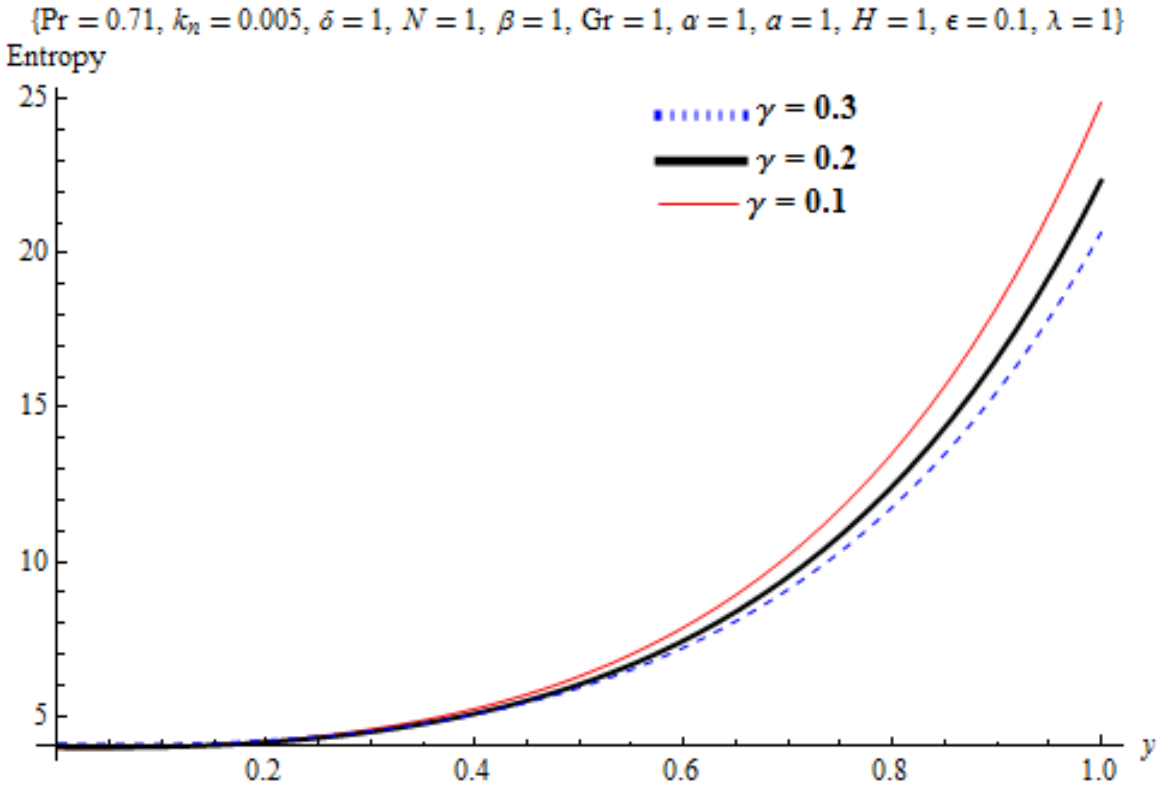

Figure 4.55: Effect of velocity slip parameter (γ) on entropy generation rate

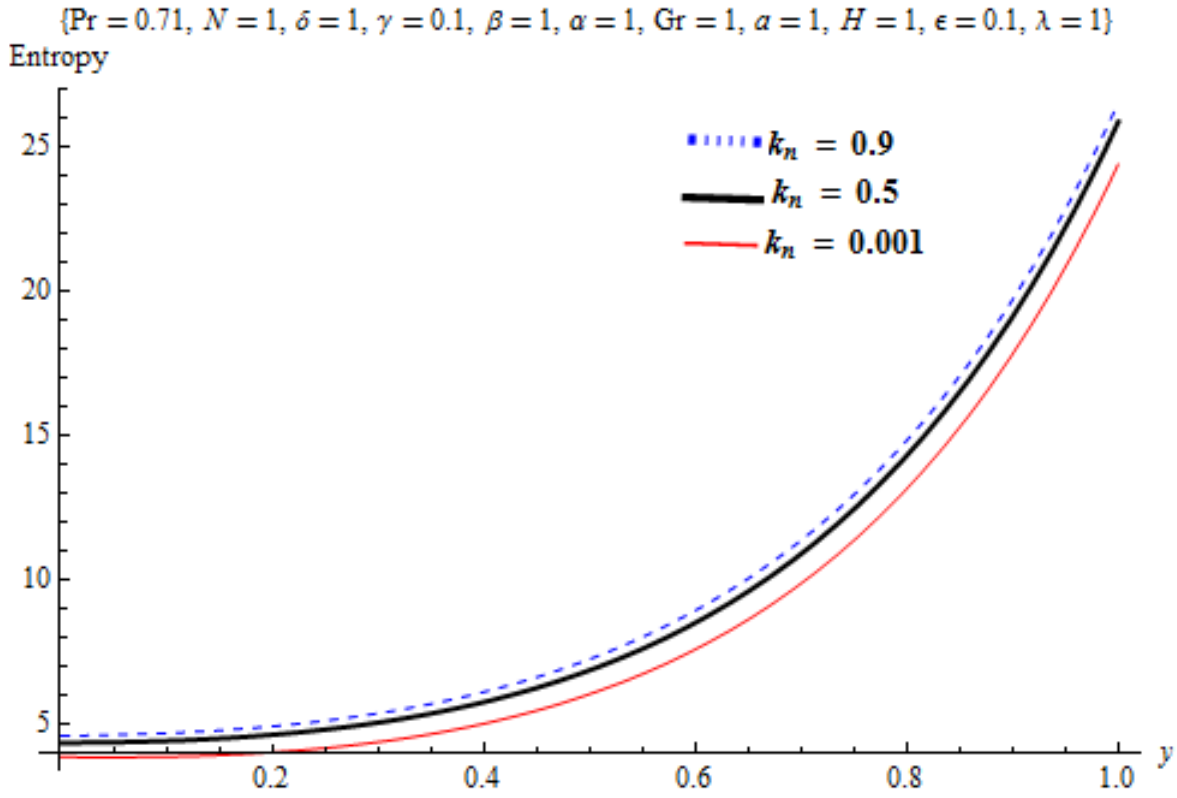

Figure 4.56: Effect of temperature jump parameter (k_n) on entropy generation rate

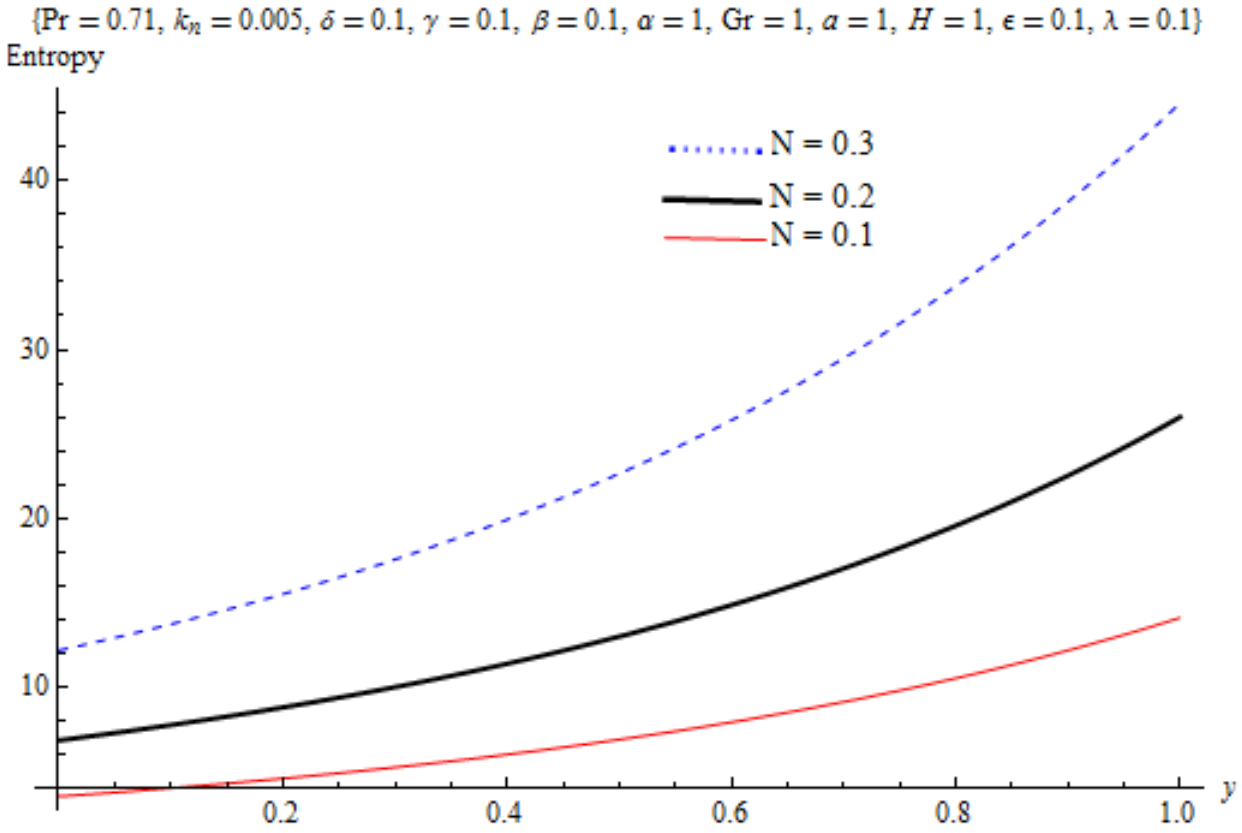

Figure 4.57: Effect of thermal radiation parameter (N) on entropy generation rate

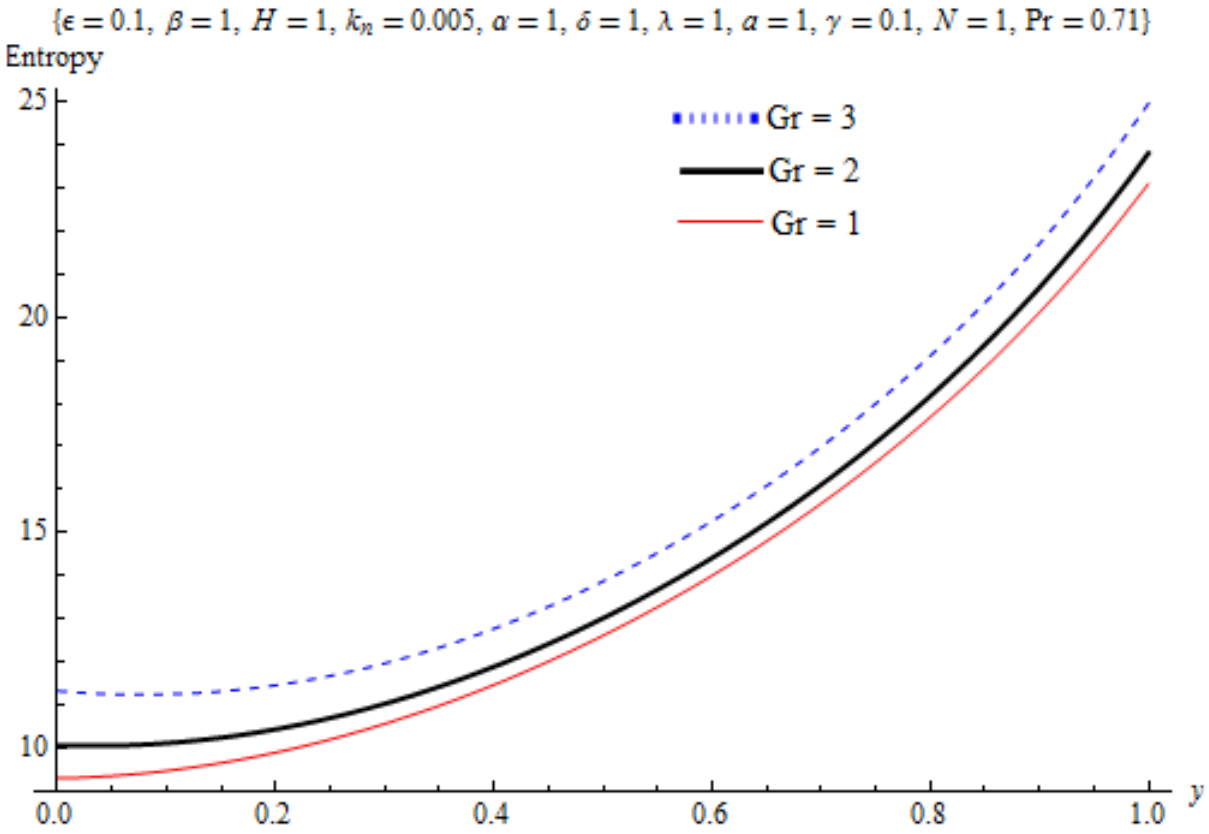

Figure 4.58: Effect of Grashof number (Gr) on entropy generation rate

4.5.4 Effects of Parameters Variation on Bejan number

In this section, the contributing factors to entropy production as each of the thermo-physical parameters is varied is presented in Figures 4.59-4.62. In Figures 4.59 and 4.62 similar result is observed, it is noticed that as the velocity slip parameter and Grashof number increase Bejan number reduces at the lower wall with Newtonian heating and increases at the upper wall. Furthermore, Figures 4.60 and 4.61 depict the influence of temperature jump and radiation parameters on Bejan number, the plots show an increase in Bejan number as the values of the parameters rise. This implies that destruction of exergy is due to the effect of heat transfer at the upper wall.

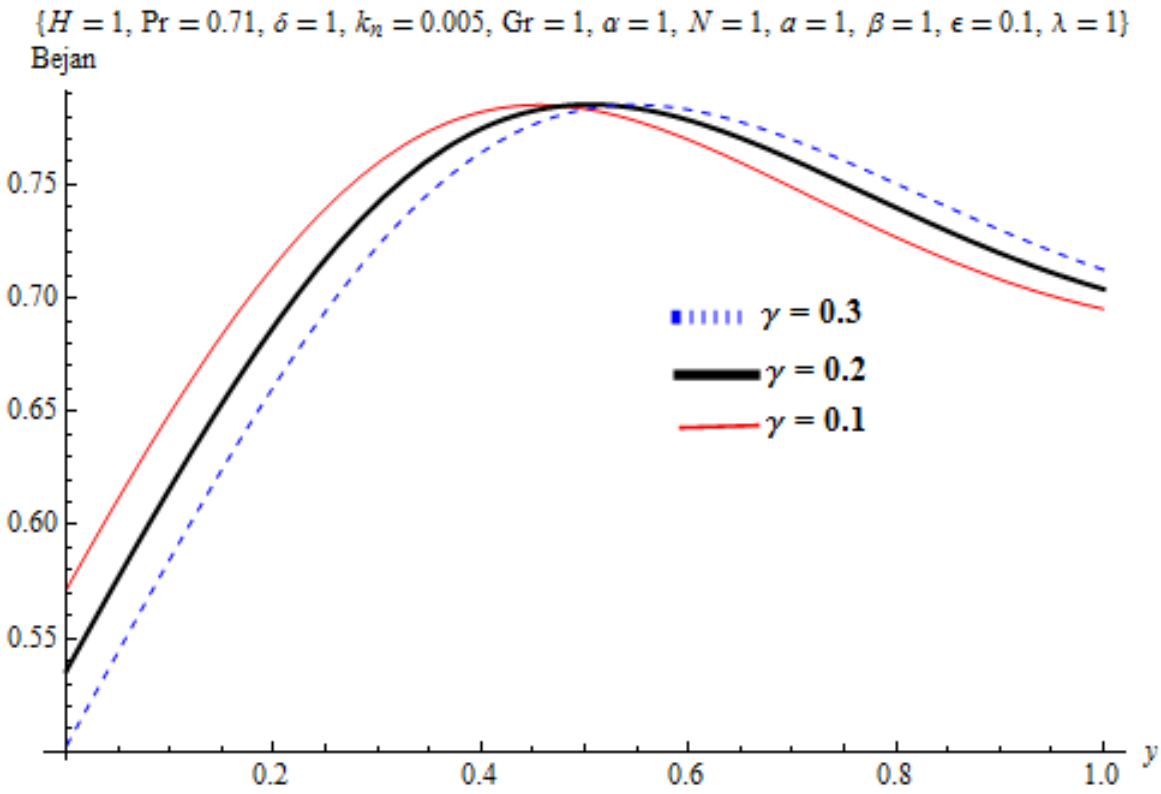

Figure 4.59: Effect of velocity slip parameter (γ) on Bejan number

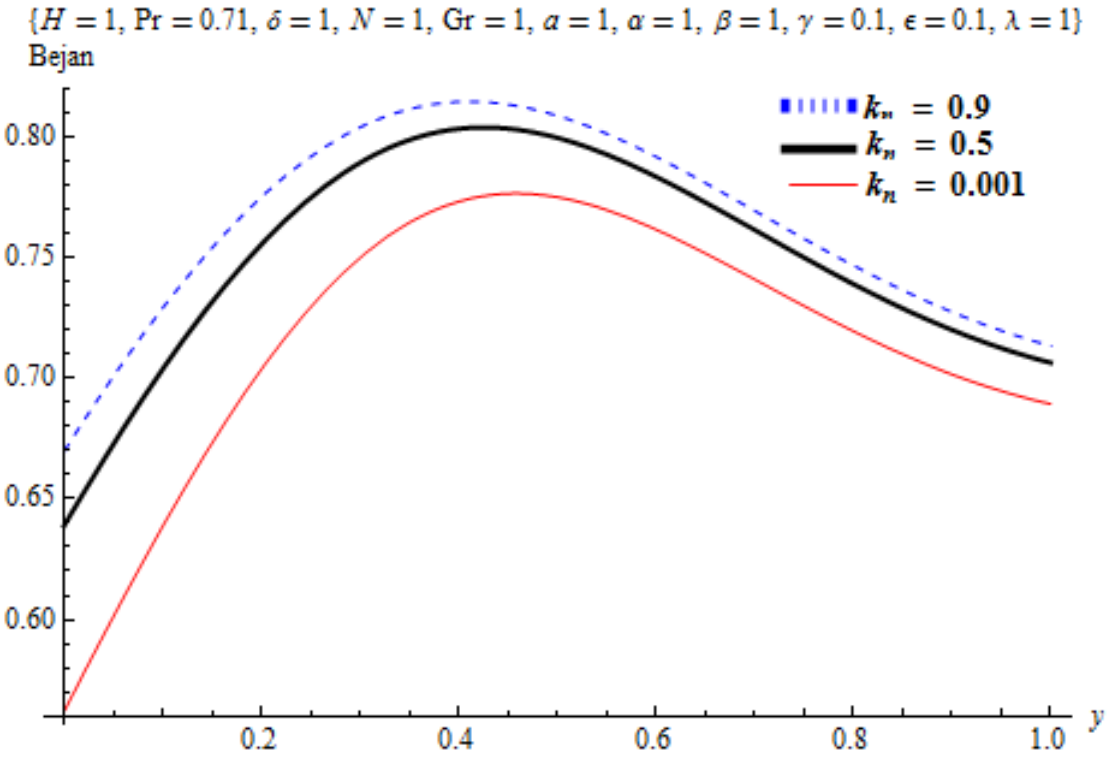

Figure 4.60: Effect of temperature jump parameter (k_n) on Bejan number

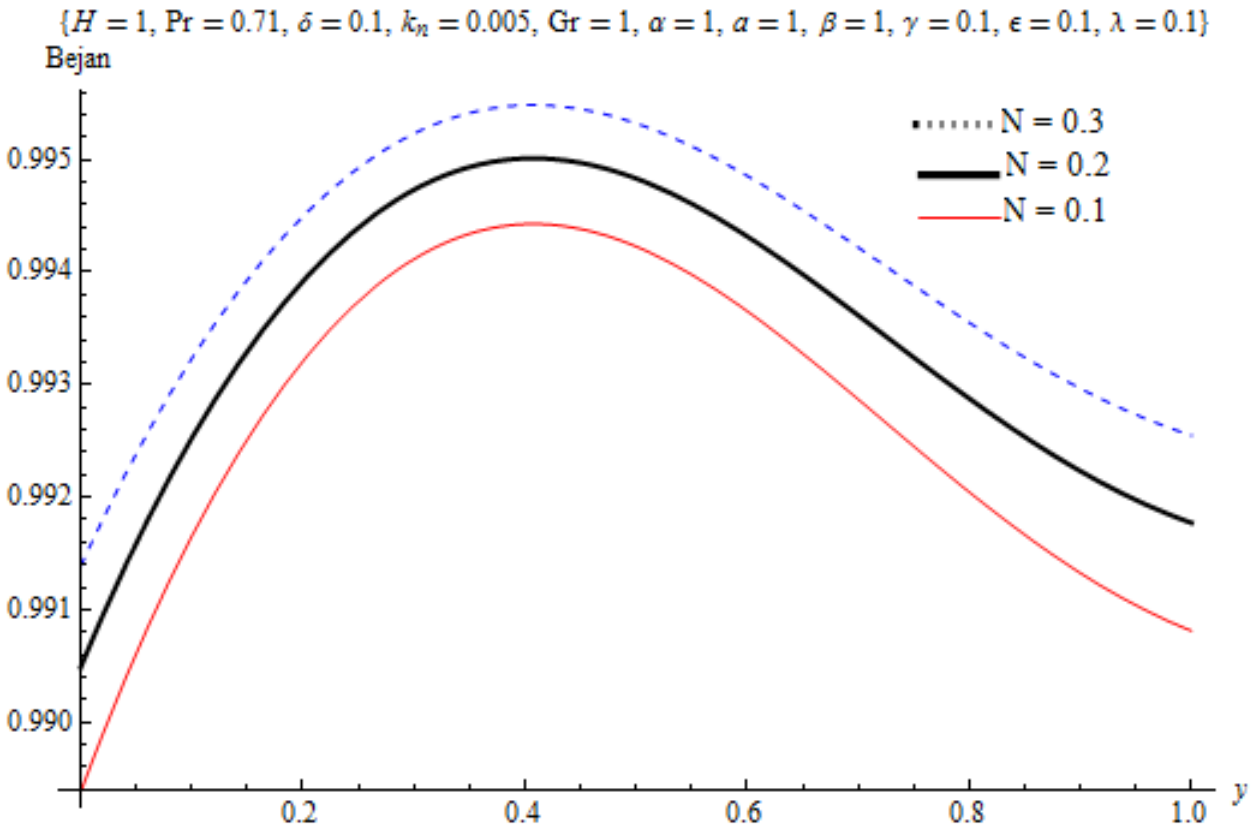

Figure 4.61: Effect of thermal radiation parameter (N) on Bejan number

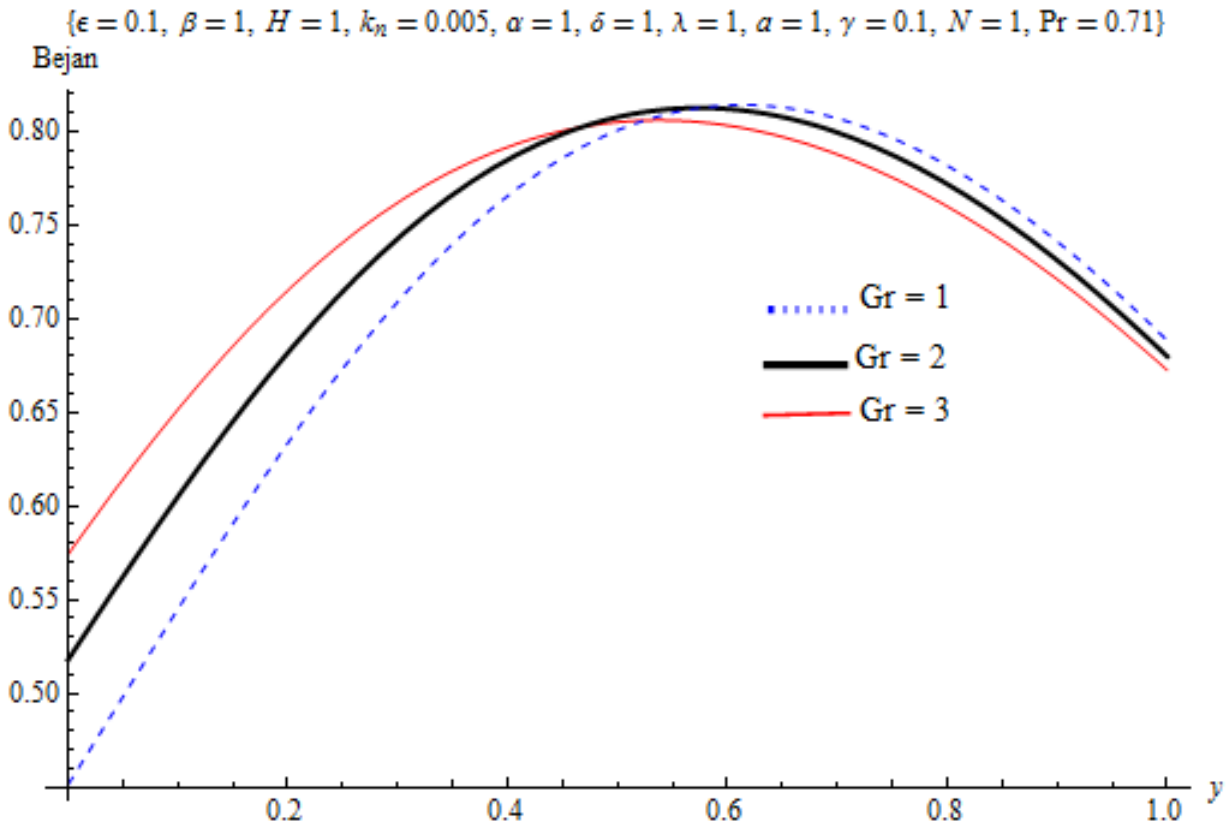

Figure 4.62: Effect of Grashof number (Gr) on Bejan number

CHAPTER FIVE

CONCLUSION AND RECOMMENDATIONS

5.1 Introduction

In this chapter, the results of the analysis in chapter four are presented and explained. The conclusions based on the findings are stated together with the contributions to knowledge.

5.2 Summary of the Research Aim and Objectives

There is an increase in entropy generation as magnetic field and couple stress inverse parameters increase, while entropy generation increases only at the upper wall for suction/injection parameter. Also, increase in magnetic field parameter increases Bejan number while increase in couple stresses retards Bejan number. However, suction/injection decreases the Bejan number at lower wall and centre of the channel. This is an indication that both irreversibility due to heat transfer and viscous dissipation contributed to entropy generation.

Magnetic field increased entropy generation while couple stress and porosity parameters decreased entropy generation. Porous media shape factor parameter, magnetic field parameter and Brinkman number respectively increased Bejan number, while Bejan number decreases slightly at the lower wall with a significant increase in the middle and upper walls of the channel as Prandtl number increases. These results indicate that irreversibility due to heat transfer dominates the flow in the middle and upper walls of the channel.

Grashof number, magnetic field parameter, suction/injection parameter and Biot numbers increased entropy generation rate. It is further noted that Grashof number reduced Bejan number while magnetic field parameter, suction/injection parameter and Biot numbers respectively retarded Bejan number. The implication of this is that

both viscous dissipation and heat transfer contributed to entropy generation.

Entropy generation was reduced with an increase in velocity slip parameter while temperature jump parameter, thermal radiation parameter and Grashof number increased entropy generation significantly. Moreover, velocity slip parameter and Grashof number reduced Bejan number at the lower wall with Newtonian heating and increased it at the upper wall with Newtonian cooling; while temperature jump and radiation parameters reduced Bejan number. This implies that destruction of exergy is due to the effect of heat transfer at the upper wall.

5.3 Conclusion

In this thesis, analysis of entropy generation due to magnetohydrodynmic couple stress fluid in a porous channel, porous medium and vertical porous medium was investigated. The conclusions based on this study are as follows:

(i) Magnetic field parameter (H^2) reduced fluid velocity, increased fluid temperature and enhanced entropy generation. Both irreversibility due to heat transfer and viscous dissipation contributed to entropy generation.

(ii) Porosity parameters decreased fluid velocity and retarded the entropy generation rate. Entropy generation due to heat transfer dominated the flow at the middle and upper walls of the channel.

(iii) Buoyancy force increased fluid velocity, fluid temperature and entropy generation rate. Both viscous dissipation and heat transfer contributed to entropy generation

(iv) Slip velocity parameter increases fluid velocity, increased fluid temperature and retarded entropy generation while temperature jump parameter reduced fluid velocity and temperature but increased entropy generation. Moreover, heat transfer irreversibility dominated entropy generation at the upper wall.

5.4 Contributions to Knowledge

This research has contributed the following to the existing knowledge in the study of MHD couple stress fluid:

(i) Increase in magnetic field and buoyancy force increases entropy generation. The implication of this is that careful measure must be put in place to avoid losses due to rise in entropy generation.

(ii) Increase porosity reduces entropy generation rate, velocity slip and temperature jump parameters retards entropy generation entropy generation rate.

(iii) Entropy generation is contributed by both irreversibility due to viscous dissipation and heat transfer.

(iv) The above submissions would be of interest to engineers and scientists who applied magnetic field to fluids and lubricants to increase the load carrying capacity and improve lubrication capacity.

(v) The findings would be useful in metallurgical industries where magnetic field is applied to control the motion of hot fluid.

5.5 Further Study

Future work can be directed to entropy generation of a couple stress fluid in different flow geometry like pipe flow channel as well as rotational pipe flow. Effect of parameter like hall currents could be an interesting area of research.

REFERENCES

Abdou, M., (2007). Introduction to MHD and applications to Thermofluids of fusion blankets: Lecture notes, *Institute for Plasma Research (IPR), Gandhinagar, India*.

Adesanya, S.O. and Makinde, O.D. (2012). Heat transfer to magnetohydrodynamic non-Newtonian couple stress pulsatile flow between two parallel porous plates. *Zeitschrift für Naturforschung* **67a**: 647—656.

Adesanya, S.O. (2013). Thermal stability analysis of reactive hydromagnetic third-grade fluid through a channel with convective cooling, *Journal of the Nigerian Mathematical Society*, **32**: 61–72.

Adesanya, S.O. Babadipe, E.S., and Arekete, S.A. (2013). A new result on Adomian decomposition method for solving Bratu's problem, *Mathematical Theory and modeling*, **3(2)**: 116–120.

Adesanya, S.O. (2014). Second law analysis for third-grade fluid with variable properties. *Journal of Thermodynamics*, 8 pages http://dx.doi.org/10.1155/2014/452168.

Adesanya, S.O. and Makinde, O.D. (2014). Entropy generation in couple stress fluid flow through porous channel with fluid slippage, *International Journal of Exergy*, **15(3)**: 344–362.

Adesanya, S.O. (2015). Free convective flow of heat generating fluid through a porous vertical channel with velocity slip and temperature jump, *Ain Shams Engineering Journal*. http://dx.doi.org/10.1016/j.asej.2014.12.008.

Adesanya, S.O. and Makinde, O. D. (2015a). Thermodynamic analysis for a third grade fluid through a vertical channel with internal heat generation. *Journal of Hydrodynamics*, **27(2)**: 264–272.

Adesanya, S.O. and Makinde, O.D. (2015b). Effects of couple stresses on entropy generation rate in a porous channel with convective heating. *Computational and Applied Mathematics*, **34**: 293-307.

Adesanya, S.O. and Makinde, O.D. (2015c). Irreversibility analysis in a couple stress film flow along an inclined heated plate with adiabatic free surface. *Physica A.*, **432(15)**: 222–229.

Adesanya, S.O. and Falade, J.A. (2015). Thermodynamics analysis of hydromagnetic third grade fluid flow through a channel filled with porous medium. *Alexandria Engineering Journal*, **57**: 615–622.

Adesanya, S.O., Kareem, S.O., Falade, J.A. and Arekete, S.A. (2015). Entropy generation analysis for a reactive couple stress fluid flow through a channel saturated with porous material. *Energy*, **93**: 1239–1245.

Adomian, G. (1989). Nonlinear stochastic systems: Theory and application to physics. *Kluwer Academic Press*. ISBN 978-90-277-2525-7.

Adomian, G. (1994). Solving Frontier problem of Physics: The Decomposition Method. *Kluwer Academic Press*. ISBN 978-94-015-8289-6.

Ajibade, A.O., Jha, B.K. and Omame, A. (2011). Entropy generation under the effect of suction/injection. *Applied Mathematical Modelling*, **35**: 4630–4646.

Akyildiz, F.T. and Vajravelub, K. (2008). Magnetohydrodynamic flow of a viscoelastic fluid. *Physics Letters A* , **372**: 3380–3384.

Alfven, H. (1956). The Sun's general magnetic field. *Svenska Geofysiska Foreningen*, **8(1)**: 1–12.

Al-nimr, M.A. and Khadrawl, A.F. (2003). Transient free convection fluid flow in domains partially filled with porous media. *Transport in Porous Media*, **51**: 157–172.

Arikoglu, A. and Ozkol, I. (2005). Solution of boundary value problems for integro-differential equations by using differential transform method. *Applied Mathematics and Computation*, **168**: 1145–1158.

Arikoglu, A., Ozkol, I. and Komurgoz, G. (2008). Effect of slip on entropy generation in a single rotating disk in MHD flow. *Applied Energy*, **85**: 1225–1236.

Arikoglu, A., Komurgoz, G., Ozkol, I. and Gunes, A. Y. (2010). Combined effects of temperature and velocity jump on the heat transfer, fluid flow, and entropy generation over a single rotating disk. *Journal of Heat Transfer*, **132(11)**: 111703–111710.

Ayeni, R.O. (1982). On the explosion of chain-thermal reaction. *Journal of Australia. Mathematical Society Series*, **24**: 194–202.

Awaisa, M., Malika, M.Y., Bilala, S., Salahuddinb, T., Hussain, A. (2017). Magnetohydrodynamic (MHD) flow of Sisko fluid near the axisymmetric stagnation point towards a stretching cylinder,. *Results in Physics*, **7**: 49–56.

Barletta, A., Magyari, E., Pop, I. and Storesletten, L. (2007). Mixed convection with viscous dissipation in a vertical channel filled with a porous medium. *Acta Mechanica* **194**: 123–140.

Basak, T., Kaluri, R.S. and Balakrishnan, A.R. (2012). Entropy generation during natural convection in a porous cavity: Effect of thermal boundary condition. *Numerical Heat Transfer, Part A*, **62**: 336-364.

Batchelor, G.K. (1949). On the spontaneous magnetic field in a conducting liquid in turbulent motion, *Proceedings of the Royal Society of London. Series A, Mathematical and Physical Sciences*, **201(1066)**: 406–416.

Beg, O.A., Zueco, J. and Takhar, H.S. (2009). Unsteady magnetohydrodynamic Hartmann-Couette flow and heat transfer in a Darcian channel with Hall current, ionslip, viscous and Joule heating effects: Network numerical solutions. *Communications in Nonlinear Science and Numerical Simulation*, **14**: 1082–1097.

Bejan, A. (1980). Second law analysis in heat transfer. *Energy*, **15**: 720–732.

Bejan, A. (1982). Second law analysis in heat transfer and thermal design. *Advances in Heat Transfer*, **15**: 1–58.

Bejan, A. (1984). Convection heat transfer. Wiley, New York. ISBN 978-0-470-90037-6.

Bejan, A. (1996). Entropy generation minimization, CRC Press: New York, NY, USA.ISBN 0-471-1-4880-6.

Bouabid, M., Maggerbi, M., Hidouri, N. and Brahim, A. B. (2011). Entropy generation at natural convection in inclined rectangular cavity. *Entropy*, **13(5)**: 1020–1033.

Chang, C.C. and Lundgren, T.S. (1961). Duct flow in Magnetohydrodynamics. *Zeitschrift für Angewandte Mathematik Und Physik*, **12**: 100–114.

Chandra, A. and Chhabra, R.P.(2012). Effect of Prandtl number on natural convection heat transfer from a heated semi-circular cylinder. *International Journal of Chemical and Biological Engineering* **6**: 45–56.

Chandran, P., Sacheti, N.C. and Singh, A.K. (1992). Effect of rotation on unsteady hydromagnetic Couette flow. *Astrophysics and Space Science*, **202(1)**: 1–10.

Chao, B.H., Wang, H. and Cheng, P. (1996). Stagnation point flow of a chemically reactive fluid in a catalytic porous bed. *International Journal of Heat and Mass Transfer*, **39**: 3003–3019.

Chauhan, D.S. and Kumar, V.(2009). Effects of slip conditions on forced convection and entropy generation in a circular channel occupied by a highly porous medium: Darcy extended Brinkman-Forchheimer model. *Turkish Journal of Engineering and Environmental Sciences*, **33**: 91–104.

Chauhan, D.S. and Rastogi, P. (2010). Radiation effects on natural convection MHD flow in a rotating vertical porous channel partially filled with a porous medium. *Applied Mathematical Sciences*, **4(13)**: 643–655.

Chen, C.K. and Ho, S.H. (1999). Solving partial differential equations by two-dimensional differential transform method. *Applied Mathematics and Computation* **106**: 171–179. doi:10.1016 S0096-3003(98)10115-7.

Collins, R.E. (1961). Flow of fluids through Porous Materials. Reinhold Publishing Co., New York. DOI: 10.1002/aic.690080102.

Cramer, K.R. and Pai, S.I. (1973). Magnetofluid dynamics for engineers and applied physicists. New York, USA: McGraw-Hill.

David, L.M., Lawrence, H. and Alejandro, L.G. (1992). Slip length in a dilute gas. *Physical Review A*, **46(8)**: 52–79.

Dainton, F.S. (1960). Chain Reaction. An introduction, New York: Willey. ISBN: 9781468476873.

Das, S. and Jana, R.N. (2014). Entropy generation due to MHD flow in a porous channel with Navier slip. *Ain Shams Engineering Journal* **5**: 575–584.

Das, S., Banu, A.S., Jana, R.N. and Makinde, O.D. (2015). Entropy analysis on MHD pseudo-plastic nanofluid flow through a vertical porous channel with convective heating. *Ain Shams Engineering Journal* **54**: 325–337.

Dawson, P.A. (2001) An introduction to magnetohydrodynamics. *Cambridge Texts in Applied Mathematics*, ISBN-10: 0-521-79487-0.

Devakar, M. and Iyengar, T.K.V.(2010). Run up flow of a couple stress fluid between parallel plates. *Nonlinear Analysis: Modelling and Control*, **15(1)**: 29–37.

Dinesh P.A., Nalinaksh N. and Sandeep, N. (2015). Double diffusive mixed convection in a couple stress fluids with variable fluid properties. *Advances in Physics Theories and Applications*, **14**: 30–42.

Eegunjobi, A.S. and Makinde, O.D. (2012). Effects of Navier slip on entropy generation in a porous channel with suction/injection. *Journal of Thermal Science and Technology*. **7(4)**: 522–535.

Fang, T., Zhang, J. and Yan, S. (2009) Slip MHD viscous flow over a stretching sheet-An exact solution. *Communications in Nonlinear Science and Numerical Simulation*, **14**: 3731–3737.

Fox, R.W., McDonald, A.T. and Pritchard, P.J. (2004). Introduction to Fluid Mechanics. 6th edition, John Wisely and Sons, Inc, United States of America.

Frank-Kamenetskii, D.A. (1969). Diffusion and heat transfer in chemical kinetics. New York: Plenum Press.

Gbadeyan, J.A., Daniel, S. and Kefan, E.G. (2005). The radiative effect on electrohydrodynamic froth flow in vertical channel. *Journal of Mathematical Association of Nigeria*, **32**: 388–396.

Gbadeyan, J.A. and Idowu, A.S. (2006) Radiation effect of magnetohydrodynamic flow of gas between concentric spheres. *Journal of the Nigerian Association of Mathematical Physics*, **10**: 305–314.

Gbadeyan, J.A., Idowu, A.S., Areo, A.O. and Olaleye, P.O. (2010). The radiative effect on velocity, magnetic and temperature fields of a magnetohydrodynamic oscillatory flow past a limiting surface with variable suction. *Journal Of Mathematical Sciences*, **21(4)**: 395–411.

Gbadeyan, J.A. and Hassan, A.R. (2012). Multiplicity of solutions for a reactive variable viscous Couette flow under Arrhenius Kinetics. *Mathematical Theory and Modeling*, **2(9)**: 39–50.

Gerbeth, G., Eckert, K. and Odenbach, S. (2013). Electromagnetic flow control in metallurgy, crystal growth and electrochemistry. *The European Physical Journal Special Topics*, **220**: 1–8.

Gupta, A.S., (1972). Magnetohydrodynamic Ekmann layer. *Acta Mechanica*, **13(1)**: 155–160.

Hadaad, O.M., Abuzaid, M.M. and Al-Nimr, M.A. (2005). Developing free-convection gas flow in vertical open-ended michrochannel filled with porous media. *An international Journal of computation and methodology*, **48(7)**: 693–710.

Hamad, M.A.A. and Pop, I. (2011), Unsteady MHD free convection flow past a vertical permeable flat plate in a rotating frame of reference with constant heat source in a nanofluid. *Heat Mass Transfer*, **47**: 1517–1524. DOI:10.1007/s00231-011-0816-6.

Hassan, A.R. and Gbadeyan, J.A. (2014). Thermal stability of a reactive hydromagnetic Poiseuille fluid flow through a channel. *American Journal of Applied Mathe-*

matics, **2(1)**: 14–20.

Hassan, A.R. and Gbadeyan, J.A. (2015). A reactive hydromagnetic internal heat generating fluid flow through a channel. *International Journal of Heat and Technology*, **33(3)**: 43–50.

Hassan, H.I. (2008). Comparison differential transformation technique with Adomian decomposition method for linear and nonlinear initial value problems. *Chaos Solitons Fractals*, **36(1)**: 53–65.

Hayat, T., Hina, S. and Ali, N. (2010). Simultaneous effects of slip and heat transfer on the peristaltic flow. *Communications in Nonlinear Science and Numerical Simulation*, **15**: 1526–1537.

Hayat, T., Shafiq, A., Alsaedi, A. and Asghar, A. (2015). Effect of inclined magnetic field in flow of third grade fluid with variable thermal conductivity *AIP Advances*, 5, http://dx.doi.org/10.1063/1.4928321.

Hooman, K. (2007), Entropy generation for microscale forced convection: effects of different thermal boundary conditions, velocity slip, temperature jump, viscous dissipation, and duct geometry. *International Communications in Heat and Mass Transfer*, **34**: 945–957.

Hughes, W.F. and Elco, R.A. (1962). MHD lubrication flow between parallel rotating disks. *Journal of Fluid Mechanics*, **13**: 21–32.

Hunt, J.C.I. and Shercliff, J.A. (1971). Magnetohydrodynamics at high Hartman number. *Annual Review of Fluid Mechanics*, **3**: 37–62.

Jamalabadi, M.A., Park, J.H. and Lee, C.Y. (2015), Optimal design of magnetohydrodynamic mixed convection flow in a vertical channel with slip boundary conditions and thermal radiation effects by using an entropy generation minimization method. *Entropy*, **17**: 866–881.

Jawad, A., Azeem, S., Masood, K. and Ramzan, A. A (2015). Note on convective heat transfer of an MHD Jeffrey fluid over a stretching sheet, *AIP Advances*, **5**: 1–11.

Jery, A.E., Hidouri, N., Magherbi, M. and Brahim, A.B. (2010). Effect of an external oriented magnetic field on entropy generation in natural convection. *Entropy*, **12**: 1391–1417.

Jha, B. K. and Ajibade, A.O. (2009). Free convective flow of heat generating/absorbing fluid between vertical porous plates with periodic heat input. *International Communications in Heat and Mass Transfer*, **36**: 624–631.

Jha, B.K., Samaila, A.K. and Ajibade, A.O. (2011). Transient free-convective flow of reactive viscous fluid in a vertical. *International Communication in Heat and Mass Transfer*, **38**: 633–637.

Jha, B.K., Samaila, A.K. and Ajibade, A.O. (2013). Unsteady/steady natural convection flow of reactive viscous fluid in a vertical annulus. *International Journal of Applied Mechanics and Engineering*, **18(1)**: 73–83.

Jha, B.K., Daramola, D. and Ajibade, A.O. (2015). Mixed convection in a vertical annulus filled with porous material having time-periodic thermal boundary condition:

steady- periodic regime. *Meccanica: An international Journal of Theoretical and Applied Mechanics*: 1–14.

Karamallah, A.A., Mohammad, W.S. and Khalil, W.H. (2011). Numerical study of entropy generation in a vertical square channel packed with saturated porous media. *Engineering and Technology Journal*, **29(9)**: 1721–1736.

Khan, Md.S., Karim, I., Islam, Md.S. and Wahiduzzaman, M. (2014). MHD boundary layer radiative, heat generating and chemical reacting flow past a wedge moving in a nanofluid, *NanConvergence*. **1(20)**. http://www.nanoconvergencejournal.com.

Kumar, K., Singh, V. and Sharma, S. (2015). On the onset of convection in a dusty couple stress fluid with variable gravity through a porous medium in hydromagnetics. *Journal of Applied Fluid Mechanics*, **8(1)**: 55–63.

Lienhard IV, J.H. and Lienhard V, J.H. (2006). A heat transfer textbook (version 1.24), 3rd ed., *Phlogiston Press*, Cambridge, MA, pp. 707–718.

Liu, H. and Song, Y. (2007). Differential transform method applied to high index differential- algebraic equations.*Applied Mathematics and Computation* **184(2)**: 748–753.

Makinde, O.D. (2009). On thermal stability of a reactive third–grade fluid in a channel with convective cooling the walls. *Applied Mathematics and Computation* **29**: 1773–1777.

Makinde, O.D. and Eegunjobi, A.S. (2013). Effects of convective heating on entropy generation rate in a channel with permeable walls. *Entropy* **15**: 220–233.

Magherbi, M., Jery, A.L, Hidouri, N. and Brahim, A.B. (2010). Evanescent magnetic field effects on entropy generation at the onset of natural convection. *Sadhana*, **35(2)**: 163–176.

Maxwell, J.C. (1879). On stresses in rarefied gases arising from inequalities of temperature. *Philosophical Transactions of the Royal Society London*, **170**: 231–256.

Michael, A.D. (1990). The no-slip condition of fluid dynamics, *Erkenntnis*, **33(3)**: 285–296.

Moffatt, H.K. (1970). Turbulent dynamo action at low magnetic Reynolds number.*Journal of Fluid Mechanics*, **41(2)**: 436–462.

Molokov, S., Moreau, R . and Moffatt, H.K. (2007). Magnetohydrodynamics historical evolution and trends. *Springer, Dordrecht, The Netherlands* ISBN 978-1-4020-4833-3.

Mutuku-Njane, W.N. and Makinde, O.D. (2013). Combined effects of buoyancy force and Navier slip on MHD flow of a Nanofluid over a convectively heated vertical porous plate. *The Scientific World Journal*, http://dx.doi.org/10.1155/2013/725643.

Nakayama, Y. and Boucher, R.F. (1999). Introduction to fluid mechanics. *John Wiley and Sons Inc.*, New York.ISBN 0 340 67649 3.

Navier, C.L.M.H. (1832), Mémoire sur les lois du mouvement des fluids, Mém. Acad. *Royal Science Institute France* 6, 389-440, ISBN 978-0387-29096-6.

Nield, D.A. and Bejan, A. (2006). Convection in porous media, 3rd edition,*Springer*, New York.

Noor, N.F.M., Abbasbandy, S. and Hashim, I. (2012). Heat and mass transfer of thermophoretic MHD flow over an inclined radiate isothermal permeable surface in the presence of heat source/sink. *International Journal of Heat and Mass Transfer* **55**: 2122–2128.

Noreen S. A., Nadeem, S. and Changhoon, L. (2013). Characteristics of Jeffrey fluid model for peristaltic flow of chyme in small intestine with magnetic field. *Results in Physics* **3**: 152–160.

Okoya, S.S. (2006). Thermal stability for a reactive viscous flow in a slab. *Mechanics Research Communication*, **33**: 728–733.

Olanrewaju, M.A., Gbadeyan, J.A. and Idowu, A.S.(2016). Flow and heat transfer analysis of a second grade fluid with Newtonian heating in the presence of elastic deformation in a porous medium. *The Pacific Journal of Science and Technology*, **17(1)**: 30–48.

Opanuga, A.A., Okagbue, H.I., Edeki, S.O. and Agboola, O.O. (2015a). Differential transform technique for higher order boundary value problems, *Modern Applied Science*, **9(13)**: 224–230.

Opanuga, A.A., Agboola, O.O. and Okagbue, H,I. (2015b). Approximate solution of multipoint boundary value problems. *Journal of Engineering and Applied Sciences*, **10(4)**: 85–89.

Opanuga, A.A., Okagbue, H.I., Owoloko, E.A., and Agboola, O.O. (2016). Modified Adomian decomposition method for thirteenth order boundary value problems. *Gazi University Journal of Science*(in press).

Ozkol, I., Komurgoz, G. and Arikoglu, A. (2007). Entropy generation in laminar natural convection from a constant temperature vertical plate in an infinite fluid. *Journal of Power and Energy* **221(5)**: 609–616.

Pakdemirli, M. (2006). Entropy generation in a pipe due to non-Newtonian fluid flow: Constant viscosity case. *Sadhana*, **31(1)**: 21–29.

Patel, V. and Kassegne, S. K. (2007). Electroosmosis and thermal effects in magnetohydrodynamic (MHD) micropumps using 3D MHD equations. *Sensors and Actuators B*, **122**: 42–52.

Prasad, V.R, Vasu, B., Beg, O.A. and Parshad, R.D. (2012). Thermal radiation effects on magnetohydrodynamic free convective heat and mass transfer from a sphere in a variable porosity regime. *Communications in Nonlinear Science and Numerical Simulation*, **17**: 654–671.

Rao, R.D.R.V., Krishna, D.V. and Devnath, L. (1982). Combined effect of free and forced convection on MHD flow in a rotating porous channel.*International Journal of Mathematics and Mathematical Sciences*, **5**: 165–182.

Rajashekar, M. and Kashinath, B. (2012). Effect of roughness on MHD couples stress squeeze-film characteristics between a sphere and a porous plane surface. *Advances*

in Tribology, doi:10.1155/2012/935690.

Rajput, R.K. (2004) A textbook of fluid mechanics and hydraulic machines. *S. Chand and Company L.T.D., RAM NAGAR*, New Delhi-110055, ISBN: 9789385401374.

Rani, H.P., Reddy, G.J., and Kim, C.N. (2011). Numerical analysis of couple stress fluid past an infinite vertical cylinder. *Engineering Applications of Computational Fluid Mechanics*, **5(2)**: 159–169.

Raptis, A. Perdikis and Takhar, H.S. (2004). Effect of thermal radiation on MHD flow, *Applied Mathematics and Computation*, **153**: 645–649.

Rashidi, M.M., Erfani, E., Bég, O.A. and Ghosh, S.K. (2011). Modified differential transform method (DTM) simulation of hydromagnetic multi-physical flow phenomena from a rotating disk. *World Journal of Mechanics*, **1**: 217–230.

Rashidi, M. M. and Freidoonimehr, N. (2012). Effects of velocity slip and temperature jump on the entropy generation in MHD flow over a porous rotating disk. *Journal of Mechanical Engineering*, **1(3)**: 3–14.

Renksizbulut, M., Niazmand, H. and Tercan, G. (2006). Slip-flow and heat transfer in rectangular microchannels with constant wall temperature. *International Journal of Thermal Sciences*, **45**: 870–881.

Rudraiah, N. and Chandrashekara, G. (2010). Effects of couple stress on the growth rate of Rayleigh-Taylor instability at the interface in a finite thickness couple stress fluid. *Journal of Applied Fluid Mechanics*, **3(1)**: 83–89.

Sabersky, R.H., Acosta, A.J., Hauptamann, E.G. and Gates, E.M. (1999). A First course in fluid mechanics, Prentice Hall International, Inc, fourth edition.ISBN-13: 978-0135763728.

Sahiti, N., Krasniqi, F., Fejzullahu, X., Bunjaku, J. and Muriqi, A. (2008). Entropy generation minimization of a double-pipe pin fin heat exchanger. *Applied Thermal Engineering*, **28**: 2337–2344.

Seth, C.S., Jana, R.N. and Maiti, M.K. (1982). Unsteady hydormagnetic Couette flow in a rotating system. *International Journal of Engineering Science.* **20(9)**: 989–999.

Schetz, J.A. and Fuhs, A.E. (1999). Fundamentals of fluid mechanics, New York, *John Wiley and Sons.* ISBN 0-471-34856-2.

Schnack, D.D. (2009). Lectures in magnetohydrodynamics: With an appendix on extended MHD.*Lecture Notes in Physics.* 780 (Springer, Berlin Heidelberg) DOI 10.1007/ 978-3-642-00688-3.

Sharma, P.R., Sharma, K. and Mehta, T. (2014). Radiative and free convective effects on MHD flow through a porous medium with periodic wall temperature and heat generation or absorption. *International Journal of Mathematical Archive*, **5(9)**: 119–128.

Shehzad, S.A., Hayat, T. and Alsaedi, A. (2015). Influence of convective heat and mass conditions in MHD flow of nanofluid. *Bulletin of The Polish Academy of Sciences Technical Sciences*, **63(2)**: 465–474.

Singh, V.P., and Kumar, B. (1996). Subsurface-Water Hydrology. *Proceedings of the International Conference on Hydrology and Water Resources* **2**, 1538160.

Singh, A.K., Sacheti, N. C. and Chandran, P. (1994). Transient effects on magneto-hydrodynamic Couette flow with rotation: Accelerated motion. *International Journal of Engineering Science*, **32**: 133–139.

Singh, K.D. (2000), An oscillatory hydromagnetic Couette flow with transpiration cooling. *Zeitschrift für Angewandte Mathematik Und Mechanik (ZAMP)*, **80**: 429–432.

Singh, K.D. (2013). Exact solution of MHD mixed convection periodic flow in a rotating vertical channel with heat radiation. *International Journal of Applied Mechanics and Engineering* **18(3)**: 853–869.

Sloan, D.M. (1973). Extremum principles for magnetohydrodynamic channel flow. *Journal of Applied Mathematics and Physics (ZAMP)*, **24(5)**: 689–698.

Smith, P. (1972). Some extremum principles for pipe flow in magnetohydrodynamics. *Journal of Applied Mathematics and Physics (ZAMP)*, **23(5)**: 753–764.

Srivastava, L.M. (1985). Flow of couple stress fluid through stenotic blood vessels. *Journal of Biomechanics*, **18(7)**: 479–485.

Srinivasacharya, D. and Kaladhar, K. (2012a). Analytical solution of mixed convection flow of couple stress fluid between two circular cylinders with Hall and ion-slip effects. *Turkish Journal of Engineering and Environmental Sciences* , **36**: 226–235.

Srinivasacharya, D. and Kaladhar, K. (2012b). Mixed convection flow of couple stress fluid between parallel vertical plates with Hall and Ion-slip effects.
Communications in Nonlinear Science and Numerical Simulation, **17**: 2447–2462.

Stokes, V.K. (1966). Couple stresses in fluid. *The Physics of Fluids*, **9**: 1709–1715.

Sunil, Sharma, R.C. and Chandel, R. S. (2002). On superposed couple-stress fluids in porous medium in hydromagnetics. *Zeitschrift für Naturforschung* **57a**: 955–960.

Turkyilmazoglu, M. (2011). Multiple solutions of heat and mass transfer of MHD slip for the viscoelastic fluid over a stretching sheet. *International Journal of Thermal Sciences*, **50**: 2264–2276.

Turner, J.S. (1973). Buoyancy effects in fluids, *Cambridge University Press*, ISBN: 052108623X.

Walicki, E. and Walicka, A. (1999). Inertial effect in the squeeze film of couple-stress fluids in biological bearings. *International Journal of Applied Mechanics and Engineering*, **4**: 363–373.

Wazwaz, A.M. (1999). A reliable modification of Adomian's decomposition method. *Applied Mathematics and Computation* **102(1)**:77–86.

Wendt, J.F. (2009). Computational fluid dynamics. 3rd edition, Springer-Verlag, Berlin Heidelberg.

Xu, X., Lian, S. and Pop, I. (2007). Series solutions of unsteady three-dimensional MHD flow and heat transfer in the boundary layer over an impulsively stretching

plate. *European Journal of Mechanics B/Fluids*, **26**: 15–27.

Yapici, H., Basturk, G., Nkayatas, N. and Yalcin, S. (2005). Numerical study on transient local entropy generation in pulsating turbulent flow through an externally heated pipe. *Sadhana*, **30(5)**: 625–648.

Zakaria, M., (2002). Hydromagnetic fluctuating flow of a couple stress fluid through a porous medium. *The Korean Journal of Computational and Applied Mathematics Archive*, **10(1-2)**: 175–191.

Zhenga, L., Niua, J., Zhangb, X. and Gaoc, Y. (2012). MHD flow and heat transfer over a porous shrinking surface with velocity slip and temperature jump. *Mathematical and Computer Modelling*, **56**: 133–144.

Zhou, J.K. (1986). Differential transformation and its application for electrical circuits. Huarjung University Press, Wu-uhahn, China, (in Chinese).

APPENDICES

Appendix A: Mathematica Codes for ADM

```
Subscript[u, 0][y] =
 Subscript[b, 1] + Subscript[b, 2]/3!*y^3 + a^2 \!\(
\*SubsuperscriptBox[\(\[Integral]\), \(0\), \(y\)]\(\((
\*SubsuperscriptBox[\(\[Integral]\), \(0\), \(y\)]\((
\*SubsuperscriptBox[\(\[Integral]\), \(0\), \(y\)]\((
\*SubsuperscriptBox[\(\[Integral]\), \(0\), \(y\)]\(((\(-G\))\) \
\[DifferentialD]y)\) \[DifferentialD]y)\) \[DifferentialD]y)\) \
\[DifferentialD]y\)\)

-(1/24) a^2 G y^4 + Subscript[b, 1] + (y^3 Subscript[b, 2])/6

Subscript[u, 1][y] = a^2 \!\(
\*SubsuperscriptBox[\(\[Integral]\), \(0\), \(y\)]\(\((
\*SubsuperscriptBox[\(\[Integral]\), \(0\), \(y\)]\((
\*SubsuperscriptBox[\(\[Integral]\), \(0\), \(y\)]\((
\*SubsuperscriptBox[\(\[Integral]\), \(0\), \(y\)]\(((\((\ D[D[
\(\*SubscriptBox[\(u\), \(0\)]\)[y], y], y])\) - s*D[
\(\*SubscriptBox[\(u\), \(0\)]\)[y], y] + \ \ \ H^2*
\(\*SubscriptBox[\(u\), \(0\)]\)[
                y])\) \[DifferentialD]y)\) \[DifferentialD]y)\) \
\[DifferentialD]y)\) \[DifferentialD]y\)\)

a^2 (-(1/720) a^2 G y^6 + (a^2 G s y^7)/5040 - (a^2 G H^2 y^8)/
   40320 + 1/24 H^2 y^4 Subscript[b, 1] + (y^5 Subscript[b, 2])/120 -
   1/720 s y^6 Subscript[b, 2] + (H^2 y^7 Subscript[b, 2])/5040)
```

```
Subscript[u, 2][y] = a^2 \!\(
\*SubsuperscriptBox[\(\[Integral]\), \(0\), \(y\)]\(\((
\*SubsuperscriptBox[\(\[Integral]\), \(0\), \(y\)]\((
\*SubsuperscriptBox[\(\[Integral]\), \(0\), \(y\)]\((
\*SubsuperscriptBox[\(\[Integral]\), \(0\), \(y\)]\((\((\(( D[D[
\(\*SubscriptBox[\(u\), \(1\)]\)[y], y], y])\) - s*D[
\(\*SubscriptBox[\(u\), \(1\)]\)[y], y] + \ \ \ H^2*
\(\*SubscriptBox[\(u\), \(1\)]\)[
                y])\) \[DifferentialD]y)\) \[DifferentialD]y)\) \
\[DifferentialD]y)\) \[DifferentialD]y\)\)

1/39916800 a^4 (-(1/12)
       a^2 G y^8 (11880 - 2640 s y + 132 (2 H^2 + s^2) y^2 -
       24 H^2 s y^3 + H^4 y^4) +
    990 H^2 y^6 (56 - 8 s y + H^2 y^2) Subscript[b, 1] +
    y^7 (7920 +
       y (220 H^2 y + 110 s^2 y + H^4 y^3 -
          22 s (90 + H^2 y^2))) Subscript[b, 2])

Subscript[u, 3][y] = a^2 \!\(
\*SubsuperscriptBox[\(\[Integral]\), \(0\), \(y\)]\(\((
\*SubsuperscriptBox[\(\[Integral]\), \(0\), \(y\)]\((
\*SubsuperscriptBox[\(\[Integral]\), \(0\), \(y\)]\((
\*SubsuperscriptBox[\(\[Integral]\), \(0\), \(y\)]\((\((\(( D[D[
\(\*SubscriptBox[\(u\), \(2\)]\)[y], y], y])\) - s*D[
\(\*SubscriptBox[\(u\), \(2\)]\)[y], y] + \ \ \ H^2*
\(\*SubscriptBox[\(u\), \(2\)]\)[
                y])\) \[DifferentialD]y)\) \[DifferentialD]y)\) \
\[DifferentialD]y)\) \[DifferentialD]y\)\)
```

```
1/20922789888000 a^6 y^8 (-a^2 G y^2 (5765760 - 1572480 s y +
       131040 (H^2 + s^2) y^2 - 3360 s (6 H^2 + s^2) y^3 +
       720 H^2 (H^2 + s^2) y^4 - 48 H^4 s y^5 + H^6 y^6) +
    43680 H^2 (11880 - 2640 s y + 132 (2 H^2 + s^2) y^2 -
       24 H^2 s y^3 + H^4 y^4) Subscript[b, 1] +
    16 y (3603600 - 1081080 s y + 98280 (H^2 + s^2) y^2 -
       2730 s (6 H^2 + s^2) y^3 + 630 H^2 (H^2 + s^2) y^4 -
       45 H^4 s y^5 + H^6 y^6) Subscript[b, 2])
 AxesStyle -> Directive[Black, 12],
 PlotStyle -> {{Red}, {Black, Thick}, {Blue, Dashed}}

Subscript[u, 3][y] = a^2 \!\(
\*SubsuperscriptBox[\(\[Integral]\), \(0\), \(y\)]\(\((
\*SubsuperscriptBox[\(\[Integral]\), \(0\), \(y\)]\((
\*SubsuperscriptBox[\(\[Integral]\), \(0\), \(y\)]\((
\*SubsuperscriptBox[\(\[Integral]\), \(0\), \(y\)]\(((\((\ D[D[
\(\*SubscriptBox[\(u\), \(2\)]\)[y], y], y])\) - s*D[
\(\*SubscriptBox[\(u\), \(2\)]\)[y], y] + \ \ \ H^2*
\(\*SubscriptBox[\(u\), \(2\)]\)[
                y])\) \[DifferentialD]y)\) \[DifferentialD]y)\) \
\[DifferentialD]y)\) \[DifferentialD]y\)\)

1/20922789888000 a^6 y^8 (-a^2 G y^2 (5765760 - 1572480 s y +
       131040 (H^2 + s^2) y^2 - 3360 s (6 H^2 + s^2) y^3 +
       720 H^2 (H^2 + s^2) y^4 - 48 H^4 s y^5 + H^6 y^6) +
    43680 H^2 (11880 - 2640 s y + 132 (2 H^2 + s^2) y^2 -
       24 H^2 s y^3 + H^4 y^4) Subscript[b, 1] +
    16 y (3603600 - 1081080 s y + 98280 (H^2 + s^2) y^2 -
```

```
       2730 s (6 H^2 + s^2) y^3 + 630 H^2 (H^2 + s^2) y^4 -
       45 H^4 s y^5 + H^6 y^6) Subscript[b, 2])
 AxesStyle -> Directive[Black, 12],
 PlotStyle -> {{Red}, {Black, Thick}, {Blue, Dashed}}

Subscript[u, 3][y] = a^2 \!\(
\*SubsuperscriptBox[\(\[Integral]\), \(0\), \(y\)]\(\((
\*SubsuperscriptBox[\(\[Integral]\), \(0\), \(y\)]\((
\*SubsuperscriptBox[\(\[Integral]\), \(0\), \(y\)]\((
\*SubsuperscriptBox[\(\[Integral]\), \(0\), \(y\)]\((\((\(( D[D[
\(\*SubscriptBox[\(u\), \(2\)]\)[y], y], y])\) - s*D[
\(\*SubscriptBox[\(u\), \(2\)]\)[y], y] + \ \ \ H^2*
\(\*SubscriptBox[\(u\), \(2\)]\)[
                y])\) \[DifferentialD]y)\) \[DifferentialD]y)\) \
\[DifferentialD]y)\) \[DifferentialD]y\)\)

1/20922789888000 a^6 y^8 (-a^2 G y^2 (5765760 - 1572480 s y +
       131040 (H^2 + s^2) y^2 - 3360 s (6 H^2 + s^2) y^3 +
       720 H^2 (H^2 + s^2) y^4 - 48 H^4 s y^5 + H^6 y^6) +
    43680 H^2 (11880 - 2640 s y + 132 (2 H^2 + s^2) y^2 -
       24 H^2 s y^3 + H^4 y^4) Subscript[b, 1] +
    16 y (3603600 - 1081080 s y + 98280 (H^2 + s^2) y^2 -
       2730 s (6 H^2 + s^2) y^3 + 630 H^2 (H^2 + s^2) y^4 -
       45 H^4 s y^5 + H^6 y^6) Subscript[b, 2])
 AxesStyle -> Directive[Black, 12],
 PlotStyle -> {{Red}, {Black, Thick}, {Blue, Dashed}}
```

Appendix B: Maple Codes for ADM

```
NULL;
```

```
restart;
with(Physics);
Setup(mathematicalnotation = true);
                 [mathematicalnotation = true]

y__0 := A*x;

m := 1;
for n from 0 to m do y__1 := B*x^3/(6.0)+x^4/(24.0)+int(int(int(int(diff(y__0, x,
                                  3                 4
         y__1 := 0.1666666667 B x  + 0.04166666667 x

                                4    1     5
            - 0.004166666667 A x  - --- A x
                                    120
                                  3                 4
         y__1 := 0.1666666667 B x  + 0.04166666667 x

                                4    1     5
            - 0.004166666667 A x  - --- A x
                                    120
y__2 := int(int(int(int(diff(y__1, x, x), x), x), x), x)-.1*(int(int(int(int(diff(
                                  5                 6
       y__2 := 0.008333333336 B x  + 0.001388888889 x

                               6                    7
         - 0.0001388888889 A x  - 0.0001964285714 A x

                               6                    7
```

```
          - 0.0001388888889 B x  - 0.00001984126984 x

                                 8                      7
          + 0.000004960317460 A x  - 0.0001984126984 B x

                                8                       9
          - 0.00002480158730 x  + 0.000002755731922 A x
y__3 := int(int(int(int(diff(y__2, x, x), x), x), x), x)-.1*(int(int(int(int(diff(y
                              -9  12                  -9  11
     y__3 := 2.087675698 10   x   + 5.010421676 10   x

                             -7  10                 -8    11
          - 5.483906525 10   x   + 2.505210838 10   B x

                             -10    13              -8    10
          - 1.605904383 10    A x   + 5.511463844 10   B x

                             -10    12                       9
          - 6.263027095 10    A x   - 0.000005483906525 B x

                             -8    11                      8
          + 4.935265350 10   A x   - 0.000004960317460 B x

                             -7    10                -7  9
          + 1.099537037 10   A x   - 5.511463844 10   x

                               8                     7
          + 0.00002480158730 x  + 0.0001984126984 B x
                    - 0.00002480158730 x  + 0.000002755731922 A x
```

```
y__3 := int(int(int(int(diff(y__2, x, x), x), x), x), x)-.1*(int(int(int(int(diff(y
```

$$y\_\_3 := 2.087675698\,10^{-9}\,x^{12} + 5.010421676\,10^{-9}\,x^{11}$$

$$- 5.483906525\,10^{-7}\,x^{10} + 2.505210838\,10^{-8}\,B\,x^{11}$$

$$- 1.605904383\,10^{-10}\,A\,x^{13} + 5.511463844\,10^{-8}\,B\,x^{10}$$

$$- 6.263027095\,10^{-10}\,A\,x^{12} - 0.000005483906525\,B\,x^{9}$$

$$+ 4.935265350\,10^{-8}\,A\,x^{11} - 0.000004960317460\,B\,x^{8}$$

$$+ 1.099537037\,10^{-7}\,A\,x^{10} - 5.511463844\,10^{-7}\,x^{9}$$

$$+ 0.00002480158730\,x^{8} + 0.0001984126984\,B\,x^{7}$$

$$- 0.00002480158730\,x^{7} + 0.000002755731922\,A\,x^{8}$$


```
y__3 := int(int(int(int(diff(y__2, x, x), x), x), x), x)-.1*(int(int(int(int(diff(y
```

$$y\_\_3 := 2.087675698\,10^{-9}\,x^{12} + 5.010421676\,10^{-9}\,x^{11}$$

$$- 5.483906525\,10^{-7}\,x^{10} + 2.505210838\,10^{-8}\,B\,x^{11}$$

```
                    -10    13                  -8    10
        - 1.605904383 10    A x   + 5.511463844 10   B x

                    -10    12                        9
        - 6.263027095 10    A x   - 0.000005483906525 B x

                    -8    11                        8
        + 4.935265350 10   A x   - 0.000004960317460 B x

                    -7    10                 -7  9
        + 1.099537037 10   A x   - 5.511463844 10   x

                      8                      7
        + 0.00002480158730 x  + 0.0001984126984 B x
```

Appendix C: Maple Codes for DTM

```
NULL;
restart;
with(Physics);
Setup(mathematicalnotation = true);
                [mathematicalnotation = true]

F(0) := 0; F(1) := A; F(2) := 0; F(3) := B/factorial(3);

m := 40;
for n from 0 to m do F(n+4) := ((n+1)*(n+2)*F(n+2)-(n+1)*F(n+1)-F(n)+KroneckerDelt
print(m+4);
                              44
C := sum(F(k), k = 0 .. m+4);
```

```
      284778046720914326136990151203543609138312454230450 37
 C := ------------------------------------------------------
      664567893697112192010906452753653972579909632000000000

      210145671437592761956266866310514081058696422926596173
    + ------------------------------------------------------ A
      221522631232370730670302150917884657526636544000000000

      464288763934534892741913938887657934951220475922 3
    + ------------------------------------------------ B
      267507102079906690822729321238841513738240000000 0
C1 := sum(k*(k-1)*F(k), k = 0 .. m+4)+0;
         174223091014454885045175251990827936893374215 99
   C1 := ---------------------------------------------
         326912866525403671306980921923893985280000000 00

        496315333921825213894162384243957871116526718315307
      - ---------------------------------------------------- A
        702503058876439949271571303122255784968192000000000

        394175619417037415048982176939430816044408547364253
      + ---------------------------------------------------- B
        351251529438219974635785651561127892484096000000000
evalf(solve({C, C1}, {A, B}));
             {A = 0.03740645580, B = -0.4513503438}
G := sum(y^i*F(i), i = 0 .. m+4);
        1    7         1  3      4 /1    1   \
G := - ---- y  + y A + - y  B + y  |-- - -- A|
       5040            6           \24   24  /
```

```
   5 / 1       1   \    6 / 1     1       1   \
+ y  |--- B - --- A| + y  |--- - --- A - --- B|
     \120     120  /      \720   720     720  /

   8 /  1         1    \    9 /    1        1     \
+ y  |----- A - ----- B| + y  |- ------ + ------ A|
     \40320     20160  /      \  181440   181440  /

   10 /   1           1     \
+ y   |------- A - ------- B|
      \1814400     3628800  /

   11 /     1          1            1      \
+ y   |- -------- + -------- A + -------- B|
      \  39916800   39916800     19958400  /

   12 /      1            1            1    \
+ y   |- --------- A + --------- B + ---------|
      \  479001600     479001600     239500800/
```

```
  G := sum(y^i*F(i), i = 0 .. m+4);
```

```
       1    7         1  3      4 /1    1   \
G := - ---- y  + y A + - y  B + y  |-- - -- A|
      5040            6           \24   24  /
```

```
   5 / 1       1   \    6 / 1     1       1   \
+ y  |--- B - --- A| + y  |--- - --- A - --- B|
     \120     120  /      \720   720     720  /
```

$$+ y^{8} \left(\frac{1}{40320} A - \frac{1}{20160} B \right) + y^{9} \left(- \frac{1}{181440} + \frac{1}{181440} A \right)$$

$$+ y^{10} \left(\frac{1}{1814400} A - \frac{1}{3628800} B \right)$$

$$+ y^{11} \left(- \frac{1}{39916800} + \frac{1}{39916800} A + \frac{1}{19958400} B \right)$$

$$+ y^{12} \left(- \frac{1}{479001600} A + \frac{1}{479001600} B + \frac{1}{239500800} \right)$$